Assessing the potential of applying energy saving measures and renewable energy resources in the campus of Lund University

Yurui Huang, Yuchen Yang
Master thesis in Energy-efficient and Environmental Building Design
Faculty of Engineering | Lund University

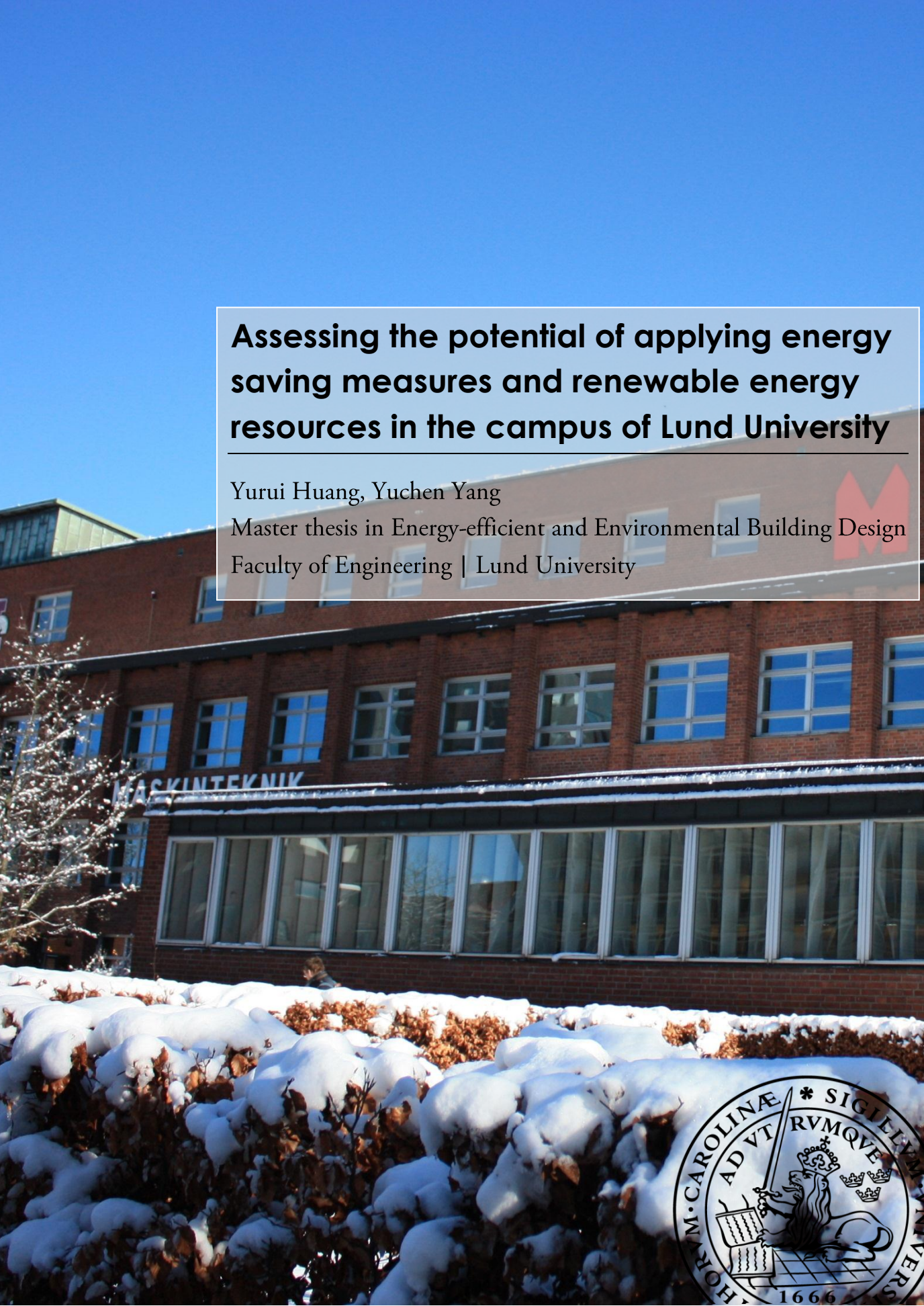

Lund University

Lund University, with eight faculties and a number of research centers and specialized institutes, is the largest establishment for research and higher education in Scandinavia. The main part of the University is situated in the small city of Lund which has about 112 000 inhabitants. A number of departments for research and education are, however, located in Malmö and Helsingborg. Lund University was founded in 1666 and has today a total staff of 6 000 employees and 47 000 students attending 280 degree programs and 2 300 subject courses offered by 63 departments.

Master Programme in Energy-efficient and Environmental Building Design

This international programme provides knowledge, skills and competencies within the area of energy-efficient and environmental building design in cold climates. The goal is to train highly skilled professionals, who will significantly contribute to and influence the design, building or renovation of energy-efficient buildings, taking into consideration the architecture and environment, the inhabitants' behaviour and needs, their health and comfort as well as the overall economy.

The degree project is the final part of the master programme leading to a Master of Science (120 credits) in Energy-efficient and Environmental Building Design.

Examiner: Elisabeth Kjellsson (Building Physics)

Supervisor: Vahid M. Nik (Building Physics)

Keywords: Energy simulation, Future climate, Renewable energy use, Solar energy, Photovoltaics, Wind energy, Wind turbine, Shallow geothermal energy, Ground source heat pump, Future energy consumption, Future renewable energy potential, Life cycle cost, Life cycle assessment.

Thesis: EEBD - 06 / 17

Abstract

Several problems concern about energy are frequently discussed in recent decades, such as the shortage of traditional energy resource, the increase of energy price and the destruction of living environment by energy conversion. To solve these problems, sustainable development of energy become a preferential task all around the world. Under current circumstances, applying energy saving measures and using renewable energy resource are two of the best choices. The goal of this study is to assess the potential of applying energy saving measures and adding renewable energy resource for two object buildings inside the campus of Lund University in Sweden. Heating and cooling energy consumption calculations towards both buildings were performed for both current and future climatic conditions. Meanwhile, the potential of adding solar energy, wind energy and shallow geothermal energy were investigated. Also, the economic profit and environmental feasibility were estimated through life cycle cost and life cycle assessment. For applying energy saving measures perspective, results show that adding insulation material to old walls, adjusting heating and cooling set point, applying high-efficient heat recovery system, and adding shading device would have significant effect on decreasing heating or cooling energy consumption. Moreover, heating and cooling energy consumption in future scenarios would decrease and increase respectively, which indicates the same phenomenon as the trend of global warming. From adding renewable energy resources perspective, the results show that the campus of Lund University have enough potential to apply solar, wind and shallow geothermal energy resources by installing PV panels, small-scale wind turbines and ground source heat pump. Besides, future climatic condition would not have huge or certain influence on renewable energy applications.

Acknowledgements

We would like to express our gratitude to Akademiska Hus for collaboration, supporting to this thesis by providing the drawings of case building, local measured weather file, and measured energy consumptions. Our special thanks to Li Lövehed and Tina Andersson, who helped us kindly during the project.

We would like to thank Guoqing Hao for his support and help on python programming. His programming makes data analysis much easier.

We would also like to thank our family respectively for their unconditional support and motivation.

Finally, we are particularly grateful to our supervisor Vahid M. Nik. His professional guidance, support and accurate critique for our thesis had significant influence on our thesis.

Table of content

Nomenclature

Abbreviations

ACH	Air changes per hour
ADPE	Depletion of abiotic resources - elements, ultimate reserves
ADPF	Depletion of abiotic resources - fossil fuels
AM	Air mass value
AP	Acidification potential
a-Si	Amorphous Silicon
BBR	Boverkets byggregler
BHE	Borehole heat exchanger
CdTe	Cadmium telluride
CH_4	Methane
CIS	Copper indium disulfide
COP	Coefficients of performance
CO_2	Carbon dioxide
ECY	Extremely cold year
EP	Eutrophication potential
ESTC	Exhaust air and solar energy
EU	European Union
EWY	Extremely warm year
FAETP	Freshwater aquatic ecotoxicity
GCM	Global climate model
GHG	Greenhouse Gas
GIS	Geographic Information System
GSHP	Ground source heat pump
GWHP	Ground water heat pump
GWP	Global warming potential
HH	Human toxicity
HVAC	Heating, ventilation and air conditioning
IKDC	Ingvar kamprad designcentrum
LGBC	Laser grooved buried contact
LiDAR	Light Detection and Ranging data

LTH	Lunds tekniska högskola
MAETP	Marine aquatic ecotoxicity
M-huset	Maskinteknik huset
MT	Clearness index
mc-Si	Mono-crystalline
NOx	Nitrogen emissions
NPV	Net present value
ODP	Ozone depletion potential
POCP	Photochemical ozone creation potential
pc-Si	Poly-crystalline
RCM	Regional climate model
SAM	System Advisor Model
SO_2	Sulphur dioxide
ST	Solar thermal
TDY	Typical downscaled year
Te	Telluride
TETP	Terrestrial ecotoxicity
UTES	Underground thermal energy storage
VAV	Variable air volume

Notation

A_1	Annual payment at first year [SEK]
A_i	Anisotropic-index [-]
A_{pv}	Area of the pv modules [m^2]
E	Equation of time [s]
g	Inflation rate [%]
$G_{b,h}$	Hourly diffuse irradiation [kW/m^2]
$G_{d,h}$	Hourly direct irradiation [kW/m^2]
G_h	Hourly global irradiation [kW/m^2]
h	Ross coefficient [-]
H_0	Extraterrestrial solar radiation [kW/m^2]
i	Interest rate [%]
L	Borehole depth [m]

L_l	Local meridian [°]
L_{st}	Time zone standard meridian [°]
n	Day number of the year [day]
N_{pv}	Number of PV modules [-]
Q_{BHE}	Shallow geothermal potential [MWh/year]
r_b	Borehole radius [m]
R_b	Thermal resistance [mK/W]
T_0	Undisturbed ground temperature [^oC]
t_c	Length of heating (or cooling) season [day]
T_{lim}	Minimum (or maximum) temperature of the carrier fluid during heating (or cooling) mode [^oC]
t_s	Simulation time [year]
U	Wind speed at anemometer height [m/s] [km/h]
U-value	Thermal Conductance [W/m^2K]
V	Wind speed at hub level height [m/s] [km/h]
Z_{ane}	Anemometer height [m]
Z_{hub}	Hub level height [m]
α	Wind power law exponent [-]
α_s	Solar height [°]
β	Tilt of the surface from horizontal [°]
γ_s	Solar azimuth [°]
δ	Declination [°]
$\eta_{inverter}$	Efficiency of inverter [%]
η_{pv}	Efficiency of PV panels [%]
θ_a	Ambient temperature of PV panels[^oC]
$\theta_{z.}$	Zenith angle [°]
λ	Thermal conductivity [W/mK]
ρ_c	Thermal capacity [$10^6 J/m^3K$]
ρ_g	Reflectance of ground [-]
ω	Hour angle [°]

1 Introduction

The energy consumption for residential and commercial buildings account for a substantial proportion of total energy consumptions in the European Union countries with approximately 40% according to the data from the European Commission of Energy. Meanwhile, traditional energy resources like coal and oil are still the main resources to produce both thermal energy and electricity. The EU has set up targets to decrease the Greenhouse gas (GHG) emissions and innovate the 20-20-20 strategies, which stands for reducing 20% greenhouse gases emission, 20% building primary energy and increasing renewable energy usage by 20% between 1990 and 2020 (Karlsson et al, 2016). Besides, study by Atanasiu et al. (2011) finds that when retrofitting the EU's existing buildings which were built more than 50 years ago with energy saving measure, total energy consumption and carbon dioxide emissions would be decreased by about 6% and 5% respectively. In addition, with the rapid growing demand of housing, the energy consumptions of buildings increase dramatically, which is equivalent to approximately 48% of total energy use in Sweden (Berggren & Wall, 2011). Study by Langer & Bekö (2015) also shows that the amount of energy-efficient buildings like passive houses has been increased rapidly to 7.2% of total amount of buildings in Sweden. The phenomenon above indicates that sustainable development of energy become a preferential task in Sweden.

Despite using building retrofitting method for energy saving, applying renewable energy resource also plays a significant role. Renewable energy resources like solar, wind, and shallow geothermal energy has become increasingly popular since last century for their characteristics of abundant, unexhausted and environment friendly (Elhadidy & Shaahid, 2000). Since Sweden is located in high latitudes with extreme cold climatic condition, more heating energy consumption would be needed to keep a satisfied indoor environment. Thus, it is of immense importance to decrease the use of traditional unrenewable energy resources and apply the clear and renewable energy resources from environment protection and sustainable development point of view. Several studies show that the uncertainties of climate changes in future would affect the energy performance of buildings even though modern retrofitting measures were applied (Nik et al., 2016). Therefore, from sustainable development perspective, the performance of buildings and renewable energy resource for future climatic condition are necessary to be estimated. The study aims to assess the potential of applying energy saving measures and add renewable energy resources for both current and future climatic conditions in the campus of Lund University in Sweden.

1.1 Objectives

The main objective of the study is to assess the potential of applying energy saving measures and adding renewable energy resources for both current and future climatic conditions in the campus of Lund University in Sweden. The second objective is to determine the feasibility of both retrofitting measures and renewable energy from the economic and environmental point of view which includes the Life Cycle Cost and Life Cycle Assessments.

1.2 Scope

The scope of this project is to investigate the energy performance for current and future climate conditions of two studied buildings considering the potential of applying possible retrofitting techniques. The potential assessment of adding renewable energy resources performing for the whole buildings in the LTH campus is also investigated for current and future climatic conditions. Moreover, the study of Life Cycle Cost and Life Cycle Assessment were carried out for long-term economic profit and environmental protection point of view.

1.3 Research question

The thesis was carried out to solving the following research questions:

1. Estimation of old and modern building energy consumption variations in current and future climate conditions.
2. Potential of energy saving when appling retrofitting measures to the buildings
3. Estimation of possible energy generation by applying renewable energy sources in current and future climate conditions.
4. Economic and environmental feasibility of retrofitting building and adding renewable energy resource.

1.4 Limitation

The entire study was carried out through numerical simulation of the energy performance of buildings, while the models were validated against measured data provided by Akademiska Hus. However, few measured data were insufficient. Thus, some inputs were assumed by the authors which are described thoroughly in the report. The data summary lists in table 1.

Table 1: Summary of provided data by Akademiska Hus.

Data type	**Building IKDC**	**Building M**
Heating consumption	Sufficient	Sufficient
Cooling consumption	Sufficient	Insufficient
Building material	Insufficient	Sufficient
Electricity	Sufficient	Sufficient
HVAC system	Insufficient	Insufficient
Heating/cooling set point	Insufficient	Insufficient
Schedule	Insufficient	Insufficient

2 Background knowledge

2.1 Energy saving techniques

Building retrofitting is a highly-raised focus in recent decades. Many building retrofitting techniques and science approach are proposed for energy savings. However, the efficiency of these measures is uncertain for specific buildings as it would be affected by plenty of parameters, like location, climate and so on. Nik et al. (2016) pointed out nine retrofitting measures which are available for residential buildings in Sweden in current climate and future climate scenarios: Basement insulation improvement; Façade insulation improvement; Attics insulation improvement; Window replacement; Ventilation system upgrade with heat recovery for Single Family Dwelling; Ventilation system upgrade with heat recovery for Multi Family Dwelling; Efficient lighting equipment; Efficient appliances; Heating and cooling set back point-minimum indoor air temperature to 20 ℃ (Nik et al., 2016).

To find out the proper building retrofitting methods from masses of energy retrofitting options, one key point is their long-term benefits (Nik et al., 2016). Previous study for buildings in the campus of Lund University, carried out by Jensen (2016), mainly assessed the long-term performance of various energy retrofitting measures for exterior wall and roof for current and future climate conditions. Results show a probable heating energy saving of 20-30% for wall retrofitting and 5% savings for roof retrofitting. Meanwhile, the retrofitting measures are economic infeasible but environmental feasible (Jensen, 2016).

Except wall retrofitting, window change is also a considerable measure for energy saving. Poor windows and frames could lead to several problems, such as draught and acoustic. Also, window with poor water tightness would have the risk of moisture problem. Van and Janssens (2016) carried out a test of 437 windows. The results showed that the vinyl frames windows have slightly lower airtightness and water tightness than wooden and aluminum window (Van & Janssens, 2016). Another experiment performed by Cuce (2016) compared two windows with one ordinary window with U-value of 2.67W/m^2k and another airtight window with U-value of 1.79W/m^2K. The results show that about 33% of heat could be saved by using airtight windows (Cuce, 2016).

Besides, adjustments of HVAC system settings are another viable and efficient measures. Research by Mata et al. (2010) estimated the validation of building retrofitting measures through a sample of 1400 buildings in Sweden based on the

data in 2005. The two most efficient measures are adding or improving heat recovery systems and adjusting indoor air temperature. (Mata et al., 2010).

Due to the amount of heat transferred through windows have some effect on energy balance inside building, changing windows replacement and adding shading devices would have a high potential for energy saving (Beck et al., 2010). Many recent researches show that windows and shading devices with optimized design would significantly reduce energy consumption and increase thermal comfort (Stevanović, 2013). Due to office buildings are popular to be designed with large glazed windows, most of the related researches were performed for office buildings (Atzeri et al., 2014). Research by Carletti et al. (2014) investigated in the effects that replacing windows with and adding shading devices would have on energy consumption for an Italian building. Results show that the use of shading devices has an improved thermal sensation as well as cooling energy saving (Carletti et al., 2014). As Italy has higher outdoor air temperature than Sweden in summer, the cooling energy saving might be higher than Sweden. Thus, the effect of shading device for cooling demand in Sweden need to be investigated.

2.2 Renewable energy resource application

2.2.1 Solar energy

2.2.1.1 Solar radiation

Solar radiation is an important factor when assessing the solar potential. However, solar radiation would be different from area to area as plenty of parameters have influence on its level variation. Researches by Wong et al. (2016) and Pfeifer et al. (2009) show that parameters like aerosols, water vapour contents, air particulates, elevation, slope, aspect, and shadow all would affect the radiation levels. Thus, estimating solar radiation under the consideration of local climate and building surroundings is necessary.

2.2.1.2 Solar pontential

Applying solar energy is a new rising trend of urban development. The method for quantifying the solar potential which presented by Compagnon (2004) is setting up threshold values to qualify external envelope of buildings for active or passive heating, photovoltaic electricity production and daylighting. For early design phases, thresholds value could determine the minimum amount of solar radiation on a surface which would be appropriate for solar energy system installation, see table 2 (Compagnon, 2004). Nevertheless, Kanters & Wall (2014) suggest that Compagnon's threshold method is based on Europe region, for other regions the result would be different. Also, as solar energy application technologies have dramatically developed in nowadays, the threshold value proposed by Compagnon

(2004) might not suitable for current simulations. Thus, based on Lund Solar map (Kraftringen, 2012), Kanters & Wall (2014) presented a new threshold value for acceptable categories, see table 3.

Table 2: Threshold values for varies solar techniques (Compagnon, 2004).

Solar technique	Threshold for façade system	Threshold for roof systems
Passive thermal heating	216 kWh/m^2 (heating season)	Same as for facades
PV system	800 kWh/m^2 (Total)	1000 kWh/m^2(Total)
Solar collectors	400 kWh/m^2(Total)	600 kWh/m^2 (Total)

Table 3: Threshold values for different categories (values in kWh/m^{2}a). *(Kanters & Wall, 2014).*

	Unsuitable	**Suitable**	**Suitable**	**Suitable**
		Reasonable	Good	Very good
Façade	0-650	651-900	900-1020	>1020
Roof	0-800	800-900	900-1020	>1020

By analyzing solar potential of four building blocks in Lund in Southern Sweden in DIVA for Grasshopper, Kanter & Wall (2014) found out the results that the flat roof orientated between 15 ° and 60 ° appears to have the highest solar potential when only take building density, orientation and roof type into consideration. The building density have the most influence on the solar potential (Todorov,2015).

Besides the DIVA for Grasshopper, several other solar radiation open source models are also frequently used, the most well-known softwares are the ArcGIS (Fu & Rich, 1999) and GRASS (Hofierka & Su ří, 2002). Based on the geographic information layer, those models take consideration of inclination, orientation and latitude (Redweik et al., 2013). In municipal level, the models have been successfully applied to determine solar potential of entire region based on a digital man-made model (Hofierka & Kanuk, 2009). The solar radiation models which cited above are in general not take the building's façades into account as the façade are lean over in

2.5D model. The model with inclined surface was not reliable on any computation (Redweik et al., 2013). Carneiro (2011) refers to a method using 3D Models which requires not only a pre-existence model but also a separated calculation for building façades. Geographic Information System (GIS) is also a way of appraising the solar potential in urban context which provides information on annual solar irradiation on building surfaces, potentially solar energy output data and Light Detection and Ranging data (LiDAR) (Nguyen et al, 2012). Moreover, a façade assessment tool-FASSADE, was introduced by Kanters et al. (2013) for solar energy, based on the DIVA for Rhino plug-in. Simulation engines like EnergyPlus and Radiance/Daysim are combined by the implement for performing hourly solar irradiation computations, used for the PV production and possible solar thermal (ST) production (Kanters et al., 2013). The tool also has the flexibility of 21 plug-ins to calculate the investment cost and payback time according to the local electricity and heating price (Kanters et al., 2013). An analysis of distinctive Swedish building block was implemented and the results point out the shadow effect from the surrounding façade influence the solar energy output and leads to more retentive payback time (Kanters et al., 2013).

Solar map is a visible way to show solar potential level. A study from Kanters et al (2014) classified the solar map into three categories with basic, medium and advance. Meanwhile, hinging on the information furnished as output. Also, based on an evolved method to forecasting the electricity output from PV panes by LiDAR and GIS data amalgamated with hourly building simulation program Daysim, Jakubiec & Reinhart (2013) created an innovative photovoltaic potential map for Cambridge's city, MA, USA. An extension module for ArcGIS in solar potential analysis based on the DEM data and input DSM also evolved solar radiation map (Fu & Rich, 1999). The slope, solar angle, shadow effect by surrounding façade, and several factors are reckoned during the simulation (Lukac et al., 2014). Another solar radiation model called SRAD, which is able to simulate the interaction between the long wave and short wave solar radiation within the surface of the earth and atmosphere (Wong et al., 2016). Hofierka & Súri (2002) also pointed out that although the model is capable to describe the spatial variability of landscape processes, the calculation is still limited over large territories as it mainly focuses on topographical and mesoscale processes.

2.2.1.3 Photovoltaic technology

The solar photovoltaic (PV) systems have rapidly developed. The domination of the PV module market was modules made by traditional technologies such as crystalline silicon. New raised PV module technologies are also applied worldwide (Baharwani et al. 2015).

Two frequently used technologies are poly crystalline technology and cadmium telluride (CdTe) technology. Poly Crystalline technology started using in 1940s and

become the ripest technology currently. Several researches show investment still can be saved by technology development. CdTe technology was invented in 1972 and the efficiency was 6% at that time. After that, significant improvement successfully made the efficiency increase to 16.5% (Solanki, 2011). Although CdTe would be stable for a longer lifetime (Boer, 2011), this technology has some negative environmental impact when using telluride (Te) as raw material (Resnick Institute, 2011).

Different PV module technologies have variable effeciency under different climate conditions (Sharma et al., 2013). A lot of researches were invested in the performance of PV module technology. Carr (2004) compared five PV modules' power generation in Perth, Western Australia with different technology: c-Si, p-Si, a-3j-Si, CIS and LGBC c-Si. Results show that if all the modules are stable and have same kWp values, the one having the best performance would be the thin film modules. The a-3j-Si modules have 15% and 8% higher power generation than c-Si module in summer and winter respectively. Meanwhile, the CIS module would have 9% to 13% more energy generation than c-Si module. Skoplaki (2009) researched the relationship between operating temperature and the photovoltaic conversion, which showed linearly variation as a result. Huld (2010) estimated three different PV modules with same installations around Europe. For the CdTe modules, moderate irradiance areas would have the highest efficiency. Makrides et al. (2010) performed a research on the performance of thirteen types of PV systems in Cyprus. The results show that the PV system which has the lowest temperature coefficient would have the best power generation performance, as the temperature losses plays a significant role when in hot climatic condition. Study by Baharwani et al. (2015) evaluated the relationship of two PV technologies and two electronic circuitries in India: polycrystalline and CdTe; MPPT and PWM. CdTe module performed better with MPPT for its highly open circuit voltage. However, polycrystalline module is better for PWM. CdTe module has higher energy generation and operational efficiency compared to polycrystalline. Study by Quansah et al (2017) estimated performance of five PV systems with different solar cell technologies: poly-crystalline (pc-Si), mono-crystalline (mc-Si), copper indium disulfide (CIS) thin-film, Amorphous Silicon (a-Si), and heterojunction incorporating thin (HIT) film. The performance experiments were done in Kwame Nkrumah University Science and Technology, Ghana. Results show that pc-Si is the most suitable solar PV technology for the site condition, followed by a-Si, HIT, mc-Si, and CIS. Besides, the HIT based system is the most suitable solar PV technology for this site and potentially If space is not a constraint.

2.2.2 Wind energy

2.2.2.1 Wind turbine

Wind, one of the most popular renewable energy resources, has been applied in many countries for decades. Almost 15-30% of total electricity production were generated by wind power in some European countries (IEA, 2013) (Higgins, 2014). Although hydropower and nuclear power take a great proportion in electricity supply in Sweden, an enlargement of renewable energy use has come into sight from twenty-first century, in which wind power contribute the most (Swedish Energy Agency, 2015). In 2016, 605 MW of new wind power has been installed in Sweden. There is a total of 6422 MW wind power was distributed over 3335 projects in Sweden until 2016 (Swedish Energy Agency, 2016).

Following the development of wind energy application technology, small-scale wind energy generators has made significant and speedy development. According to incomplete statistics, about 250 small-scale wind turbine salers was running business in about 26 countries. Small-scale wind turbine business starts from early 1980s. Not only numbers of application but also the capacity of energy generation is expected to be increased triple than before (Rolland & Auzane, 2012). Study by Bilal et al. (2013) show that the energy generation of the small-scale wind turbine would vary from 312 kWh/year (for Inclin 600W) and 1470 kWh/year (EOLSenegal 500W) in Gandon and Sakhor respectively.

It is important to assess local air density to predict the potential of wind energy (Ko et al., 2015). According to the ideal gas law, the air density is decided by average atmospheric pressure, absolute temperature, and ideal gas constant (Lee et al., 2013). Also, wind speed is a particularly important parameter to assess wind energy using potential. The distribution functions proposed by Weibull and Rayleigh were frequently used for wind speed simulation as it is regarded as a suitable distribution functions to actual wind speed (Ko et al., 2015). Then, the maximum generation per area could be predicted by knowing the mean value of air density and wind speed (Dahmouni et al, 2010). Meanwhile, using this distribution, the occurrence rate of wind can be calculated (CDIT,2001). Afterwards, the energy generation for a year could be simulated by combine the turbine power curve and the occurrence rate of wind speed (Ko et al, 2015). Based on wind speed and wind power density, wind energy resource can be classificayed, show in table 4 (Ko et al, 2015).

Table 4: Classification of wind energy resource (Ko et al, 2015).

Wind resource category	Wind class	Wind speed [m/s]	Wind power density [W/m^2]
Poor	1	3.5-5.6	50-200
Marginal	2	5.6-6.4	200-300
Moderate	3	5.4-7.0	300-400
Good	4	7.0-7.5	400-500
Excellent	5	7.5-8.0	500-600
Excellent	6	8.0-8.8	600-800
Excellent	7	> 8.8	>800

Wind is a more clean and infinite energy sources compared with fossil fuels and nuclear power, as it would not cause acidification or other damaging emissions. Whereas, it also has some limitations. First, there is a lack of undisputed evidence that could prove wind energy has siginificant effect on reducing global warming phenomenon (Kealy, 2017). Also, for noises generated by wind turbines and moving shadows, wind power has been considered as environmental harmful in some rules (Wizelius, 2007). The noise is mostly come from the moving mechanical turbine and aerodynamic sound from blades, which are affected by local wind characteristics, terrain and turbine characteristics (Thorstensson, 2009). However, according to the sound level, only when wind speed is between 3-8 m/s, the noise from the turbine would disturb (Larsson, 2003). One feasible solution is building filters in same speed as turbines (Thorstensson, 2009). The shadows are from the tower and blades, which may show a moving shadow over the surroundings and disturb others. But this bad influence can be avoided by optimal urban planning (Thorstensson, 2009).

The main advantage of investing in small-scale wind turbines could be generating electricity for personal need and reduce energy dependence on unrecycled energy source like fossil fuel. Also, it is appreciated to make personal or corporate contribution to the environment of human lives (Thorstensson, 2009).

2.2.3 Shallow geothermal energy

2.2.3.1 Shallow geothermal resource

Shallow geothermal resource, which is defined in several countries as geothermal resource from ground depth less than 400 meters, play a vital part when producing heating and cooling for domestic or commercial applications (Koroneos et al. 2017).

According to the technology applied, the geothermal potential has two definitions: closed-loop system or open-loop system. Closed-loop systems is a system that yearly average thermal load is exchanged with the ground by a borehole heat exchanger (BHE) with a length L, coping with a minimum / maximum temperature threshold of the heat carrier fluid (Casasso & Sethi, 2016). Based on ground thermal parameters and BHE's characteristics, a limitation is imposed to the thermal alteration of the heat carrier fluid (Casasso & Sethi, 2014). On the contrary, although thermal conductivity has slight effect on the heat diffusion into the aquifer, the hydrodynamic parameters of the aquifer play an important role in heat transfer in Ground Water Heat Pump (GWHP) (Russo et al. 2017). Analytical or numerical models is needed in designing phase as the system efficiency would be impaired by thermal recycling (Casasso & Sethi, 2015). The propagation of thermal plumes downstream the injection well is another important aspect when design GWHPs, for it would have a negative impact on drinking water wells or other geothermal installations (Casasso & Sethi, 2016).

Closed-loop ground source heat pumps is universally used as the abstraction of groundwater is not required. However, various parameters affect the techno-economic feasibility of BHEs: usage profile (heating or cooling mode, building type, location climate condition), thermal properties of the ground (thermal conductivity λ, thermal capacity ρ_c, undisturbed ground temperature T_o), and BHE and plant properties (length L, minimum/maximum threshold fluid temperature T_{lim}, thermal resistance R_b. borehole radius r_b, pipe radius r_p, number of U-pipes n and geothermal grout λ_{bf}) (Casasso & Sethi, 2016).

For thermal properties of the ground, vadose and saturated zone have different thermal conductivity. Typical thermal conductivity for some zones are listed in Table 5 (Sipio et al., 2014; VDI, 2010).

Table 5: Values of thermal conductivity and thermal capacity adopted for different lithologies (Sipio et al., 2014; VDI, 2010).

Nº	**Lithology**	**λ[W/mK]**	**ρ_c [10^6J/m^3K]**
1,2	Alluvial/moraine sediments(dry)	2.4	1.5

1.2	Alluvial/moraine sediments (saturated)	0.5	2.4
3,9	Clay/Alternated clayey layers	1.8	2.5
4	Fine sand	1.8	2.5
5	Clay and clayey marl	2.1	2.25
6	Marl	2.3	2.25
7	Marl and siltstone	2.1	2.25
8	Sandstone	2.8	2.2
10	Serpentinite	2.5	2.8
11	Calceschyst	2.5	2.4
12	Limestone and dolostone	2.7	2.25
13	Fine grained gneiss	2.5	2.1
14	Coarse grained gneiss	2.9	2.1
15	Granite	3.2	2.5

Most shallow geothermal energy systems in Sweden use hard rock to make vertical drilling. At the same time, the boreholes are usually filled with groundwater. The temperature of ground generally varies between +2 ^{o}C in the winter and +8 ^{o}C in summer (Swedish Energy Agency, 2015).

2.2.3.2 Ground source heat pump

Ground source heat pump (GSHP), the most frequent applications of utilizing shallow geothermal resource. When GSHP is used as heating supplier, ground is the heat source. On the contrary, when it is used as cooling supplier, ground works as a heat sink. Ground source heat pump have rapid development since 1995, especially in United States, Europe and China (Lund & Boyd, 2015).

As temperature underground is approximately constant, GSHP operates with smaller temperature differences than conventional heat pumps. Therefore, GSHP is more energy-efficient and have higher coefficients of performance (COP) than other heat pumps (Sarbu. et al, 2014). Also, from weather variations point of view, geothermal

energy is more stabilized than other renewable energies such as solar, wind and hydro. Thus, it is ideal for providing a base load energy supply (Fridleifsson, 2001).

Geothermal power plants in Lund are the largest ground source heat pumps used in Sweden in the twentieth century. It was first reported in Bjelm and Schärnell (1983). Until 2015, the largest BTES system in Sweden is in the Campus of Karlstad University, which has 204 boreholes at depth of 240-250 m (Svensk Geoenergi, 2014).

In 2015, there are around twenty percent of two million single-family houses using GSHP as heat source in Sweden (Swedish Energy Agency 2015). The application of these small GSHP systems has rapidly grown for several years until the last few years it was slightly levelled out. The reported sales of GSHPs up to 10kW can be seen in figure 1.

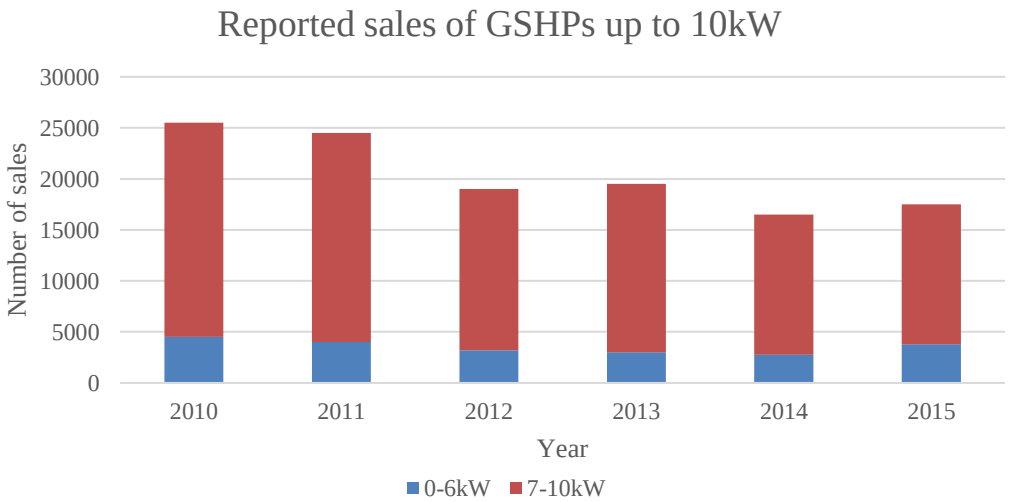

Figure 1: Reported sales of GSHPs up to 10kW (Swedish Energy Agency 2015).

The application of larger GSHP systems large underground thermal energy storage (UTES) also steadily growing, see figure 2. Besides, when heat pump capacities are above 60 kW, system would be divided to several heat pump units. Single larger heat pumps used in UTES systems are not included in the statistics (Swedish Energy Agency 2015).

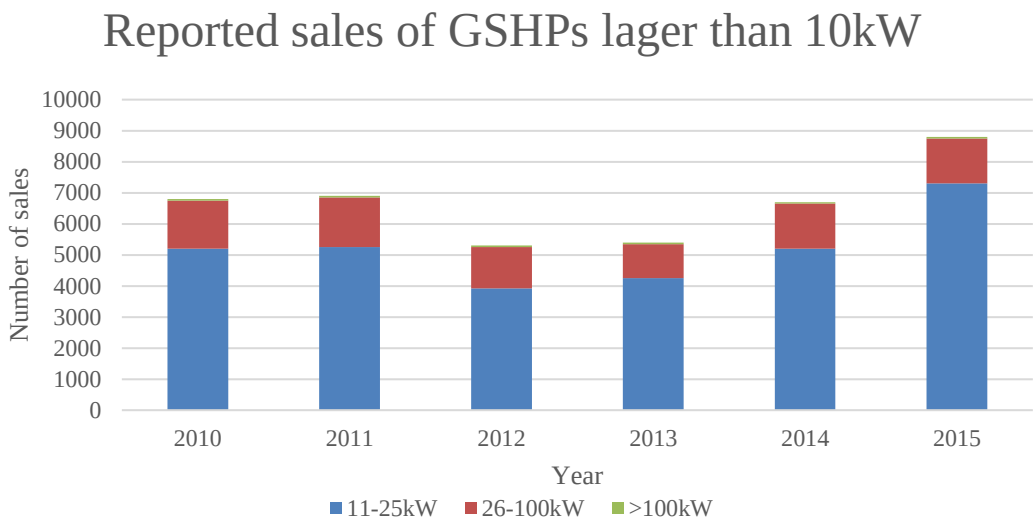

Figure 2: Reported sales of GSHPs larger than 10kW (Swedish Energy Agency 2015).

Depth, capacity and efficiency of boreholes for GSHPs and BTES systems all have an increasing trend. Figure 3 shows how the numbers of drilled boreholes and the depths of borehole change during 2000-2015. The rapid development of average depth of drilled boreholes is a result of development in drilling equipment and higher COP in newer heat pumps (Swedish Energy Agency 2015).

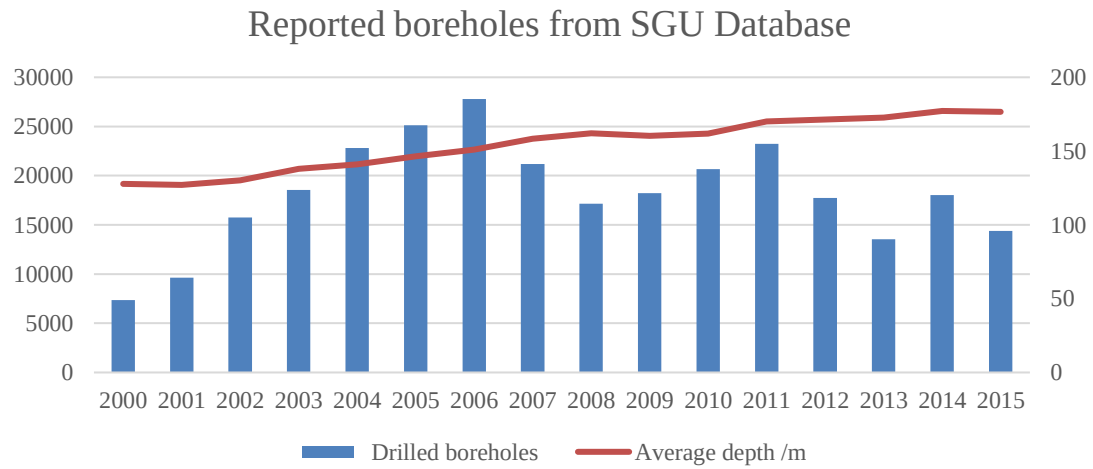

Figure 3: Reported boreholes from SGU Database.

Due to underground thermal imbalance, the efficiency of GSHP systems decreases over long-term operation (Wang et al., 2017). Some solutions were proposed such as increasing borehole radiuses or depth, adding heat exchangers, or adding natural heat recovery time and so on (Yang et al., 2013). However, geological conditions,

construction difficulties, and engineering costs would create limitations to these solutions (Ji et al., 2015).

Solar systems could be added to hybrid-GCHP system as a heat compensation in cold climatic condition (Emmi et al., 2015). A GSHP system assisted by solar collector was analyzed by Si et al (2014) to find the addendum with solar energy for keeping GSHP system running effeciently during a long period. In another research about solar collector and ground heat exchangers combined system, result shows that this system could effectively keep the temperature on the wall of boreholes (Yang et al., 2015). Whereas, weather variations and low outdoor temperature in cold climate areas make the assumptions of stability, actual working hours and heating loads unrealistic (Wang et al., 2010). Also, adding solar energy could increase temperature of soil and decrease the efficiency in hot climate (Zhu et al., 2014).

Aiming to solve the thermal imbalance problem of GSHP system, You et al (2015) proposed a combined system by adding air source heat compensator. However, the air-source heat compensator would need large investment and high operation energy consumption. Meanwhile, to promoting efficiency of GSHP systems in cold regions, a combined compensation system with exhaust air and solar energy (ESTC) was proposed in the research by Wang et al. (2017). Results showed that the ESTC system can effectively compensate heat to the ground heat exchanger. During the 10-year simulation period, the simulated thermal imbalance ratio of the ESTC - GSHP was below 2.5%. Furthermore, the thermal compensation capacity per unit energy consumption of this approach was 25% higher than the traditional method (Wang et al., 2017).

2.3 Life cycle cost

2.3.1 Energy price

The research of energy price was done for grid electricity, district heating and energy tax in Sweden.

2.3.1.1 Price of grid electricity in Sweden

For grid electricity, the price was gathered from Energimarknadsinspektionen(Ei), which is the inspectorate organization of Swedish energy markets. From their weekly report of week nine in 2017, the system price from NPS in 2015, 2016, and 2017 can be seen in figure 4 (Energimyndigheten, 2017). NPS is the marketplace for whole sale markets in Sweden, Norway, Finland, Denmark, Estonia, Latvia and Lithuania (Energimyndigheten, 2017). Spot price in Malmö, which city is close to

Lund, was 30.2 EUR per MWh in week nine in 2017. It is slightly lower than the system price from NPS, which was 30.5 EUR per MWh at the same time.

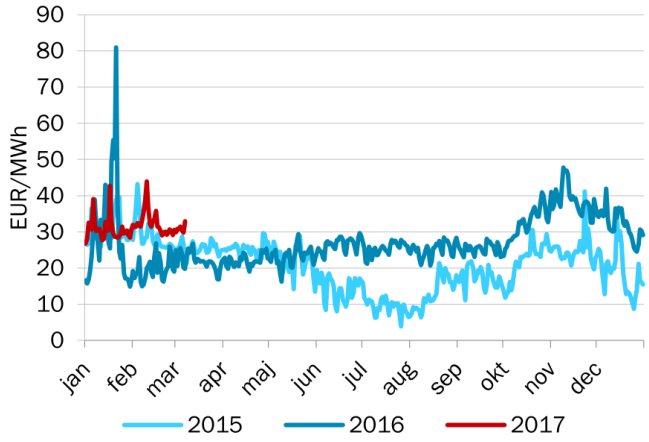

Figure 4: The system price from NPS in 2015,2016 and 2017 (Energimyndigheten, 2017).

From the Ei Annual report in 2016, price trend over the year 2015 for different areas was compared (Swedish Energy Markets Inspectorate, 2016). Lund located at southern Sweden, which bidding area was named SE4. The price in this area show as the lightest blue line in figure 5. The highest price in bidding area SE4 in 2015 was on 2nd February when the average day price was 46.4 öre/kWh, and the lowest prices was 3.3 öre/kWh in the 26th July.

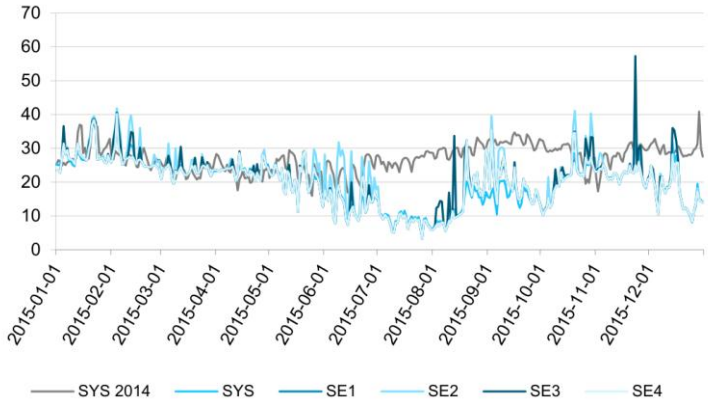

Figure 5: Daily average rates on El spot during 2015, öre/kWh (Swedish Energy Markets Inspectorate, 2016).

Also, the electricity price for the customers is somehow different from the electricity suppliers and their supply contracts. According to the annual report from Ei in 2016, customers living in apartments who signed one-year fixed price contract, the period's

difference between the most expensive and the cheapest contracts of fixed price type in one year was 42 percent difference with averaged 37 öre in the period from 2010 to the end of 2015, see figure 6 (Swedish Energy Markets Inspectorate, 2016).

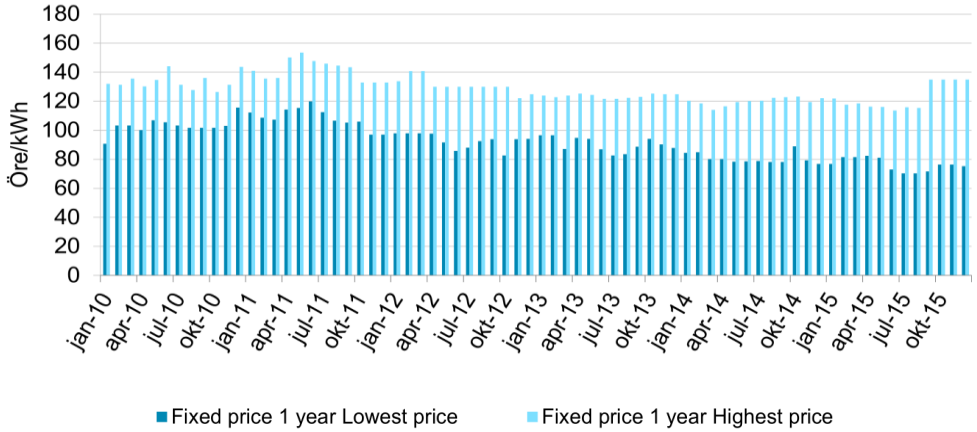

Figure 6: The highest and lowest prices for the contract type fixed price in one year, customer in apartment, 2,000 kWh/year (Swedish Energy Markets Inspectorate, 2016).

In recent years, the rate of household customers choosing a variable rate contract has increased significantly, which becomes the most common contract in Sweden since the end of 2013 (SCB, 2016). For customers living in apartments who owned the contract type with variable price, the difference of the highest price and the lowest price amounted to 63 percent with averaged 53 öre difference in the period, see figure 7 (Swedish Energy Markets Inspectorate, 2016).

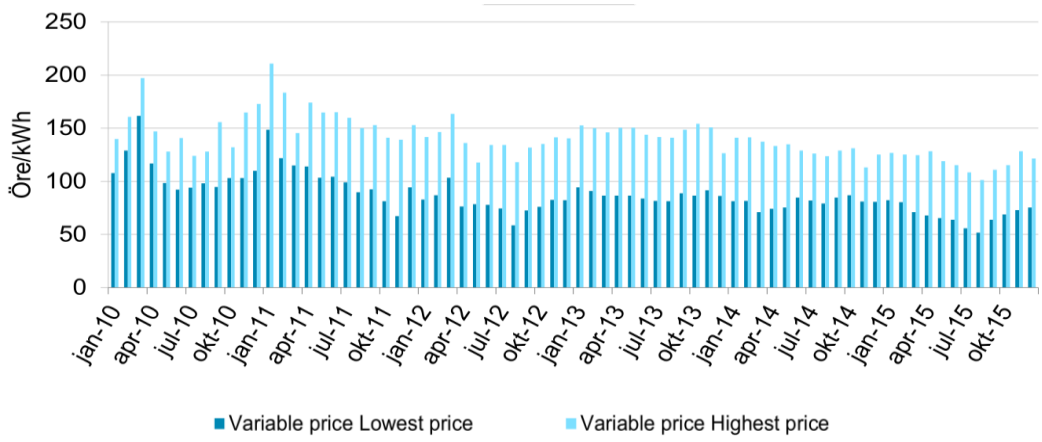

Figure 7: The highest and lowest prices for the contract type variable price, customer in apartment, 2,000 kWh/year (Swedish Energy Markets Inspectorate, 2016).

Based on the realistic data provided by Statistics Sweden(SCB), the average total price of electricity paid by household customers in every six months is showed in

figure 8. The total price includes electricity, grids, certificates, electricity tax and VAT, which is given in öre / kWh. Also, electricity also can be used by household customers in detached houses for electric heating. The price in different contracts can be find in figure 9 (SCB,2016).

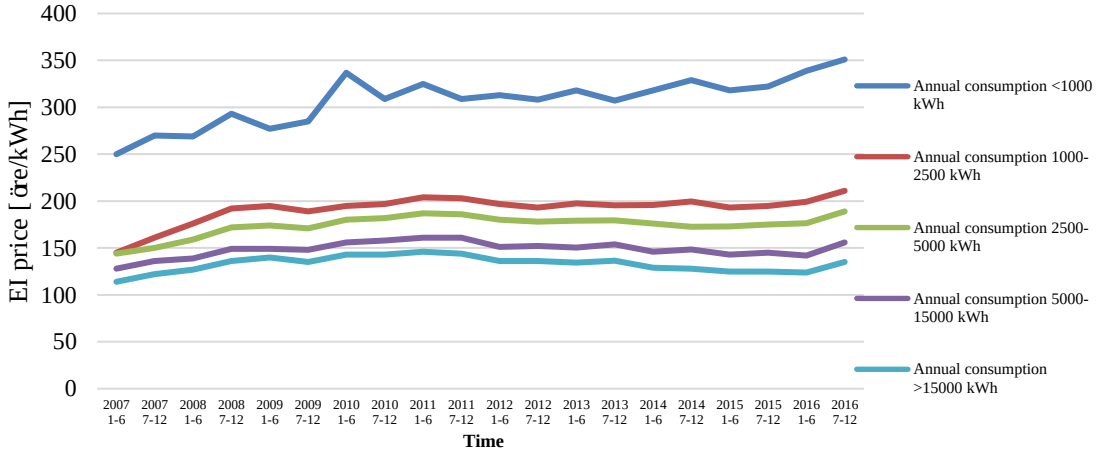

Figure 8: Prices of electricity for residential customers (SCB,2016).

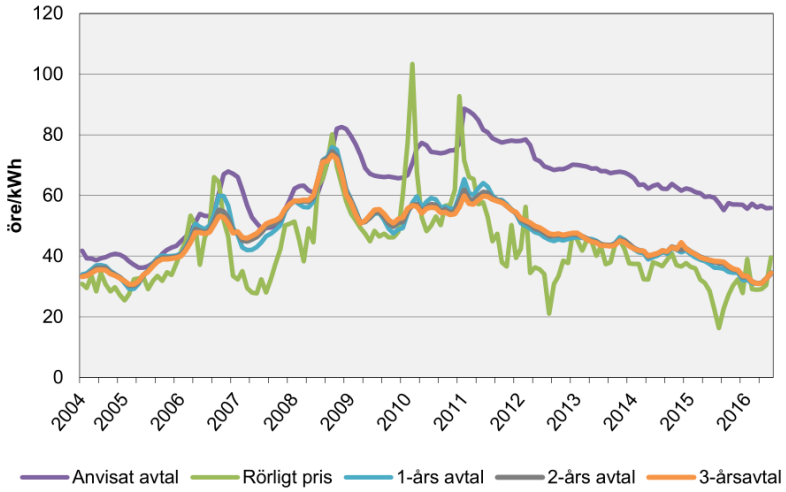

Figure 9: Average electricity prices for household customers in detached houses with electric heating, öre/kWh (excl. taxes) (SCB,2016).

2.3.1.2 District Heating

Annual average district heating prices 1980-2013 in euro per GJ in Sweden, which collected by Energi Forsk (2016), is showed in Figure 10. In the large scheme of view, it has a steadily rise trend. But for each year, the price changes also combine with ups and downs.

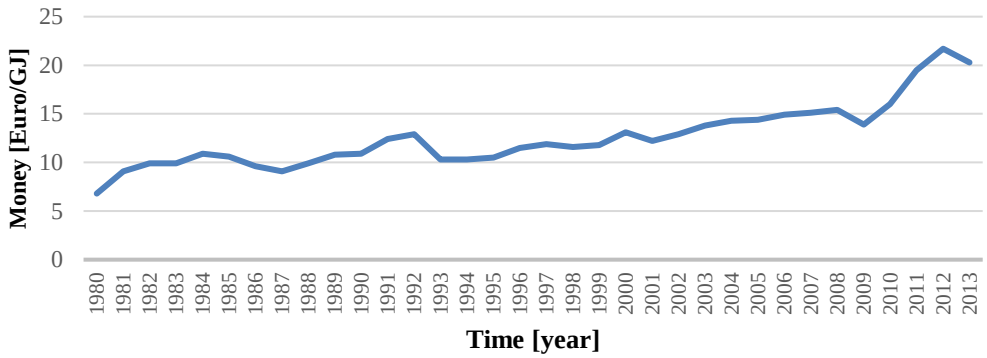

Figure 10: Annual average district heating prices 1980-2013 in euro per GJ in Sweden (Energi Forsk, 2016).

SCB's survey (2016) on district heating prices collected 15 district heating companies both have fixed price contract and variable price contract, and added together as an average price in SEK / MWh (incl. VAT). District heating prices have obvious seasonal variations, see table 6 (SCB, 2016).

Table 6: District heating prices for multi-dwelling buildings (incl. VAT), mean values, SEK/MWh (SCB, 2016).

	2006	2007	2008	2009	2010	2011	2012	2013	2014	2015	2016
Jan	692.2	705.5	732.6	769.4	786.7	799.8	858.8	888.4	905.7	923.8	933.1
Feb	693.6	705.4	735.7	769.4	786.7	799.8	858.6	888.2	905.4	923.6	944.8
Mar	687.3	705.5	735.8	769.4	786.7	799.8	852	876.7	882.7	883.6	904.7
Apr	657.2	683	710.7	731.5	748.7	767.7	733.8	755.7	764.9	765.8	778.2
May	541	563.2	587.1	597.5	591.3	592.1	601.2	612.5	622	641.8	636.6
Jun	517.8	537.6	565.9	574.9	568.5	583.7	554.2	563.9	597	590.7	586.1
Jul	517.8	537.6	566	574.9	568.5	583.7	553.5	563.2	596.5	589.9	
Aug	517.7	537.6	566	574.9	570.5	583.7	553.5	563.2	596.5	589.9	
Sep	541.7	561.9	594.1	603.1	597.9	621.6	598	609.2	630.9	615.1	
Oct	618.3	634.6	682.6	723.8	747.2	760.3	729.3	751.3	759.1	769.4	
Nov	688.6	699.7	730.3	743.5	766.5	767.7	736.7	758.7	766.9	768.9	
Dec	695	706.2	736.4	769.4	788.7	799.8	857.7	887.3	895	922.6	

Except district heating energy price, the power starting price and the flow price are also needed to be taken into consideration if customer is desired to using district heating. The price for these two types of cost as well as energy prices for 2014 from municipality in Helsingborg is showed in table 7.

Table 7: District heating Prices in 2014 in Sweden from municipality in Helsingborg.

Power Starting price (meter price)	10 458 kr/year
Energy, November-March	55,6 öre/kWh
Energy, April-May and September-October	32,0 öre/kWh
Energy, June-August	9,8 öre/kWh
Flow	3,78 kr/m ^{3}

2.3.1.3 Comparison of the price for the energy carriers

Prices of all traditional energy source between 1996 and 2014collected by Swedish Energy Agency (2015) is showed in figure 11. The electricity price has increased from 1996 but decreased since 2011 for both domestic electricity and electric heating. The oil price in Sweden have same trend as the price on the global oil market, which is a mostly continual rise trend. The price of natural gas, similar as electricity price, rapid growth 2000s, but slowly fall down since 2011. The price of district heating keeps increasing during the 2000s.

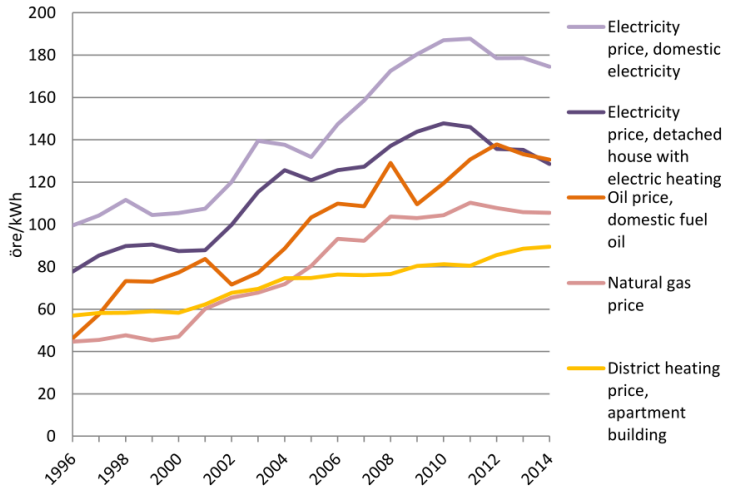

Figure 11: Energy prices for the residential and services sector, 1996–2013, real (2014) öre/kWh (Swedish Energy Agency, 2015).

2.3.1.4 Energy tax

The tax on energy consumption is a collective noun for fuel and electricity, including energy taxes, carbon dioxide taxes and sulfur taxes (Swedish Energy Agency, 2015). The payment of energy tax is decided according to the energy type. The carbon dioxide tax is paid per kilogram of carbon dioxide emissions for all energy resources except biomass and peat fuel. The sulfur tax is equivalent to 30 SEK per kilogram of sulfur gram for coal and peat fuel, and 27 SEK per cubic meter of 10% the weighted sulfur content of the oil (Swedish Energy Agency, 2015). The maximum sulfur content of the oil which is tax free is 0.05% by weighted value. (Swedish Energy Agency, 2015). General energy taxes excluding VAT are showed in table 8 (Swedish Energy Agency, 2015).

Table 8: General energy taxes excluding VAT from 1st January 2015 (Swedish Energy Agency, 2015).

	Energy tax	CO2 tax	Sulphur tax	Total tax	Tax [öre/kWh]
Fuel oil 1, SEK/m³(<0.05% sulphur)	850	3218	-	4068	40.9
Fuel oil 5, SEK/m³(<0.4% sulphur)	850	3218	108	4176	39.5
Coal, SEK/tonne (0.5% sulphur)	646	2800	150	3596	46.7
Natural gas, SEK/1000m³	939	2409	-	3348	30.3
Electricity, northern Sweden, öre/kWh	19.4	-	-	19.4	19.4
Electricity, rest of Sweden, öre/kWh	29.4	-	-	29.4	29.4

2.4 Life cycle assessment

LCA, represents for Life Cycle Assessment or Life Cycle Analysis, is an analysis of the environmental effect which is caused by a product or process during the extraction of raw materials, manufacturing, installation, operation and maintenance, dismantling, recycling, and disposal at the end-of-life. LCA involves a great many steps. First, the aim and the scope of the LCA is needed to be decided. Also, a functional unit is needed. It includes all input and outputs, which would give a clear explanation of the product and results. The second step includes deciding system boundaries, designing flow charts, and gathering data for each process. Next step is impact assessment, which focus on raw material depletions and emissions process. After that, a comparison of environmental impacts with other product with an alike functional unit could be done.

LCA study of renewable energy sources is a significant point when assessing potential. Due to influencing factors such as resource availability, climate, environment, economy, society, and policies are various in different scenarios, one energy resource would not be suitable for random locations. Thus, LCA based local conditions is needed (Singh et al. 2013). LCA not only has detailed analysis on regional and global scales but also associates emissions, and the end of life process (Singh et al. 2011). Performing LCA research could identify the process of product, which greatly contributes to its environmental burden and helps companies make investment decisions (Udo de Haes & Heijungs, 2007).

However, LCA also have several limitations and uncertainties. Growing attention on Greenhouse Gas (GHG) makes LCA tends to focus mainly on those effects and weakens assessment on other impacts. The site connected with whole energy system such as electricity grid, market, etc. is rarely be take into consideration. Social standards, acceptability or supply safety are also missed in LCA. In addition, the results are influenced by different assumptions or methods, such as the choice of LCA technology, impact categories, system boundaries, lifetime, operating conditions. The risk of repeated calculations and concepts introduced or used would also affect results (WG, 2011). Thus, it is impossible to apply results worldwide for environmental impacts are heavily site dependent. Moreover, LCA is usually considered as a very cumbersome process, mainly focusing on existing facilities, but for future scenarios variations are not be taken into account. Uncertainty and limitations of the various methods might be noticed by the authors, but the decision maker would rarely consider them (WG, 2011).

As renewable energy source in this thesis are mainly centralize on solar energy, wind energy and geothermal energy, detail review of LCA study of these three types were discussed below.

2.4.1 Solar energy

Olsen et al. (2013) studied the installation of photovoltaic systems in Belgium for twenty years. The results show that lifetime and solar radiation have a strong impact on global warming potential of PV systems. The PV system in Belgium has an emission of GWP as 116 g CO_2-eq per kWh, which is twice higher than a same PV system but has a lifetime of thirty years in Switzerland with 66 g CO_2-eq. Moreover, a same PV system with a lifetime of thirty years in Spain has GWP with 44 g CO_2-eq. In general, GHG emissions from crystalline PV systems are typically between 50 and 100 g CO_2-eq/kWh. Sunny areas like Spain and Italy would hold lower value of GWP than regions like Belgium, Britain, Germany.

LCA study Frischknecht et al. (2014) provides a scenario-based environmental performance information for single-Si and CdTe PV modules for European residential roofs in 2030 to 2050. Results show that the GWP of current crystalline silicon PV system are slightly higher than CdTe PV system, approximately 30 g CO_2-eq per kWh and 80 g CO_2-eq per kWh. With the adjustment of key parameters and auxiliary systems, GWP of crystalline silicon PV system could be reduced to 65% in business as usual scenario, 31% in realistic improvement scenario and 18% in optimistic improvement scenario in future. With same adjustment, GWP of CdTe PV system would be decreased to 70% in business as usual scenario, 44% in realistic improvement scenario and 32% in optimistic improvement scenario. Other environmental impacts have similar trend as greenhouse gas emissions except for human toxicity. However, the assessment of data and uncertainty is highly depended on human toxicity results (European Commission, 2010).

2.4.2 Wind energy

Wind turbines would not exhaust any greenhouse gases during operation, but significant emissions may appear in other processes such as manufacture, transport, installation and disposal. Thus, it is necessary to consider all processes in life cycle for LCA study of wind turbine (Haapala & Prempreeda, 2014). LCA study by Munir et al. (2016) analyzes the effects that changing various parts of wind turbine would bring to LCA results, such as turbine size selection, turbine technique, turbine blade orientation. Although different assumption and conditions are considered by different researches, a general result of the effect of wind turbine size changes shows that large wind turbines have lower embodied energy output and more positive environmental effects compared to small wind turbines. For the effect bring by wind turbine size variation, Kabir et al. (2012) also studied three types of PV units' performance with same power output: a 100kW wind turbine, five 20kW wind turbines and twenty 5kW wind turbines. Result shows that for 1kWh electricity generation, single 100 kW wind turbine has lower embodied energy and lower environmental emission than other two units. It also shows that five 20 kW wind

turbines are more efficient than twenty 5 kW wind turbines. For the influence of wind turbine technology, Guezuraga et al. (2011) performed LCA of a gearless turbine and a turbine with a gearbox. Result shows that with a gear box, power output increases. But, the required energy and the GHG emissions also increase. For the influence of transportation, Tremeac and Meunier (2009) did a research of how transport condition affects LCA results for wind turbines. The results show that type and transport distance are crucial factors for human health, resources and climate change. When the distance increases, the carbon dioxide emissions as well as human health effects also increases. For the same scenario, when the transport medium changes from the train to the truck, the carbon dioxide emissions and human health effects would decrease. For the influence of blade orientation, Uddin and Kumar (2014) performed a detailed LCA study of wind turbine with vertical blade and wind turbine with horizontal blade. Results suggest that the wind turbine with vertical blade has higher CO_2 and SO_4 emissions and larger GWP per functional unit than the horizontal blade wind turbine. Luckily, it is possible to reduce the negative impact by changing blade material of the wind turbine with vertical blades.

To compare solar photovoltaic and wind turbines, Greening and Azapagic (2013) evaluated the performance of small-scale wind turbines compared with grid power generation and solar photovoltaic power generation. The results point out that for the main environmental impact of unit power generation, wind turbine has lower value than the grid electricity except the loss of abiotic elements, fresh water and human toxicity. Compared to solar photovoltaic, wind turbines are more environment friendly than solar PV except fossil resource depletion, fresh water, human and terrestrial toxicity.

2.4.3 Shallow geothermal energy

Despite geothermal energy is widely considered as clean energy source, environmental effects may occur from the lifecycle process of the GSHP system such as materials, manufacturing, transportation and so on. A recent research done by Koroneos et al. (2017) quantified environmental impacts of a GSHP system in Greece over a life cycle of 25 years. Results show that the acidification effect dominates by 73.49% and greenhouse effect holds 14.54% of all assessed impacts, which are mainly imputed to the production of materials and to the operation of the system. A possible solution could be install an automatic control system, which will regulate its operating conditions but the negative is, it will decrease electric energy consumption (Koroneos et al., 2017).

Study by Ozdogan Dolcek et al. (2015) investigates the LCA performance of a vertical GSHP configuration with three boreholes, a horizontal GSHP, a special insulated single hole GSHP system, and a split natural gas air conditioning unit by using SimaPro. Heat-exchanger operation, borehole drilling, and circulation heat

pump operation are three main parameters affect GHG emissions, which amounts to savings of 10% and 19% over vertical and horizontal GSHPs. Also, the COP is a significant factor of reduce negative environmental impacts.

The LCA study by Koroneos et al (2017) quantifies the environmental impacts of a ground heat exchanger based system of the Town Hall of Pylaia in Thessaloniki, Greece. Results show that for a life cycle of 25 years, the acidification effect is the most negative environmental effect with 73.49%, which mainly composed by SO_2 as well as by NOx exhausted from the production of raw materials and the operation of the system. About 14.54% of the negative environmental effect is greenhouse effect which mainly appears from the production of raw materials and from cement. A possible solution to reduce the environmental burdens could be the installation of an automatic control system, which will regulate its operating conditions. However, this could result in the increase of electric energy consumption.

2.4.4 All electricity generation technologies

Some LCA studies for the GWP of residential PV systems and wind turbine systems compare results from a variety of renewable and non-renewable electricity production technologies. General data show that emissions in PV system are much lower than emissions from fossil fuel power generation technology. The emissions from coal-fired or gas power plant are about ten times or five times higher than from the photovoltaic system (Jaramillo et al., 2007; Viebahn et al., 2007; Weisser, 2007). Besides, wind energy and hydro would be a better energy resource than other renewable energy resources (Martinez et al., 2009; Martinez et al., 2009 b; Varun et al., 2009).

Report by WG Environmental Management & Economics (2011) show that the LCA result for different electricity generation technologies. For CO_2 emissions, result noted that Fossil-fueled electricity generation has the highest carbon footprint which mainly produced during plant operation. On the contrary, renewable energy source and nuclear generation have a low carbon footprint which mainly caused indirectly during the construction phase. Carbon dioxide emissions from biomass power plants are sometimes not considered as carbon dioxide emissions equal to carbon dioxide absorptions in the biomass growth phase. For air pollution, the results show that non-combustible renewable energy and nuclear emissions are relatively few air pollutants in the upstream and downstream processes. For fossil fuel power generation and biomass power generation, most emissions occur during the combustion phase. Most health effects are relevant with air pollutant emissions from fossil fuels and biomass. There are also health problems related to renewable energy, such as wind turbine noise.

2.4.5 Weighting method of shadow cost

As results of LCA study has varies environmental impact and negative level is hard to compare from different environmental effects, weighting of environmental impact is imperative needed.

The first weighting is made according to the CML-2 baseline method developed by Leiden University. The weighting factor indicates the contribution of a quantity of a pollutant to a given environmental impact (De Bruyn et al., 2010). For example, one kg of CH_4 is 21 times more responsible in causing global warming than one kg of CO_2. Moreover, this weighting is objective when evaluating the environmental impact (Van et al., 1997). However, the second weighting is subjective. For example, Acidification Potential is more important than Global Warming Potential, thus it weighted more money. This weighting groups different impact categories under a single indicator (Chevalerias, 2015).

The weighting system in Netherlands includes 11 impact categories. All categories have been assigned to a shadow price per unit. Figure 12 illustrates an example of the process of weighting Global Warming Potential and Acidification Potential to a shadow cost. A single environmental indicator could be calculated when summing all shadow costs up. Shadow cost is a constructed and virtual cost which represents the investment to protect the environmental (Chevalerias, 2015).

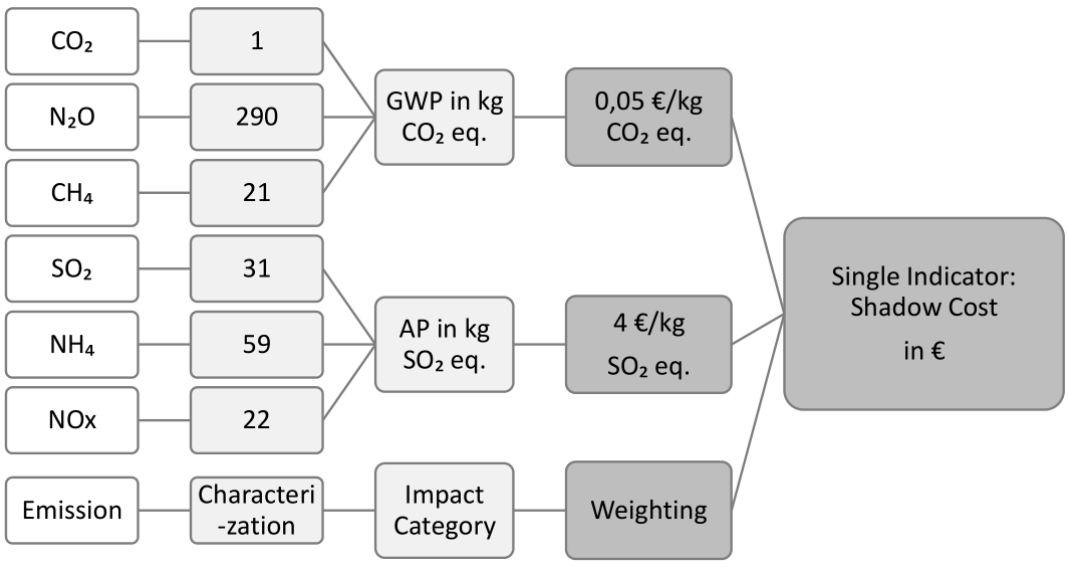

Figure 12:Workflow of weighting from different emissions to a single indicator.

3 Methodology

This chapter mainly describes the methodology applied to assess the potential of adding renewable energy resource in the campus of Lund University. Five parts are included: General information of the case study, energy consumption calculation, energy generation calculation, life cycle cost and life cycle analysis. Figure 13 shows the whole work flow for this thesis.

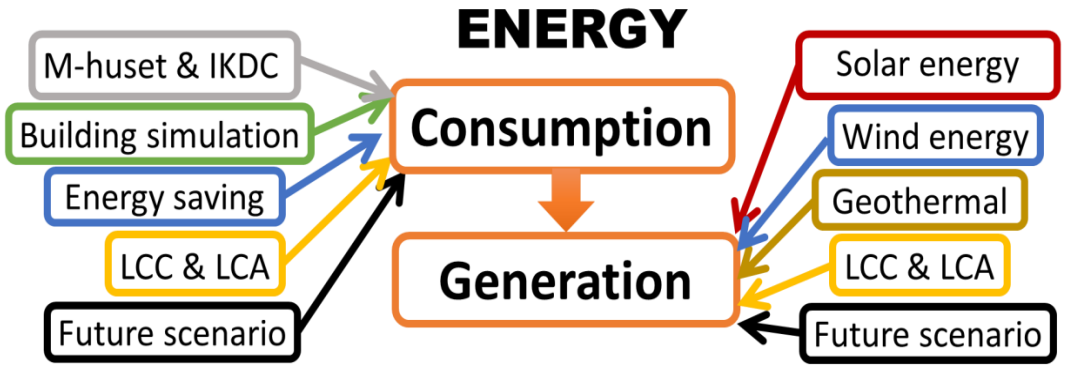

Figure 13: Work flow

3.1 General information

3.1.1 Case building description

Lund University, established in 1666, distributed throughout the centre of Lund (55.72 °N, 13.18 °E). Most of the campus buildings were built in same decades, using same construction materials and having flat roofs. In this study, the main focus of energy simulation was on two representative buildings, which were built in different decades and have different surroundings, see figure 14 green star marks. Meanwhile, the focus of assessing renewable energy potential was on whole area of Lunds Tekniska Högskola (LTH) campus, see figure 14 orange area marks. Besides, Lunds Tekniska Högskolan has developed a virtual model of whole campus and an aerial tour can be taken on the website (Lunds Tekniska Högskolan, 2017).

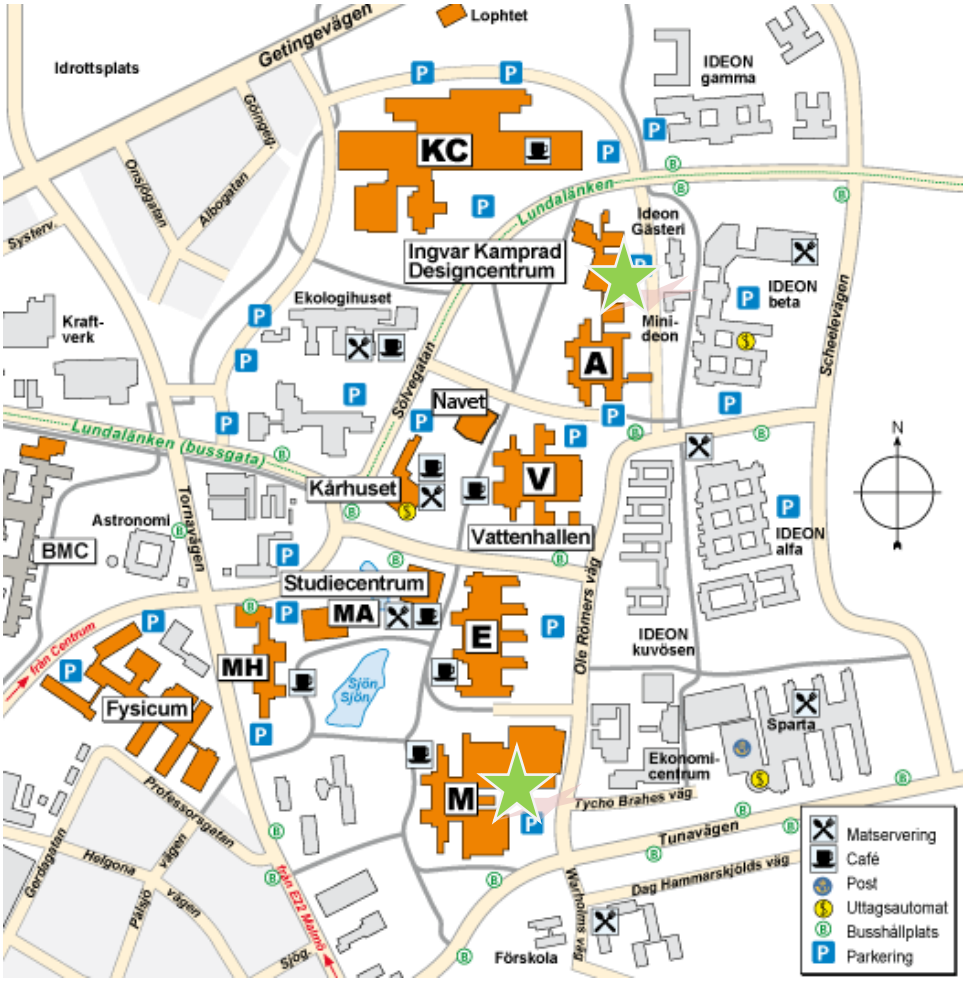

Figure 14: Map of Lunds Tekniska Högskola (LTH) campus (Lunds Tekniska Högskolan, 2017).

M-huset (see figure 15) was designed by the Swedish architect Klas Anshelm (1914-1980). Anshelm showed his talent in drawing and model building in his childhood. In 1936-1940 he went to Chalmers University studying architect (Svedberg, 2004). After he graduated from Chalmers, he was employed by Hans Westman in Lund. In 1947, he established his own office. Anshelm's largest project was the construction of Lund Tekniska Högskolan in the 1960s. The typical red brick was a signature of his work. In LTH, the mathematics building was firstly built, followed by the A-huset (School of Architecture), E-huset (Electronics techology), and M-huset (Machine Technology) (Anshelm& Qvarnström, 1998).

M-huset was located at Latitude 55.709 N, Longitude 13.211 E and 65 meters above sea level, see the lower green star in figure 14. Figure 16 below show an aerial view of the surroundings of M-huset from the virtual model of LTH. East side of the building has a large parking zone. Approximately 24 trees with average height of 6.8 meters were equally distributed in the west side along the road. The total envelope area for M-huset is 39278.6 m^2.

Figure 15: M-huset (Photo taken by author).

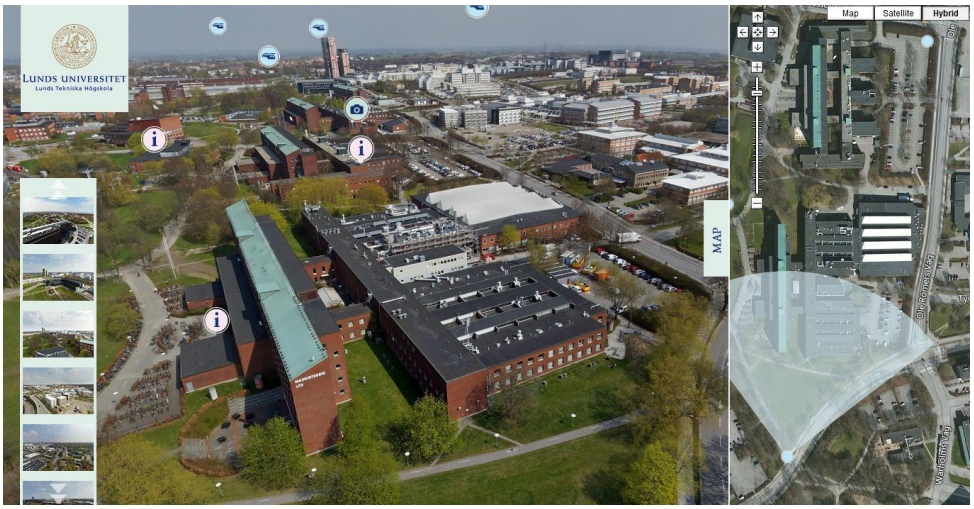

Figure 16: Aerial view of M-huset (Lund Tekniska Högskolan, 2017).

The IKDC (see figure 17) was designed by architect Gunilla Svensson who was born in the 23rd of May 1956 in Lund. Gunilla Svensson still works in Lund in her own company Gunilla Svensson Arkitektkontor AB now. The IKDC building was completed in 2002. It has been nominated for European Union Prize for contemporary Architecture (Svensson, 2017).

The IKDC is served as a design centre in Lund University. It is located at Latitude 55.715 N, Longitude 13.213 E and 74 meters above sea level, see the higher green star in figure 14. The modern construction has large window areas on the southern part (see figure 18). Meanwhile, figure 19 below shows an aerial view of the surroundings of the IKDC from the virtual model of LTH. The parking zone for the IKDC was in the east side of the building. Approximately 11 trees with average 12.7 meters was equally distributed in the west side of the building. The total envelope area of the IKDC is 13417.4 m^2.

Figure 17: IKDC (Photo from Wikimedia Commons).

Figure 18: IKDC- view outside restaurant with large windows (Photo taken by author).

Figure 19: Aerial view of IKDC (Lund Tekniska Högskolan, 2017).

3.1.2 Software

Plenty of professional software were used in this thesis for energy consumption simulation, renewable energy potential assessment, and data statistical analysis. Specifically, AutoCAD and IDA ICE were used to performing energy consumption simulation. Meanwhile, SketchUp, Rhinoceros, System Adviser Model, Autodesk Flow Design, Autodesk ECOTECT, and WRPLOT View were used for renewable energy assessing simulation. Furthermore, Excel, MATLAB, and Python were used for data statistical analysis. Detailed function descriptions of software were listed below:

For energy consumption simulation:

Autodesk AutoCAD is a 2D and 3D computer-aided-design and drafting software, which was frequently used to reveal details of constructions (AutoCAD,2017). In this thesis, provided construction plans by Akademiska Hus were in AutoCAD format.

IDA Indoor Climate and Energy is a detailed and dynamic multi-zone simulation software, which can analyze energy performance and thermal comfort (IDA ICE, 2017). The energy consumption simulation in this thesis was performed by IDA Indoor Climate and Energy.

For renewable energy potential assessment:

SketchUp is a 3D modelling software with a wide range of drawing applications and an easy-to-use interface, allowing the users to build fast 3D models (SketchUp, 2017). SketchUp was used to build target building models and surroundings in this thesis.

Rhinoceros is a commercial 3-D computer graphics and computer-aided design software using Non-Uniform Rational Basis Spline (NURBS), which are mathematical representations of 3D geometry (Rhinoceros, 2017)

Rhinoceros Plug-ins:

- **Grasshopper** is a graphic editor with 3D model integrated within Rhinoceros. Grasshopper was used as the main working interface while working with Ladybug, DIVA, and another convenient small plug-in (Grasshopper, 2017).

- **Ladybug** is an open source environmental plug-in for Grasshopper, used to create environmental-conscious building designs (Ladybug, 2017). It was mainly used for importing climate data and analyzing annual solar radiation in this thesis.

- **TT toolbox** is a tool acted on connecting Grasshopper with Microsoft Excel, which makes it convenient to import input data or export generated results of simulations.

- **DIVA** is an analysis tool integrated within both Rhinoceros and Grasshopper (DIVA-for-Rhino and DIVA-for-Grasshopper). Some software like Radiance, DAYSIM and EnergyPlus are integrated in DVIA which makes DIVA be able to do environmental evaluations such as solar irradiation, daylighting, and energy use simulation for thermal zone (Jakubiec & Reinhart, 2011).

System Advisor Model (SAM) is a performance and financial model designed for the simulation of renewable energy (System Advisor Model, 2017). The function of solar PV simulations was used in this thesis to estimate PV generation.

Autodesk Flow Design is a software which can build a virtual wind tunnel based on geometry drawings and model air flows (Autodesk Flow Design,2017).

Autodesk ECOTECT is energy simulation software which has an excellent weather analyze tool. This tool was used in this thesis to analysis wind condition in current and future climate.

WRPLOT View is a program with visual wind rose plots and frequency analysis.

For data analysis:

Microsoft Excel was used for performing theoretical calculation of PV outputs as well as assess energy and radiation simulation results, Life Circle Cost and Life Circle Analyze.

Python is a programming language which was used to transform simulation results from random sequence to ordered sequence.

3.1.3 Weather data

Weather data is a necessary element to assess the building energy performance of buildings as well as the potential of renewable energy generation. A new technique to evaluate the climate impact of building energy performance was carried out by Nik (2016). Statistical or downscaled future weather data from global dynamic climate models were used, which are from RCA3 regional climate model (RCM), downscaling climate data from several global climate models (GCMs) (Nik (2016)). RCMs provide more detailed and more precise local extreme occurrences for predictions for local events than other models.

Uncertainties of future climate data make it essential to take long-periods into consideration. Nik (2016) creates three sets of one-year weather data from RCMs for

period of thirty years. These three sets are Typical downscale year (TDY), Extreme cold year (ECY), and Extreme warm year (EWY) based on the distribution of dry bulb temperature. The generated data sets represent typical and extreme weather conditions in 30-year periods. The intension and advantage of the method is decreasing the numbers of the simulation for building impact evaluation, also providing a precise approximation of future condition.

Future weather data for period 2009-2038, 2039-2068, and 2069-2098 were used in this study for energy simulation in IDA ICE energy, solar potential simulation in DIVA for Rhino, PV output simulation in System Advisor Models, and wind analysis in WRPLOT View.

For current climate simulations, the climate data used for building energy simulations in IDA ICE as "reference year" were originally existed in IDA ICE for Malmö region, which is 18 km to Lund region. The climate data used for solar irradiation and PV generation calculation for reference year was provided by Akademiska Hus, which was made by local measures inside Lund university in 2015. For wind speed analysis, weather file for Lund, which is originally existed in Energy plus as "epw" format was used as reference.

3.2 Energy consumption calculations

The energy consumption simulation for both the IKDC and M-huset were performed in IDA ICE. Architectural drawings, realistic consumption data, and some part of input parameters were provided by Akademiska Hus in Lund. Akademiska Hus is a governmental owned company which provide construction, management, and rental service for academic facility in Sweden (Akademiskahus, 2017). The simulation process was carried out in six phases, see detailed work flow in figure 20.

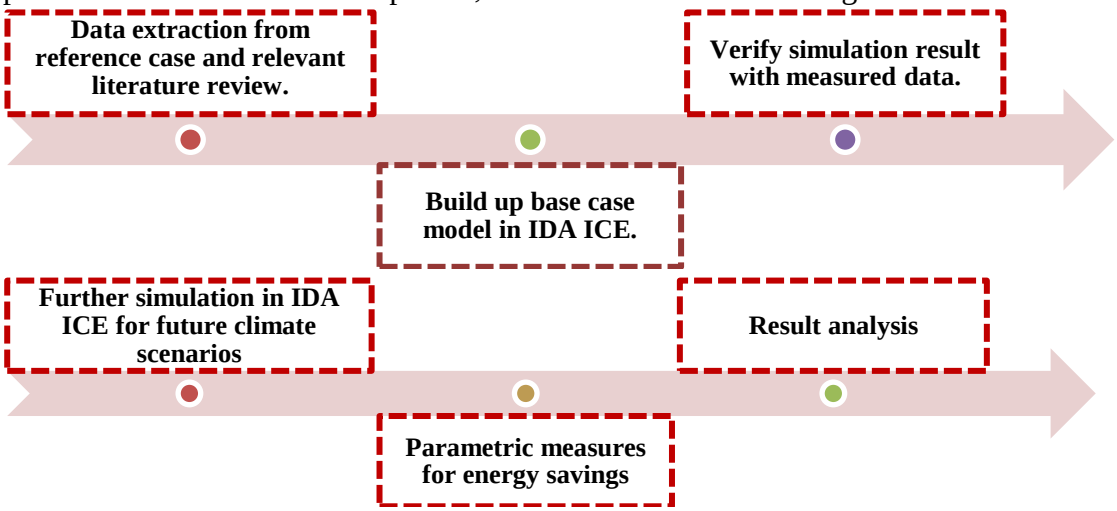

Figure 20: Energy consumption simulation work flow.

3.2.1 Model geometry

Based on the AutoCAD drawings from Akademiska Hus, both buildings were built in IDA ICE accurately as the realty. Views of IDA ICE 3D model from different angles are showed in figure 21. The left side are the views of the IKDC model and the right side are the views of M-huset model.

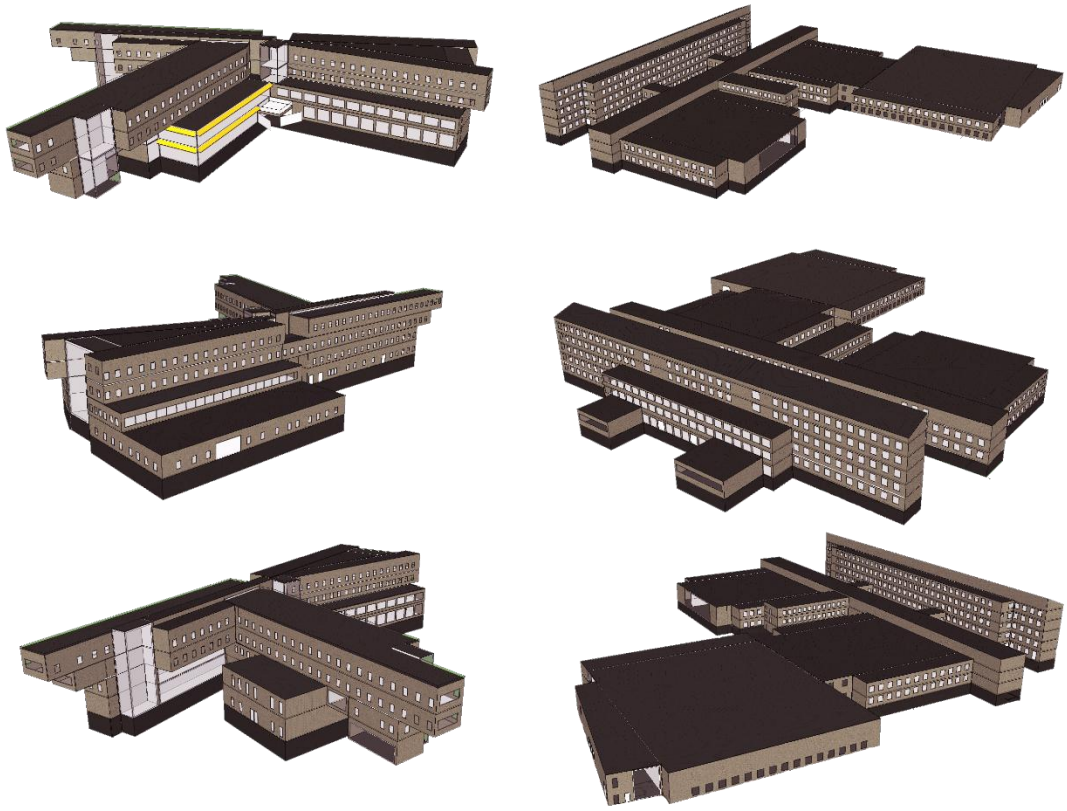

Figure 21: IDA ICE 3D model: IKDC in the left, M-huset in the right.

IKDC was divided in several zones, teacher offices, student workshop, classroom, student meeting spot, hallway, storage room, exhibition hall, kitchen area and free study meeting sport. The floor height for most zones were set as 3.48 meters according to laser measured data. Few exceptions such as the exhibition hall was set to be 6.8 meters and free study area was set to be 7.1 meters.

M-huset was also divided in several zones, Classroom, group room, laboratory, machine room, hallway, and storage room. Th floor height for each zone was set to be 3.28 meters except Laboratory was set as 6.56 meters according to laser measured data.

3.2.2 Input parameters

Although the energy simulation was implemented for the IKDC and M-huset, nevertheless, the input data received from Akademiska Hus was available for A-huset only. As M-huset was built during 1960-1969 when the A-huset was built as well, it was assumed that the architect Klas Anshelm used same materials for M-huset as the A-huset. Thus, the existing IDA ICE simulation model of the A-huset made by Nickolaj (2016) was considered as reference model for M-huset simulation. Same input data from Nickolaj's model was applied for M-huset. However, few input data were insufficient even for the A-huset model. Thus, some inputs were set by the authors based on logical assumptions for Swedish construction in the 1960s. Meanwhile, for the IKDC, as it is a modern construction which completed in 2002 and designed by architect Gunilla Svensson, it is different from other main buildings in the campus of Lund University. Thus, the input data for IKDC building was mainly assumed according to modern Swedish construction and adjusted with real measured data gathered by Akademiska Hus. Summary of received data are showed in table 9. Detail description of input parameters in IDA ICE for both buildings are described thoroughly in this chapter.

Table 9: Summary of received data from Akademiska Hus.

Data type	IKDC	M-huset
Heating consumption	Sufficient	Sufficient
Cooling consumption	Sufficient	Insufficient
Building material	Insufficient	Sufficient
Electricity	Sufficient	Sufficient
HVAC system	Insufficient	Insufficient
Heating/cooling set point	Insufficient	Insufficient
Schedule	Insufficient	Insufficient

3.2.2.1 Building envelope

As mentioned in former section, the building envelope input parameters of previous research on A-huset by Jensen (2016) were used as reference data for M-huset.

Table 10 below shows construction details of the received value for M-huset and the assumed value for the IKDC. The specific information for building envelope is in table 11. More specific detail regarding the assumption of thickness, material and thermal properties are showed in Appendix A-B.

Table 10: Construction details of the IKDC and M-huset.

Building envelope	IKDC U-value [W/ (m^2 K)]	M-huset U-value [W/(m^2 K)]
External wall	0.31	1.20
External wall below ground	0.13	0.21
Roof	0.10	0.10
External Slab	0.13	2.7

Table 11: Specific building envelope information for the IKDC and M-huset.

Building envelope	IKDC Area [m^2]	M-huset Area [m^2]
Walls above ground	3862.23	9428.70
Walls below ground	1224.56	2818.22
Roof	3240.62	12289.38

3.2.2.2 Windows

The window size and amount for both the IKDC and M-huset were set according to received AutoCAD drawing from Akademiska Hus. Same window materials were assumed for both constructions. The U-value for the window glass was assumed to be 1.3 W/(m^2K), and 2 W/(m^2K) for window frame. Regarding U-value and window area, Table 12 and table 13 below shows more details of windows in the IKDC and M-huset.

Table 12: Window details of the IKDC.

Windows	Area [m^2]	U Glass [W/ (m^2 K)]	U Frame [W/ (m^2 K)]	U Total [W/ (m^2 K)]	U*A [W/K]
N	65.55	1.30	2.00	1.37	89.81
NNE	146.86	1.30	2.00	1.37	201.19
E	217.71	1.30	2.00	1.37	298.27
ESE	22.69	1.30	2.00	1.37	31.09
S	204.68	1.30	2.00	1.37	280.42
SSW	460.04	1.30	2.00	1.37	630.26
W	259.88	1.30	2.00	1.37	356.04
WNW	376.87	1.30	2.00	1.37	516.32
Total	1754.30	1.30	2.00	1.37	2403.39

Table 13: Window details of M-huset.

Windows	Area [m^2]	U Glass [W/(m^2 K)]	U Frame [W/(m^2 K)]	U Total [W/(m^2 K)]	U*A [W/K]
N	360.70	1.30	2.00	1.37	494.16
E	714.73	1.30	2.00	1.37	979.18
S	372.49	1.30	2.00	1.37	510.31
W	962.90	1.30	2.00	1.37	1319.17
Total	2410.81	1.30	2.00	1.37	3302.81

3.2.2.3 Model infiltration

Building leakage could be model either depending on actual wind pressure or as an assumed fixed value in IDA ICE. The commonly used unit of infiltration around the world is in Air changes per hour (ACH), while sometimes l/sm^2 is also used in Sweden. The Swedish building regulation Boverkets byggregler (BBR) stipulate the average air leakage at a pressure difference of 50 Pa should not exceed 0.6 l/sm^2 (Boverket, 2015). According to this regulation, the infiltration rate in IDA ICE for both buildings was assumed as 0.6 ACH=0.542 l/ (sm^2) at the pressure difference of 50 Pa.

3.2.2.4 Interior heat gains

The internal heat gain includes three categories: lighting, equipment and occupancy. There is no specific setting information provided for each function zone in both buildings. A logical assumption of the density of lighting and equipment were set at first, and then the settings were adjusted by matching the actual measured electricity consumption with the simulation result. Besides, the occupancy level for each zone was assumed according to the numbers of tables and chairs. Table 14 below gives the adjusted settings of internal heat gains for different function zones.

Table 14: Settings of internal heat gains for different function zones.

Zone	Occupancy [NO/ m^2]	Lights [W/m^2]	Equipment [W/m^2]
Classroom	0.097	3.3	5.0
Lecture hall	0.1	3.3	7.5
Hallway	0.02	3.3	0
Corridor office	0.03	3.3	7.3
Group room	0.13	3.3	7.3
Workshop	0.08	3.3	17.7
Free study area	0.13	3.3	9.5
Storage room	0	3.3	0
Lab (small size)	0.1	5.5	22.3
Lab (middle size)	0.1	5.5	35.1
Lab (large size)	0.1	5.5	57.4
Fan room	0	3.3	19.7

3.2.2.5 Operating schedule

The schedule of occupancy, lighting, equipment, heating, cooling, and ventilation for each function zone in the IKDC and M-huset were made according to schedules for the reference model of A-huset made by Jensen (2016), which were provided by Akademiska Hus as well. In week days, office area would be occupied in the period of 08:00 until 17:00 and all other areas would be occupied during 08:00 until 20:00. All zones of the building would be considered as unoccupied during weekends and holidays. In addition, the auditoriums would be unoccupied during January and summer holidays. Details of operating schedules were given in Appendix C-D.

3.2.2.6 Indoor air quality

Detailed information of heating, ventilation and air conditioning (HVAC) settings for the IKDC and M-huset were not provided by Akademiska Hus. HVAC was then assumed as a variable air volume (VAV) system based on observation. According to the EN 15251-2007 for school buildings (Category II), the minimum ventilation rate is 7 l/s per person plus 0.35 l/s per square meter (CEN, 2007). As the total floor area for the IKDC is 11678.4 m^2 with 790 people, the minimum ventilation rate according to the criteria would be 9617.3 l/s, which is less than the assumed airflow rate in IDA ICE for the IKDC as 17400 l/s. Meanwhile, the total floor area for M-building is 28395.3 m^2 with 1792 occupancy, the minimum ventilation rate according to the criteria would be 22482.3 l/s, which is also less than the assumed airflow rate in IDA ICE for M-huset as 33700 l/s. Thus, the assumed air flow rate in IDA ICE for both building all meet the minimum requirements of the building criteria.

Following the reference model, the heating set point for both the IKDC and M-huset was set as 15 ℃, except for the lecture hall, 19 ℃ was set. Cooling set point was set to be 27 ℃ for whole building but 25 ℃ for the lecture hall. The heating/cooling set point indicate the heating/cooling system would be operating when the indoor air temperature is below 15 ℃ or 19 ℃ (heating) and 25 ℃ or 27 ℃ (cooling). Otherwise, the system would stop running for energy savings.

Information of heating and cooling energy source was provided by Akademiska Hus. In the IKDC, district heating and heating from ground source heat pump were used as heating energy sources. Cooling from ground source heat pump was used as the only cooling energy source. In M-huset, district heating is the only heating source and district cooling is the only cooling source. However, measured data of cooling consumption from district cooling is not gathered by Akademiska Hus yet.

3.2.2.7 Thermal bridges

As the IKDC is a quite new building, the thermal bridges in IDA ICE were considered as "Good", which indicate 20% of transmission losses by thermal bridges. M-huset, a slightly older building, the thermal bridges in IDA ICE were set as "typical", which indicate 30% of transmission losses by thermal bridges. See Appendix E for more details.

3.2.3 Parametric study of energy savings

This section assessed several retrofitting building technologies to reduce the energy consumption, mainly focus on adding insulation material to old walls, changing windows and frames, adjusting heating and cooling set point, applying high heat recovery rate and adding shading device. IDA ICE Model of M-huset was used as reference model. All parametric simulations were done based on the current weather condition.

3.2.3.1 Insulation

According to previous research on energy savings, using material with low U-value would be helpful for energy savings. As M-huset was completed in later 20th century when insulation material is not developed as today, its construction materials had very high U-values. In order to find out the energy consumpation that would be saved when adjusting construction material, new insulation material was added for parametric simulation process. New construction material with low U-value illustrates below in figure 22. The new construction material has the U-value of 0.103 W/ (m^2K) which is much lower compared to the old internal wall with the U-value of 2.21 W/(m^2 K).

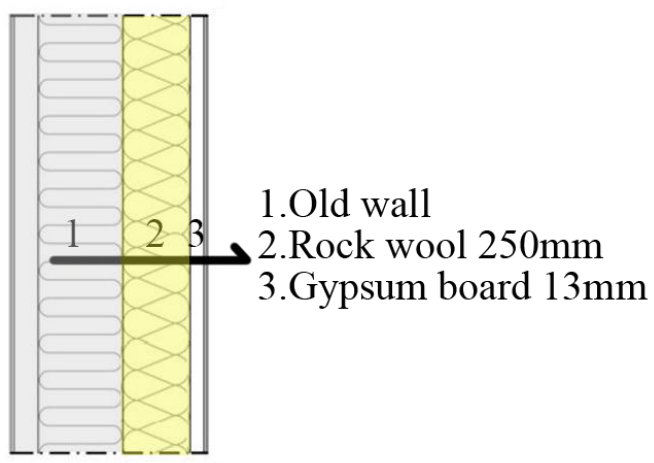

Figure 22: New construction material.

3.2.3.2 Windows

Windows is another key affecting parameter on building energy consumption. Aiming to estimate the effect of window U-value variation on energy savings, a new triple glazing window with U-value of 0.79 W/ (m^2 K) was applied for parametric simulation. For new frame (see figure 23), the wood batten inside the mineral wool layer also minimized the thermal bridge.

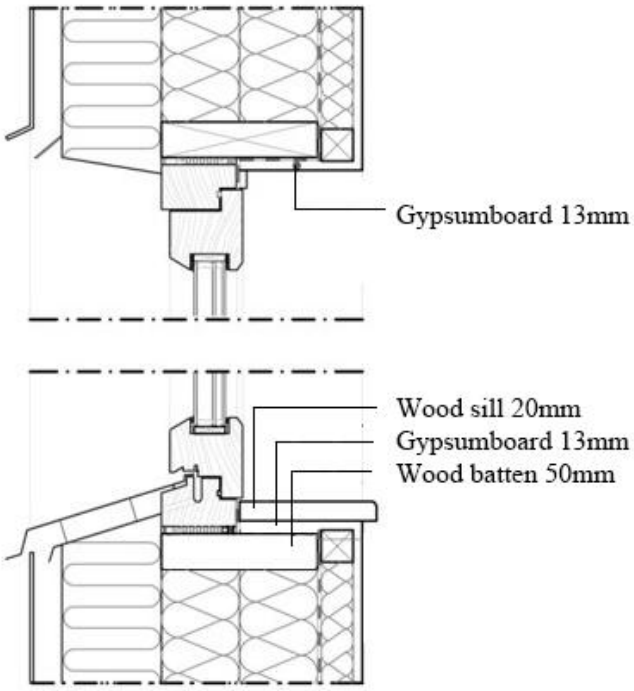

Figure 23: New window and frame.

3.2.3.3 New heating and cooling set point

The easiest way to adjust energy consumption is to change the heating and cooling set point in HVAC system. As mentioned before, the original heating and cooling set point was 15 ℃ and 27 ℃ for the whole building. In order to estimate the effect of set point variations on energy savings, heating set point was reduced to 14 ℃ and cooling set point was increased to 28 ℃ for parametric simulation. Both heating and cooling set point have 1 ℃ difference with the original case.

3.2.3.4 High efficiency heat recovery

Except change the heating and cooling set point in HVAC system, heat recovery rate in air handling unit (AHU) also affects energy consumption. Higher heat recovery rate was applied for the parametric simulation which was changed from 60% to 80%.

3.2.3.5 Shading

Although low U-value material would lower the heating demand, it would cause overheating problems. Considering reducing cooling demand, adding shading devices would be the first choice as method of passive cooling. Thus, the exterior shading "drop arm awing" has been integrated on walls in both south and west side for parametric simulation.

3.3 Energy generation calculations

Renewable energy is energy collected from renewable resource, which are naturally replenished on a human timescale (Ellabban et al., 2014). Solar, Wind, geothermal, hydropower, and biomass are the most frequently used renewable energy resources in nowadays. Considering Lund University is not near sea or river or field, potential of using hydropower and biomass power are not estimated in this study. Method of assessing the potential of adding Solar, Wind, and shallow geothermal energy resources are performed in this chapter.

3.3.1 Solar energy

3.3.1.1 Solar radiation

Solar radiation plays an important role in assessing the potential of using solar energy. Read weather file and estimate solar radiation data is the first step of the assessment. Since former researchers have done several studies for LTH campus, building geometries were already existed in SketchUp. As Ladybug and DIVA in Rhinoceros are the main tools to estimate local solar radiation, models were then exported to Rhinoceros. Ladybug was used to perform the annual solar irradiation simulations. The annual solar irradiation simulation results were used to distinguish the surfaces with large enough solar potential, to be analysed further and in more detail. In the case of possibility, roofs, facade, parking lots, green areas all have the potential to be used for installation of photovoltaic. Meanwhile, Diva for Grasshopper was used to perform the hourly solar irradiation (hourly global irradiation, hourly diffuse irradiation, and hourly direct irradiation on a horizontal plane) simulations for the surfaces with high annual solar radiation.

3.3.1.2 Surroundings

As surroundings like high-rise buildings may influence the solar potential of simulated building, all surroundings were built in SketchUp as solid geometry which have the same bottom surface outlines as Google map showed and the heights of them were measured by laser ruler on the spot. Besides, target building models were downloaded from existing SketchUp models which look as vivid as the real buildings.

3.3.1.3 Photovoltaic output calculation

This section explains the method for calculation of photovoltaic output based on solar radiation data from weather file.

3.3.1.3.1 Calculation of solar angles

As the position of sun varies from hour to hour, the global solar radiation on horizontal or incident surface will also change over time. Solar angle is an important parameter that affects photovoltaic output, which would be influenced by the hour angle ω, the declination δ, solar time, the solar azimuth γ_s, solar height α_s, and zenith angle θ_z.

The hour angle, ω, is the angular displacement of the sun, which decided by the rotation of the earth. The rotational speed is approximately 15° per hour. It is defined to be zero when solar time is at 12:00, and be positive after 12:00 solar time. The hour angle can be determined from equation 1. HH is the hour and MM is the minutes for the solar time (Duffie & Beckman, 2013).

$$\omega = ((HH - 12) + MM / 60)*15(\text{degrees}) \quad (1)$$

The declination, δ, is the angle between the sun and the equator plane. It changes from -23.45° to 23.45°, and be positive when the sun is north of the equator. The declination can be determined from equation 2 (Duffie & Beckman, 2013).

$$\delta = 23.45\sin(360(284+n)/365)\ (\text{degrees}) \quad (2)$$

n = day number during the year

Solar time is a timing method based on the position of sun. For example, when the sun directed to the south, the solar time is at 12:00. It can be calculated from equation 3 (Duffie & Beckman, 2013).

$$\text{Solar time} - \text{normal time} = 4(L_{st} - L_l) + E \quad (3)$$

$$B = 360(n-1)/365 \quad (4)$$

$$E = 229.2\,(0.000075 + 0.001868\cos(B) - 0.032077\sin(B) - 0.014615\cos(2B) - 0.04089\sin(2B)) \quad (5)$$

L_{st} = the time zone standard meridian (Sweden has L st = -15°)

L_l = the local meridian

E =”equation of time”,

n = day number of the year

Combine Eq (1), (3), (4) and (5):

$$\omega = 15*(hh-12) + (mm+E)/4 + (Lst-L_l) \text{ (degrees)} \quad (6)$$

The solar height angle α_s is the height angle of the sun which can be calculated based on the hour angle ω, the declination δ, and the latitude λ, see equation 7 (Duffie & Beckman, 2013).

$$\alpha_s = \arcsin(\cos(\delta)\cos(\omega)\cos(\lambda) + \sin(\delta)\sin(\lambda)) \quad (7)$$

The solar azimuth γ_s is the angle between the south and the projection on the ground plane of the sun which varies from -180 ° to180 ° when west is positive. It can be calculated based on equation 8a when $\omega \neq 0$, and equation 8b when $\omega=0$ (Duffie & Beckman, 2013).

$$\gamma_s = \arccos((\cos(\delta)\cos(\omega)\sin(\lambda)-\sin(\delta)\cos(\lambda))/\cos(\alpha_s))*\omega/|\omega| \quad (8a)$$

$$\gamma_s = \arccos((\cos(\delta)\sin(\lambda)-\sin(\delta)\cos(\lambda))/\cos(\alpha_s)) \quad (8b)$$

The zenith angle θ_z is the angle between solar vector and the vertical line, it is defined by equation 9 (Duffie & Beckman, 2013).

$$\theta_z = 90^o - \alpha_s \quad (9)$$

Finally, the solar angle θ, for the solar radiation on a surface was determined by parameters mentioned above, see equation 10 (Duffie & Beckman, 2013).

$$\theta = \arccos(\sin(\theta_z)\sin(\beta)\cos(\gamma_s-\gamma) + \cos(\theta_z)\cos(\beta)) \quad (10)$$

β= tilt of the surface from the horizontal, $0^o \leq \beta \leq 180^o$

γ= the rotation from south (azimuth) (west is positive), $-180^o < \gamma \leq 180^o$

3.3.1.3.2 Calculation of hourly solar irradiation on photovoltaic module.

The second step was performed based on the collected data of hourly global irradiation G_h, hourly diffuse irradiation $G_{d,h}$, and hourly direct irradiation $G_{b,h}$ on a horizontal plane from DIVA for Grasshopper. Since weather data for 2015 collected by Akademiska Hus only provided total solar irradiation of a horizontal plane (G) in Lund, diffuse solar irradiation ($G_{d,h}$) and direct irradiation $G_{b,h}$ are needed to calculate according to equation 11 and equation 12. Hourly diffuse fraction (f) was

calculated first, and later diffuse solar irradiation ($G_{d,h}$) on horizontal plane was calculated (Miguel et al., 2001).

$$f = \begin{cases} 0.995 - 0.081\,MT, MT \leq 0.21 \\ 0.724 + 2.738MT - 8.32\,MT^2 + 4.967\,MT^3, 0.21 \leq MT \leq 0.76 \\ 0.18,\ 0.76 \leq MT \end{cases} \quad (11)$$

$$Gd = f\ G \quad (12)$$

MT in equation 11 refers to the clearness index, which is calculated according to equation 13.

$$MT = G/H_0 \quad (13)$$

where H_0 denotes extra-terrestrial solar radiation.

Knowing these three values, hourly solar irradiation on the PV module can be calculated for any inclined surfaces with equation 14-16 (Duffie & Beckman, 2013).

$$G_{d,h} = G_h - G_{b,h} \quad (14)$$

$$G_{b,h} = G_{b,n} \cos(\theta_z) \quad (15)$$

$$G_b = G_{b,n} \cos(\theta) \quad (16)$$

G_b = the direct radiation towards a tilted surface

$G_{b,n}$ = the direct radiation towards a surface perpendicular to the sun

θ = angle of incidence for the direct radiation against the tilted surface

$G_{d,h}$ = diffuse radiation towards a horizontal surface

G_h = the total radiation towards a horizontal surface

$G_{b,h}$ = the direct radiation towards a horizontal surface

θ_z = angle of incidence for the radiation against a horizontal surface (zenith angle)

One model of diffuse radiation towards a tilted surface, G_d, that takes the anisotropies into account is Hays and Davies model, see equation 17 and 18 (Duffie & Beckman, 2013).

$$G_d = G_{d,h} (1 - A_i)(1+\cos(\beta))/2 + G_{d,h} A_i \cos(\theta)/\cos(\theta_z) \quad (17)$$

$$A_i = G_{b,n} / G_{o,n} \quad (18)$$

G_d = diffuse radiation towards the tilted surface (W/m^2)

β = tilt of the surface from the horizontal (°)

$G_{o,n}$ = radiation outside the atmosphere towards a surface perpendicular to the sun (W/m^2)

A_i = anisotropic-index. It refers to the measure on the transmittance of direct radiation through the atmosphere.

A simple isotropic model, where the diffuse radiation is assumed to have the same intensity from the entire sky is also possible to use, which gives in equation 19 (Duffie & Beckman, 2013).

$$G_d = G_{d,h} (1+\cos(\beta))/2 \quad (19)$$

Apart from the direct radiation G_b, and the diffuse radiation G_d, there is another radiation that reflected by ground that also radiated towards a tilted surface G_g. It can be determined using equation 20 (Duffie & Beckman, 2013).

$$G_g = \rho_g G_h (1-\cos(\beta))/2 \quad (20)$$

ρ_g = reflectance of the ground.

The total radiation towards a tilted surface is calculated using equation 21 (Duffie & Beckman, 2013).

$$G = G_b + G_d + G_g \quad (21)$$

Where G_b, G_d and G_g is determined using equation 13, 16 and17.

3.3.1.3.3 Calculation of photovoltaic generation

Durisch W has tested numbers of measurements of semi empirical efficiency models. According to the results of the research, the most suitable model that could represent all module types investigated was used to calculate PV panels' efficiency (η_{pv}), which is given in Equation 22 (Durisch et al., 2007).

$$\eta_{pv} = p[q\ G/G_o + (G/G_o)^m][1 + r\ \theta_{cell}/\theta_o + s\ AM/AM_o + (AM/AM_o)^u] \quad (22)$$

where G_o=1000 W/m^2, θ_o =25^{o}C and AM_o =1.5. Parameters p, q, r, s, m, u for different PV types were taken from Table 15 (Perera et al., 2012).

Table 15: Parameters for the efficiency model for different solar panel types (Perera et al., 2012).

	p	**q**	**r**	**s**	**m**	**u**	**h**
Monocrystalline	23.62	-0.2983	-0.09307	-0.9795	0.1912	0.9865	0.028
Polycrystalline	15.39	-0.177	-0.09736	-0.8998	0.0794	0.9324	0.026
Amorphous	36.02	-0.7576	-0.02863	-1.1432	0.6601	1.0322	0.022

AM denotes the air mass value, which can be calculated by equation 23.

$$AM = 1/\sin(\text{angle of solar and ground}) \quad (23)$$

θ_{cell} was computed using equation 24 (Durisch et al., 2007).

$$\theta_{cell} = \theta_a + h\ G \quad (24)$$

where h denotes the Ross coefficient (Table 15) and θ_a is the ambient temperature of the place PV panel installed.

Overall, the PV output was calculated based on solar radiation G, the efficiency of the PV modules η_{pv}, area of the PV modules A_{pv}, number of the PV modules N_{pv}, and the efficiency of inverter that related to the PV modules $\eta_{inverter}$ according to equation 25 (Perera et al., 2012).

$$P_{PV} = G\ \eta_{pv}\ A_{pv}\ N_{pv}\ \eta_{inverter} \quad (25)$$

3.3.1.3.4 Simulation in SAM

M-huset, one of modelled building in LTH, has installed efficient PV panels in 2014 (figure 24). MonoX Neon PV panels were used, which are from LG, Europe's largest facility with high-efficiency panels. Ten inverters from Fronius SYMO were used. With total area of 1050 m^2, the estimated peak power was about 191 kWp and annual production was approximately 182,000 kWh. Based on outdoor temperature, solar radiation, and PV output in 2015 recorded by Akademiska Hus, PV panel

simulation was run in System Advisor Model (SAM). In SAM model, all input datas such as module type, inverter type, which were exactly the same as which M-huset has installed. Also, losses of electricity generation were adjusted based on real PV output data. This model was then used for parametric study.

Figure 24: The wing-room of M-huset that installed PV panels.

3.3.1.3.5 Parametric study of optimization proposal

The next step was to find the optimization proposal of install PVs in high radiation areas. Parametric studies were done for module titled angels (0^o-90^o), module types (Monocrystalline, Polycrystalline, and Amorphous), coverage proportion of electricity consumption in case building (Covering whole consumption in May when both radiation and consumption are high; Covering whole consumption in December when radiation is lowest in the year), and future scenarios (2009-2098). The annual and hourly generation of PVs was processed and plotted against the IDA ICE modelled electricity consumption of M-huset.

3.3.2 Wind energy

3.3.2.1 Local wind analysis

To analyse the wind variation in Lund, the wind rose in ECOTECT weather tool was used to estimate the distribution of wind speed and direction. Also, histogram of wind frequency distribution in the reference year was generated in WRPLOT View.

3.3.2.2 Wind turbine modeling

The potential of wind energy is assessed by the wind accessibility, machine power and respond capability of turbine to wind variation. From statistically neutral view, wind speed has a logarithmic relationship with height in the surface layer (Sahin AD, 2004). Hourly wind speed data given by weather file was measured at anemometer height of 10 m, which was used to calculate wind speed at hub level by equation 26.

$$V/U = (Z_{hub} /Z_{ane})^{\alpha} \quad (26)$$

Where V refer to wind speeds at hub level height Z_{hub}, U refer to wind speeds at anemometer height $Z_{ane,}$ and α is the power law exponent (Petersen EL, 1998).

For space limitation in campus, big scale wind turbine is not available to install inside campus. Thus, small scale wind turbines were taken into comparison of different rated power wind turbines and estimation of wind potential. Three wind turbines with vertical blades and two wind turbines with horizontal blades from Aeolos Company were chosen in this study, appearance can be seen in figure 25. Meanwhile, characteristics of them are listed in table 16.

Figure 25: Appearance of small scale wind turbine. Left: Aeolos V-3kW; Middle: Aeolos V-5 / 10kW; Right: Aeolos H-10 / 20kW (Pictures are from product catalog).

Table 16: Characteristic of wind turbine from Aeolos.

Type	Aeolos V-3kW	Aeolos V-5kW	Aeolos V-10kW	Aeolos H-10kW	Aeolos H-20kW
Blade direction	Vertical	Vertical	Vertical	Horizontal	Horizontal
Rotor height [m]	3.0	5.3	5.3	-	-
Rotor width [m]	2.4	4.2	4.2	-	-
Rotor diameter [m]	-	-	-	8	10
Rated power w	3000	5000	10000	10000	20000
Cut in wind speed / m/s	2.5	2.5	2.5	2.5	3.0
Rated wind speed / m/s	10.0	10.0	12.0	10.0	11.5
Noise Level / dB(A)	<45	<45	<45	<55 (10m from tower); <47 (50m from tower)	<60

As power variation of different wind turbine has different relationship with wind speed, it is hard to run generic simulations for all wind turbines. Power- Wind speed diagram from product catalogue for different products were used for individualized but representative simulations. However, function of the Power-Wind speed diagram is not mentioned in catalogue. Hence, fitting function for the diagram which auto generated by Excel were used for calculation, details of how fitting function matches with the Power- Wind speed diagram can be found in Appendix H.

3.3.3 Shallow geothermal energy

3.3.3.1 Geology and hydrogeology condition

Swedish geology is composed by the massive Baltic shield, crystalline eruptive and metamorphic rocks. Sedimentary rock formations of significant thickness are found in southern part of Sweden. Also, porous sandstones with excellent hydraulic properties are found at considerable depth. The geothermal gradient is about 28-30 ^{o}C/km and bedrock is covered by glacial deposits. Granites and gneisses form crystalline rocks, which are stable for drilling and have low yield of groundwater. Thus, drilling holes down to 200-300 m would not have technical problems.

Undisturbed ground temperature varies between 8-9 ºC in southern part of Sweden. Besides, a few large aquifers are also found in the sedimentary rocks, especially younger sandstone and limestone (Gehlin & Andersson, 2016).

3.3.3.2 Existing system

The ground source heat pump system already installed in the Centre for Chemistry and Chemical Engineering (Kemicentrum) inside LTH campus, has 166 bedrock wells with depth of 230 meters and located five meters apart. As well as 38 kilometres of pipes filled with liquid containing 28% alcohol. See service room appearance in figure 26, principle drawing in figure 27 and wells location in figure 28. It is one of Europe's largest ground source heat pump system. The system provides cooling and heating for the Kemicentrum and the IKDC during summer and winter. Also, it provides heating for A-huset in winter. The GHSP system is capable to produce 1.8 MWh/year, which is enough to satisfy the heating demand of 360 single-family houses approximately.

The same type of ground source heat pump system was installed in Lund Observatory (Astronomihuset) with 20 wells and 120 kW heat output, as well as the Centre for Languages and Literature (Språk- och litteraturcentrum) with 33 wells and 600 kW heat output.

Figure 26: Appearance of ground source heat pump service room in LTH campus (Picture were taken by Akademiska Hus).

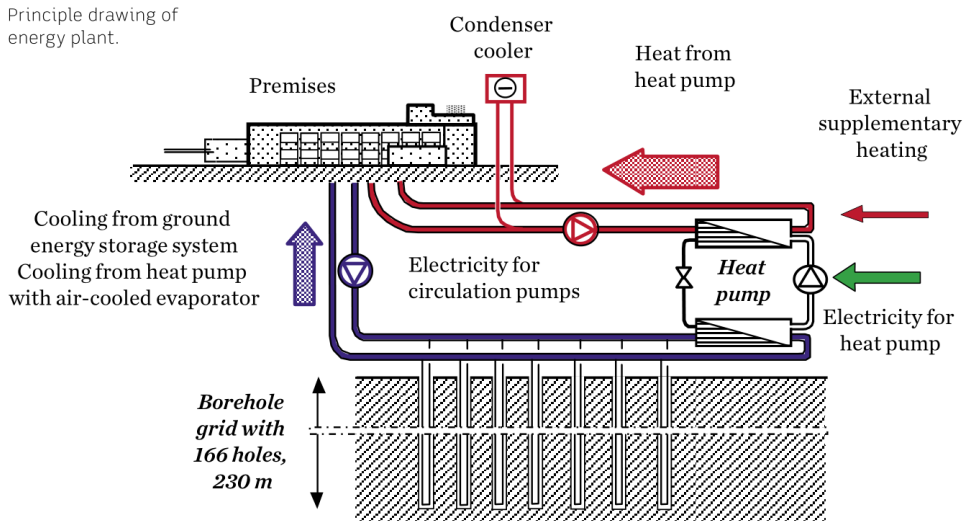

Figure 27: Principle drawing of ground source heat pump in LTH campus (Picture were provided by Akademiska Hus).

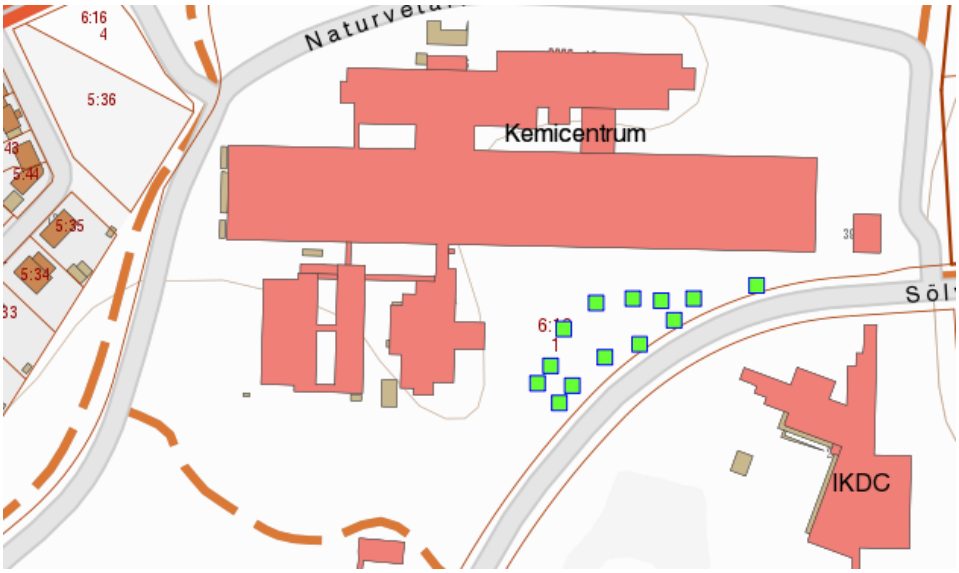

Figure 28: Boreholes in the LTH campus (Mapped by Geological Survey of Sweden (SGU).

3.3.3.3 Shallow geothermal potential estimation

Shallow geothermal potential Q_{BHE} could be estimated by a certain geothermal borehole heat exchanger. The ground energy could be sustainable, without excessive cooling or heating of the heat carrier fluid. G.POT method offers an empiric function for the calculation of Q_{BHE} based on several parameters: thermal conductivity (λ),

thermal capacity (ρ_c), undisturbed ground temperature (T_0); borehole depth (L), borehole radius (r_b), thermal resistance (R_b), minimum (or maximum) temperature of the carrier fluid during heating (or cooling) mode (T_{lim}), length of heating (or cooling) season (t_c), and simulation time (t_s) (Casasso & Sethi, 2016).

At the same time, as this method is a simplified model, several assumptions were made. First, the ground is uniform and the system's thermal load is the annual periodic with an emi-sinusoidal profile. Second, the BHE is modelled as a linear heat source with infinite length, in other words, the heat flux is purely radial (Carslaw and Jaeger, 1959); Third, for the heat transfer, the borehole resistance model made by Claesson and Eskilson (1988) was used. Finally, the minimum (or maximum for cooling mode) temperature of the carrier fluid is considered to be equal to T_{lim} (Casasso & Sethi, 2016).

Based on the aforementioned parameters and assumptions, the shallow geothermal potential Q_{BHE} was estimated by equation 27:

$$\overline{Q_{BHE}} = \frac{a\cdot(T_0 - T_{lim})\cdot\lambda\cdot L\cdot t_c'}{-0.619t_c'\cdot ln(u_s') + (0.532t_c' - 0.962)\cdot ln(u_c') - 0.455t_c' - 1.619 + 4\pi\lambda R_b} \quad (27)$$

where a=8 if Q_{BHE} is expressed in W, or a=0.0701 if Q_{BHE} is expressed in MWh/y. $u_s' = \rho_c\ r_b^2 / 4\ \lambda\ t_s$, $u_c' = \rho_c\ r_b^2 / 4\ \lambda\ t_s$, and $t_c' = t_c / t_y$, t_y is the length of the year (Casasso & Sethi, 2016).

3.3.3.4 Parametric study of assessing shallow geothermal potential.

Parametric study of how different parameter affects shallow geothermal potential was down by using G.POT method and changing relevant parameters:

Ground: thermal conductivity (λ), thermal capacity (ρc),

Borehole: borehole depth (L), borehole radius (rb),

Time: length of heating (or cooling) season (tc), simulation time (ts).

Detail values of the parameters could be found in table 17. All parametric simulations are based on a reference case which is most similar to the geothermal condition in Lund, which are also listed in table 17.

Table 17: Values of the parameters adopted in parametric study.

Parameter	Symbol	Unit	Range of variation	Step	Base case
Thermal conductivity of the ground	λ	W/mk	1.0-4.0	0.5	3.5
Thermal capacity of the ground	ρ_c	10^6J/m^{3}k	1.0-4.0	0.5	2.16
Borehole length	L	m	100-300	50	230
Borehole radius	r_b	m	0.05-0.25	0.05	0.11
Length of the heating/cooling season	t_c	day	30-240	60	180
Simulation time	t_s	year	10-100	10	25

3.4 Life cycle cost

A lot of assumptions on energy price growth rates, discount interest rates, and inflation rates were made for the complex actual situation. A parametric study on these uncertain parameters was carried out for the simulation of already installed PV panels in M-huset. A realistic scenario was chosen as assumptions for further LCC calculation of wall insulation changes, window changes, PV panels and wind turbines, with 1 % energy price growth, 2 % interest and 2 %inflation rate.

Although changing wall insulation and window are significant in reduce energy consumptions, it may have a negative economic effect. Thus, Life cycle cost was carried out by using geometric gradient equation 28.

$$\mathrm{NPV} = \begin{cases} \frac{A_1\left[1-(1+g)^N(1+i)^{-N}\right]}{i-g} \\ A_1\left(\frac{N}{1+i}\right), if\ i = g \end{cases} \quad (28)$$

Where i refers to interest rate, g refers to inflation rate, and A_1 refers to the annual payment at first year.

Also, different simulated PV systems have viable profits. Thus, a Life cycle cost was carried out. LCC s for diverse ways to calculate the inverter change was also carried out. Since the selected inverters had a warranty of ten years (Schneider Electric, 2016), where the solar panels had a warranty of 25 years, the inverters needed to be changed twice during the calculation period. Besides, LCC of wind turbines were performed using same method as PV panels.

All inputs value of investments of changing walls, windows, PVs, and wind turbines are listed in table 19, which are market price available until April of 2017. In this

study, labor cost, transportation cost and operating cost were not taken into consideration. Assumptions of Energy price are listed in table 19.

Table 18: Summary of investment price.

Type		Cost	Waranty /years	Amount	Exchange rate	total cost/SEK
Wall	Minal wool	311 kr/m^2	20	9429 m^2	1.00	2932326
	Gypsum board	103 kr/m^2	20	9429 m^2	1.00	971156
Window		4824 kr/m^2	20	2411 m^2	1.00	11629747
PV	LG 295 N1W B3	$486.75	25	640	8.97	2794552
Inverter	Fronius Symo Lite 12.0-3	$3,599	10	14	8.97	451998
Wind turbine	Aeolos-V 3000w	£ 7063.14	20	1	11.28	79657
	Aeolos-V 5000w	£ 10467.6	20	1	11.28	118053
	Aeolos-H 10000w	$27420	20	1	8.80	241296
	Aeolos-H 20000w	$35800	20	1	8.80	315040

Table 19: Energy price assumed data.

Market price	energy tax (e.t.)	other	total excl. VAT	VAT	total incl. VAT
kr/kWh	kr/kWh	kr/kWh	kr/kWh	%	kr/kWh
0.5	0.293	0.18	0.973	0.25	1.216

3.5 Life cycle assessment

The goal of the LCA analysis was to compare environmental impact from insulation material (rock wool) with different thickness for M-huset. The scope was limited to estimation of global warming potential (GWP), eutrophication potential (EP), acidification potential (AP), ozone depletion potential (ODP), photochemical ozone creation potential (POCP), human toxicity (HH), Depletion of abiotic resources - elements, ultimate reserves (ADPE), Depletion of abiotic resources - fossil fuels (ADPF), Freshwater aquatic ecotoxicity (FAETP), Marine aquatic ecotoxicity (MAETP), and Terrestrial ecotoxicity (TETP). Functional Unit is an environmental impact of rock wool for M-huset having area of 9428.7 m^2. Building lifespan was considered to be 50 years. System boundary is defined as cradle to gate, insulation

materials and energy use the usage phase was considered. Wastes decomposing or re-use of materials after the operational phase are not included. Open LCA software with "elcd_3_1.zolca" regional for Europe database was used for inventory analysis. Energy consumption of M-huset from IDA ICE was applied, see table 20. Flows presenting insulation materials and yearly energy consumption were set as an input data. As an output, emissions and wastes when produce insulation of different thicknesses and energy were received.

Table 20 Energy consumption of M-huset from IDA ICE for insulation materials with different thickness.

Thickness [mm]	U-value [W/m²K]	Heating consumption [kWh]
50	0.327	1995721
150	0.1614	1933215
250	0.103	1907702
350	0.087	1891171
450	0.0705	1894988

Afterwards, impact categories were weighted according to Dutch weighting system, where different emissions are converted to a single indicator in €, see table 21.

Table 21*: Weighting of impact categories.*

Environmental Impact Category	Unit	Shadow price/unit	Source
Abiotic Depletion Potential for Non-fossils resources(ADPE)	kg Sb eq.	€ 0.16	TNO
Abiotic Depletion Potential for Fossils resources (ADPF)	kg Sb eq.	€ 0.16	TNO
Global Warming Potential for 100 years(GWP100)	kg CO_2 eq.	€ 0.05	CE
Ozone Depletion Potential (ODP)	kg CFC-11 eq.	€ 30	CE
Photochemical Oxidant Creation Potential (POCP)	kg C_2H_2 eq.	€ 2	CE
Acidification Potential (AP)	SO_4	€ 4	CE
Eutrophication Potential (EP)	kg PO_4 eq.	€ 9	CE
Human Toxicity Potential (HTP)	kg 1,4-DB eq.	€ 0.09	TNO
Fresh water Aquatic EcoToxicity Potential (FAETP)	kg 1,4-DB eq.	€ 0.03	TNO
Marine Aquatic EcoToxicity Potential (MAETP)	kg 1,4-DB eq.	€ 0.00	TNO
Terrestrial EcoToxicity Potential (TETP)	kg 1,4-DB eq.	€ 0.06	TNO

As the process of using renewable energy have substantial number of environmental influencing factors, the LCA method mentioned above could not be simply appiled. Thus, the LCA of renewable energy is not discussed in this case study.

4 Results

4.1 Energy consumption calculations

This chapter shows results received from IDA ICA simulation of energy consumption for the IKDC and M-huset in current climate and future climate. Parametric simulations for assessing energy saving measures are showed as well.

4.1.1 Current climate scenario

4.1.1.1 Reference case simulation

Summary of measured energy consumption data received from Akademiska Hus and simulated energy consumption data gathered from IDA ICE for the IKDC and M-huset are showed in figure 29. As cooling is not installed inside M-huset yet, it is not taken into comparison for M-huset. From the comparison for heating demand, cooling demand and electricity consumption, the simulated data all have approximately 1%-3% difference from the measured data for both buildings. This indicates that simulation models in IDA ICE share the same condition as reality. Thus, this two simulation models in IDA ICE is defined as reference case for both buildings. Besides, when comparing unit energy consumptions for reference case, M-huset has heating demand and electricity demand as 79.8 kWh/m^2 year and 79.6 kWh/m^2 year, which is about 20% and 12% higher than the IKDC with 66.3 kWh/m^2 year and 71.8 kWh/m^2 year respectively. Moreover, cumulative hourly energy consumption simulation results in IDA ICE for the IKDC in reference case is showed in figure 30 for and figure 31 for M-huset, which are mainly used as reference data for further simulation.

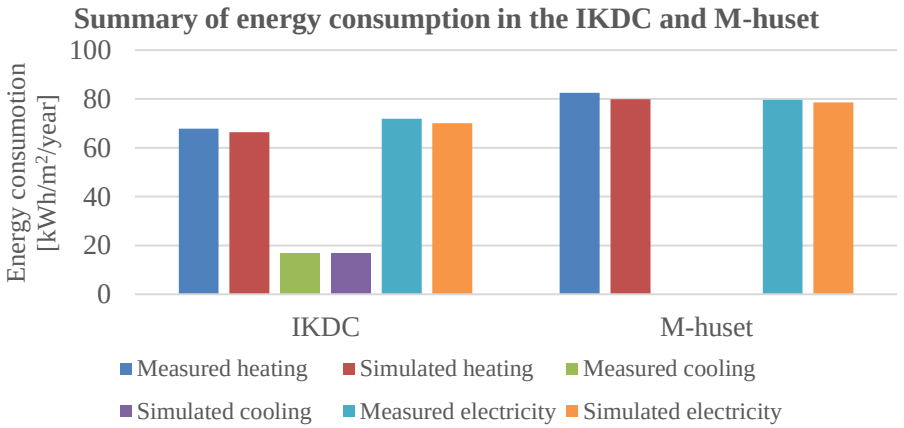

Figure 29: Summary of energy consumption in the IKDC and M-huset.

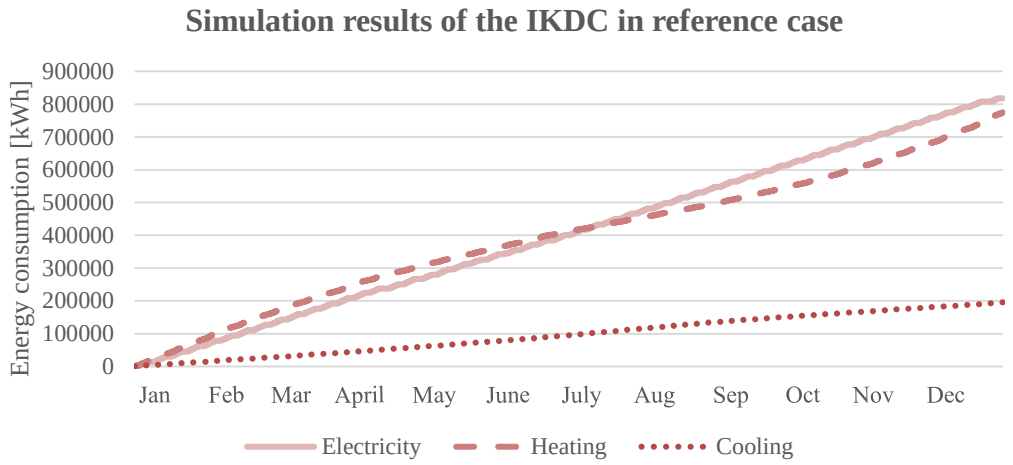

Figure 30: Simulation result in IDA ICE for the IKDC in reference case.

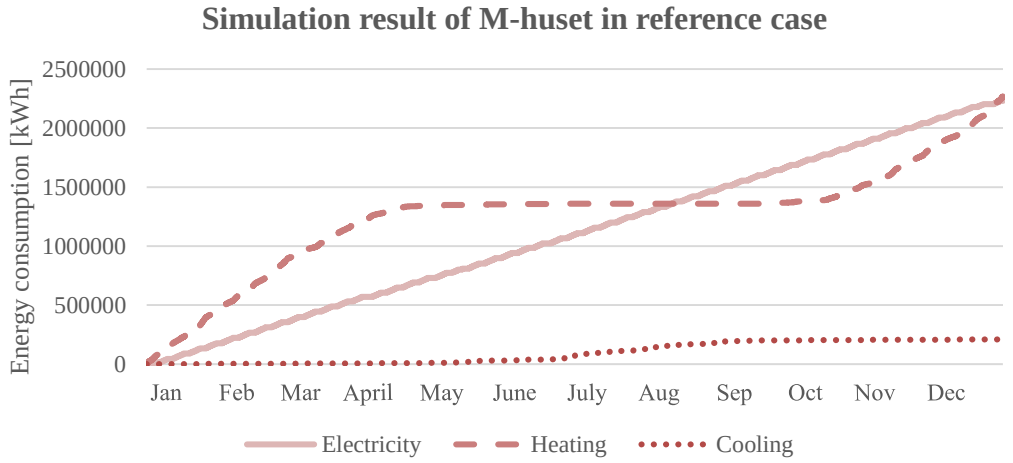

Figure 31: Simulation result in IDA ICE of M-huset in reference case.

4.1.1.2 Parametric simulation for energy savings

This section shows results of applying several energy saving measures on M-huset in IDA ICE, including adding insulation material to old walls, changing windows and frames, adjusting heating and cooling set point, applying high heat recovery rate, and adding shading device.

For construction retrofitting, figure 32 shows changes in cumulative hourly energy demand after adding insulation material to old walls. The annual heating demand reduced by 16% than reference case as it decreased from 2267501 kWh/year to

1907702 kWh/year. Annual cooling demand increased by 4.8% than reference case as it increased from 209432 kWh/year to 219410 kWh/year. Figure 33 showed cumulative hourly energy consumption variations when using new windows and frames. The annual heating demand reduced by 9% than reference case, which decreased from 2267501 kWh/year to 2077739 kWh/year. However, the annual cooling demand increased by 8% than reference case, which increased from 209432 kWh/year to 226850 kWh/year.

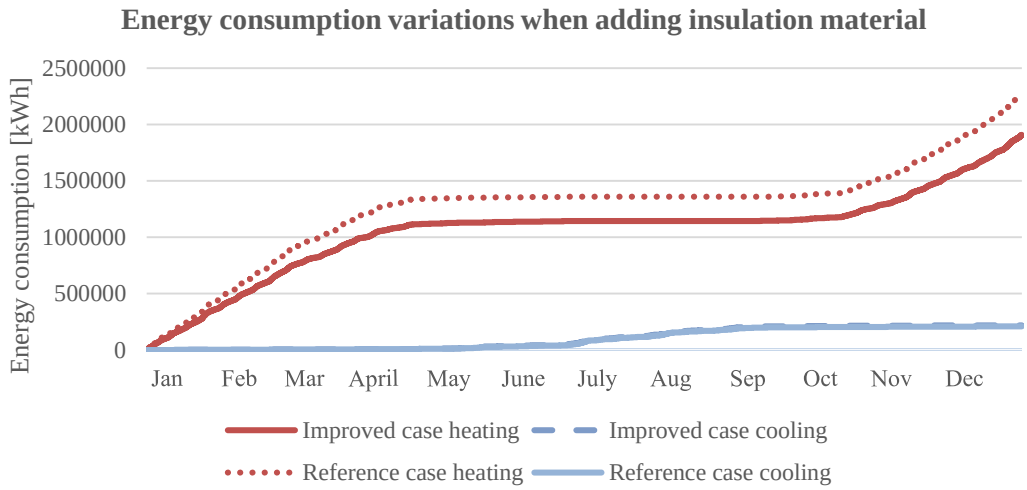

Figure 32: Energy consumption variations when adding insulation material to old walls.

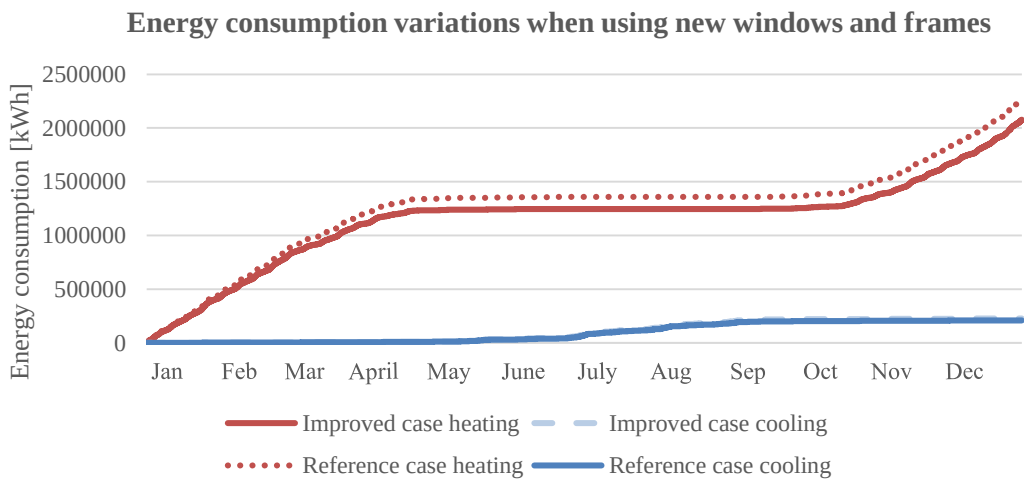

Figure 33: Energy consumption variations when using new windows and frames.

For HVAC systems, figure 34 shows the cumulative hourly energy consumption changes after adjusting heating and cooling set point. Both heating and cooling set point for the improved case have 1 ℃ difference with the reference case. The annual heating consumption reduced by 20% from 2267501 kWh/year to 1814001 kWh/year. And annual cooling consumption reduced by 28% from 209432 kWh/year to 151629 kWh/year. Figure 35 shows the cumulative hourly energy consumption changes after high-efficient heat recovery applied. When the heat recovery rate was changed from 60% to 80%, the annual heating consumption reduced by 21% from 2267501 kWh/year to 1799157 kWh/year and annual cooling consumption unvaried.

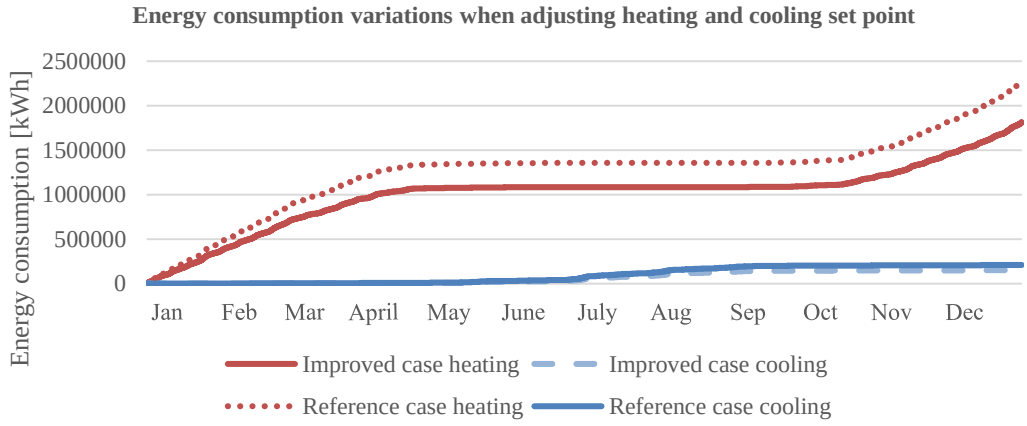

Figure 34: Energy consumption variations when adjusting heating and cooling set point.

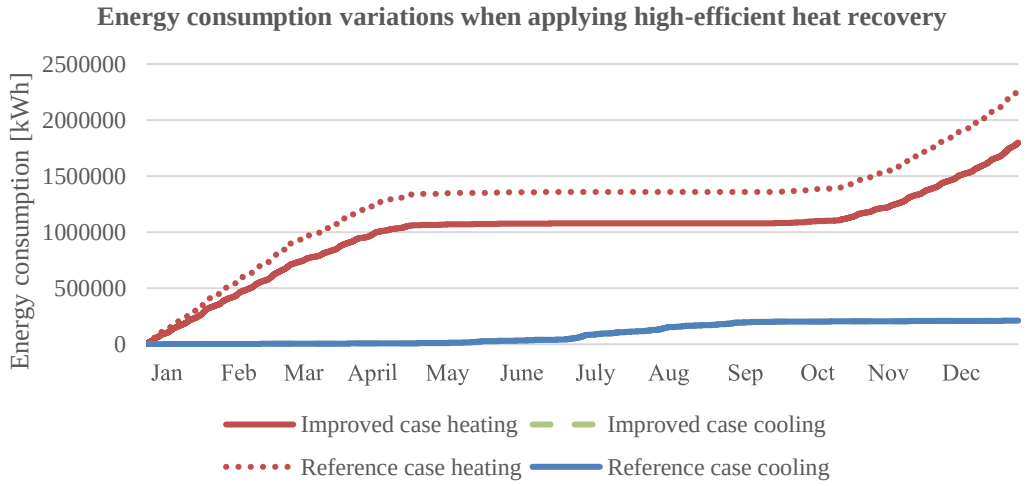

Figure 35: Energy consumption variations when applying high-efficient heat recovery.

For cooling energy saving, figure 36 showed the cumulative hourly energy consumption variations after adding more shading device on walls in south and west side. The annual heating consumption increase by 2.6 % from 2267501 kWh/year to 2327362 kWh/year but the annual cooling consumption decreased by 20% from 209432 kWh/year to 168825 kWh/year.

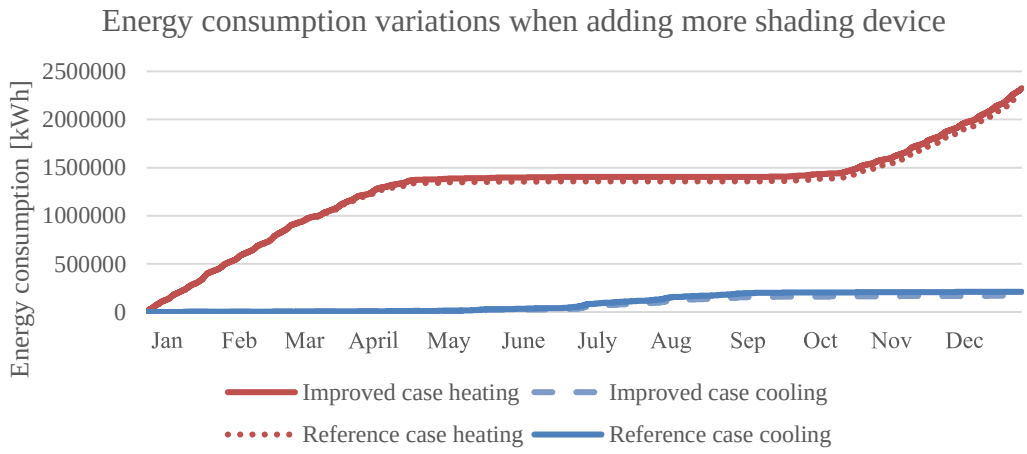

Figure 36: Energy consumption variations when adding more shading device.

When applying all five measures together for M-huset, the cumulative hourly heating and cooling consumption variations shows in figure 37 below. The annual heating consumption reduced by 27% from 2267501 kWh/year to 1662628 kWh/year and cooling consumption reduced by 12% from 209432 kWh/year to 184306 kWh/year.

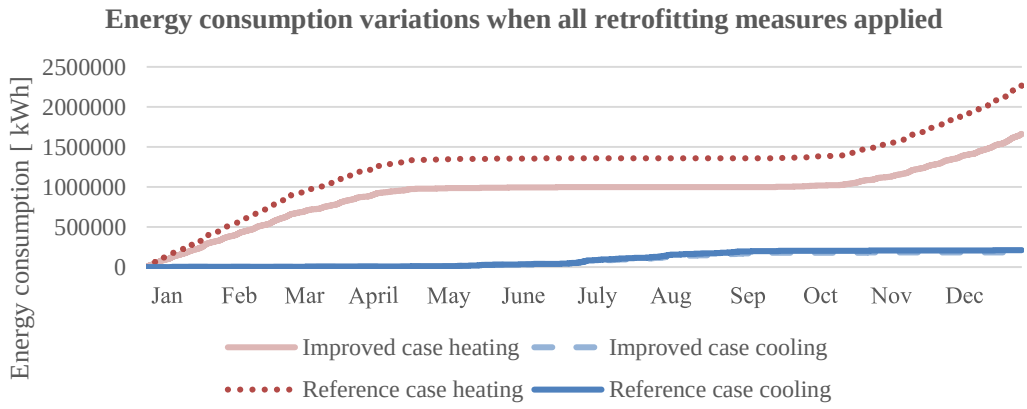

Figure 37: Energy consumption variations when all retrofitting measures applied.

4.1.2 Future climate scenario

For future climate scenario, weather files for typical downscale year (TDY), extremely cold year (ECY), and extremely warm year (EWY) for period 2009-2038, 2039-2068 and 2069-2098 were applied for simulations in IDA ICE for the IKDC and M-huset. Simulation results of TDY scenarios during 2009-2098 for both buildings as well as the energy consumption variations between TDY, ECY and EWY scenarios are showed in this section. As ECY and EMY scenarios are theoretical boundaries which would not happen in real life, detailed simulation result of this two scenarios during 2009-2098 are listed in Appendix F.

4.1.2.1 Heating demand and load variations

The heating energy simulation results received from IDA ICE for the IKDC under typical downscale year (TDY) scenario are showed in figure 38. The annual heating demand decreased by 4.5% from the first 30 year' periods (2009-2038) to the second 30 years' period (2039-2068). 5.8% decreased from the second 30 year' periods (2038-2069) to the third 30 year' periods (2069-2098). Meanwhile, heating load has a decreasing trend as time goes by in TDY scenario, see figure 39.

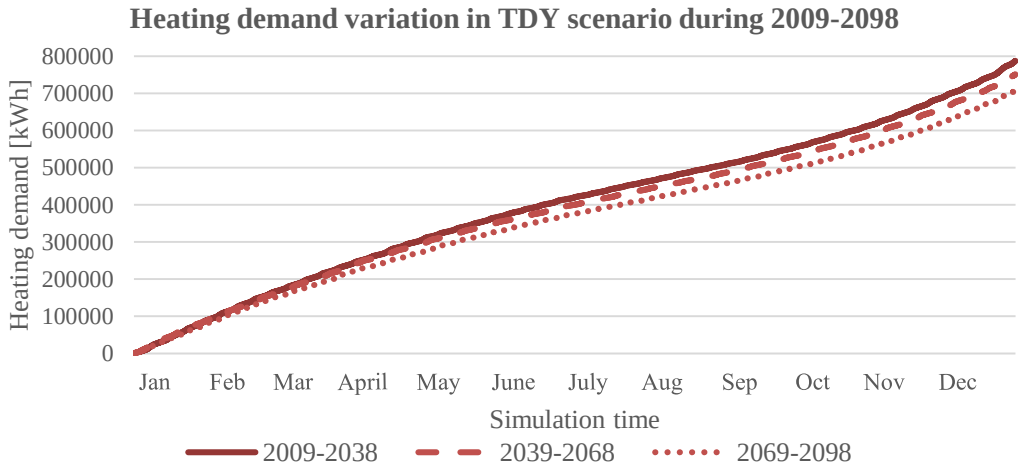

Figure 38: Heating demand variation of the IKDC in TDY scenario during 2009-2098.

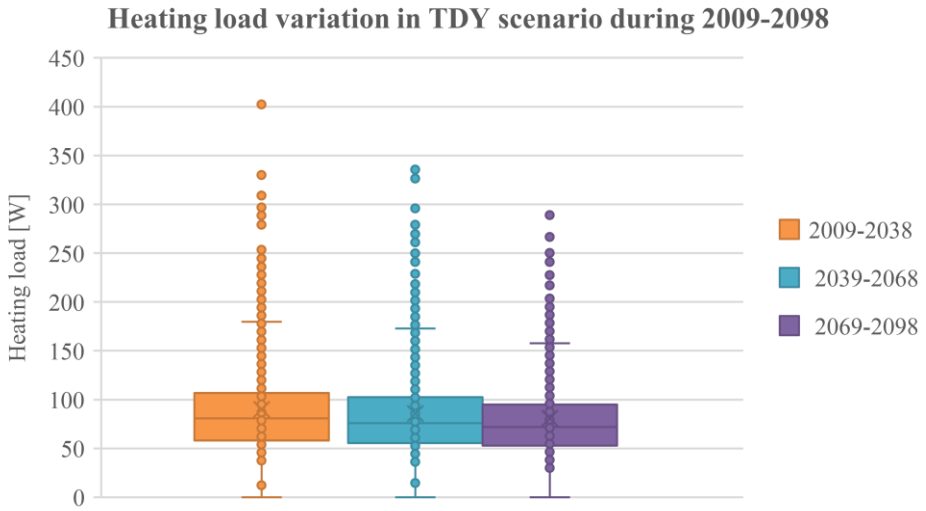

Figure 39: Heating load variation of the IKDC in TDY scenario during 2009-2098.

Heating demand and heating load variations of the IKDC in TDY, ECY and EWY scenarios during 2009-2038 are showed in figure 40 and figure 41 respectively. Both heating demand and heating load in TDY scenario all have the value between other two scenarios. Also, in figure 41, the series called Triple is a combination of heating load result in TDY, ECY and EWY scenarios. The similar result Triple series has as TDY series indicates that TDY scenario has its representativeness for the future heating energy consumption variations in the IKDC.

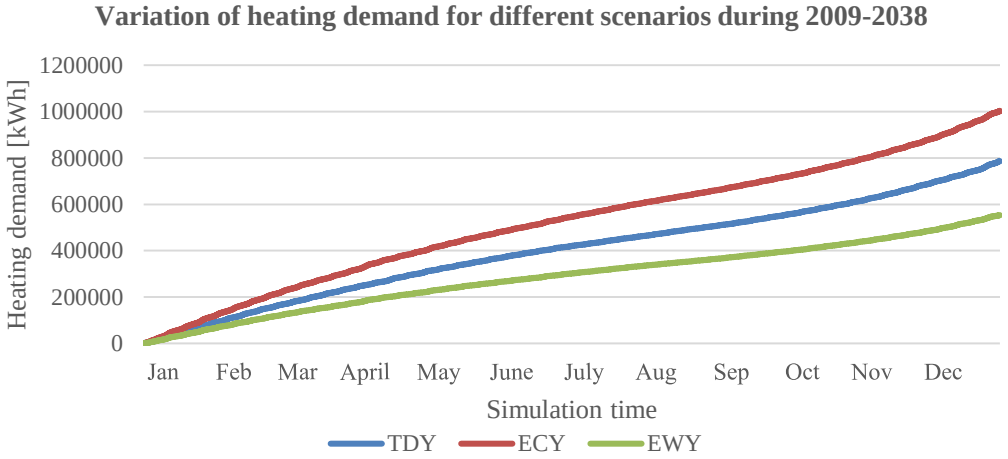

Figure 40: Heating demand variation of the IKDC in TDY, ECY, and EWY scenarios during 2009-2038.

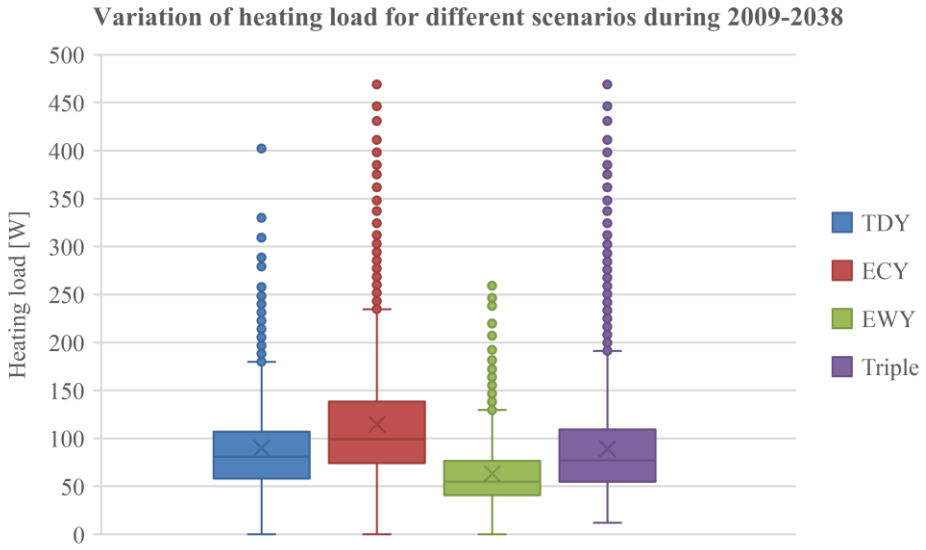

Figure 41: Heating load variation of the IKDC in TDY, ECY, and EWY scenarios during 2009-2038.

The heating energy simulation results received from IDA ICE for M-huset under typical downscale year (TDY) are showed in figure 42. It indicates that the annual heating demand decreased by 7% from the first 30 year' periods (2009-2038) to the second 30 years' period (2039-2068). 12% decreased from the second 30 year' periods (2038-2069) to the third 30 year' periods (2069-2098). Same as heating load variations in the IKDC, heating load in M-huset also has a decreasing trend as time goes by in TDY scenario, see figure 43.

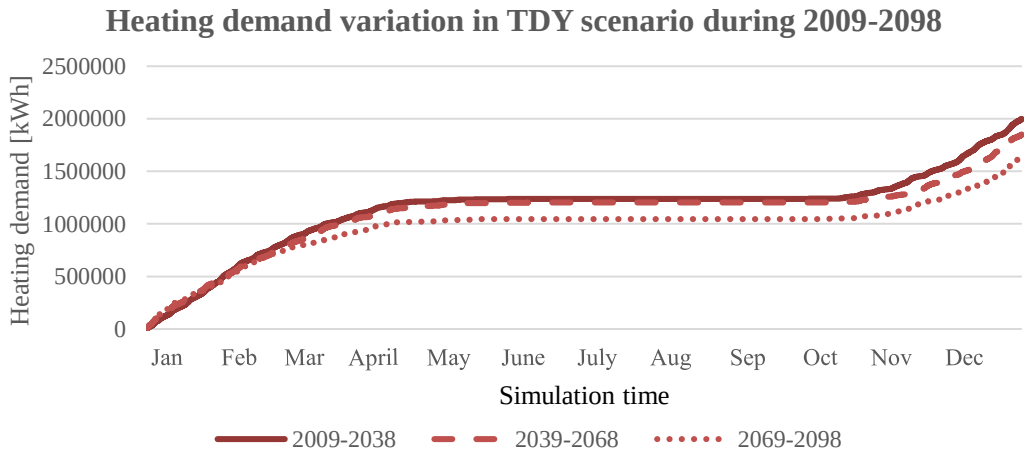

Figure 42: Heating demand variation of M-huset in TDY scenario during 2009-2098.

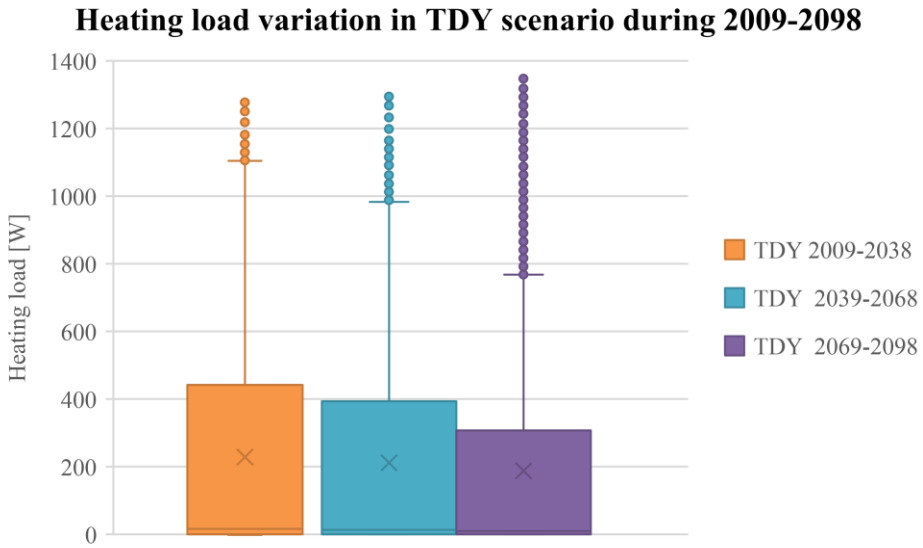

Figure 43: Heating load variation of M-huset in TDY scenario during 2009-2098.

Heating demand and heating load variations of M-huset in TDY, ECY and EWY scenarios during 2009-2038 are showed in figure 44 and figure 45 respectively. Both heating demand and heating load in TDY scenario all have the value between other two scenarios. Also, same as the IKDC, the series called Triple in figure 45 is a combination of heating load result in TDY, ECY and EWY scenarios. The similar result Triple series has as TDY series indicates that TDY scenario has its representativeness for the future heating energy consumption variations in M-huset.

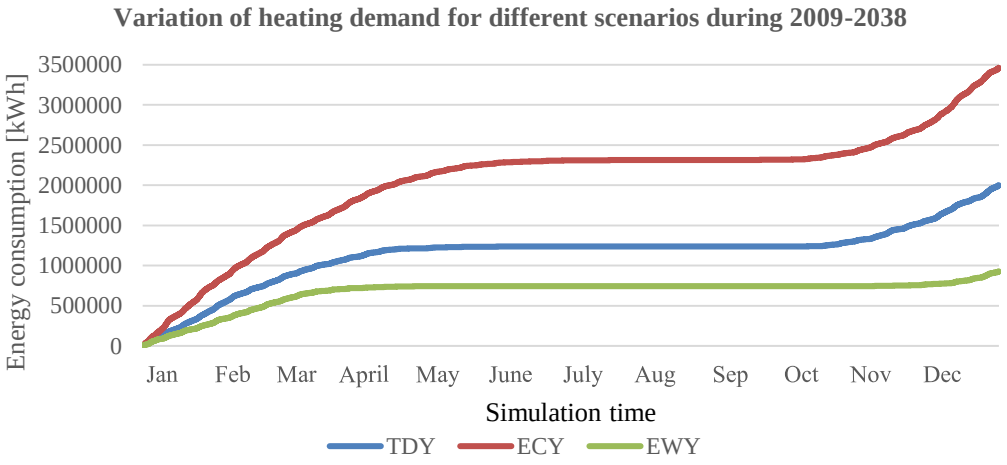

Figure 44: Heating demand variation of M-huset in TDY, ECY, and EWY scenarios during 2009-2038.

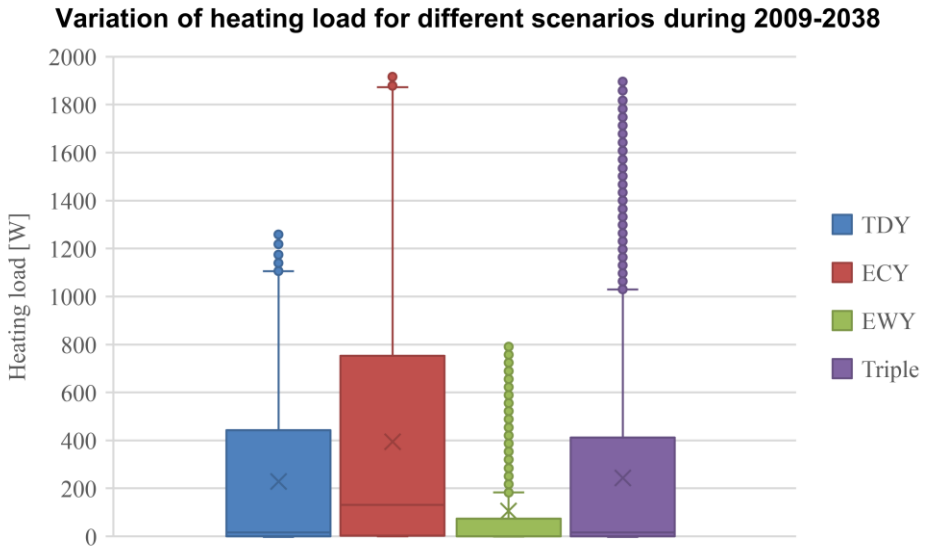

Figure 45: Heating load variation of M-huset in TDY, ECY, and EWY scenarios during 2009-2038.

1.1.2.1 Cooling demand and load variations

The cooling energy simulation results received from IDA ICE for the IKDC under typical downscale year (TDY) are showed in figure 46. It indicates that the annual cooling demand increased by 1% from the first 30 year' periods (2009-2038) to the second 30 years' period (2039-2068). 4% increase from the second 30 year' periods (2038-2069) to the third 30 year' periods (2069-2098). Also, cooling power per watts have an increasing trend as time goes by in TDY scenario, see figure 47.

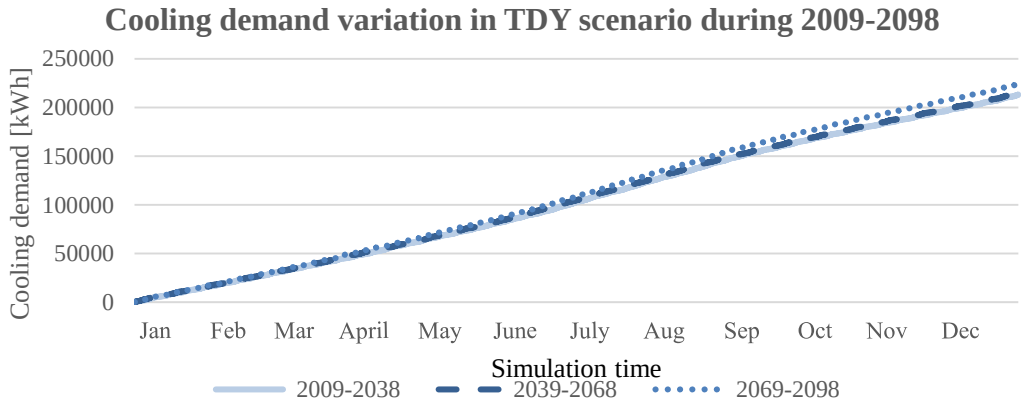

Figure 46: Cooling demand variation of the IKDC in TDY scenario during 2009-2098.

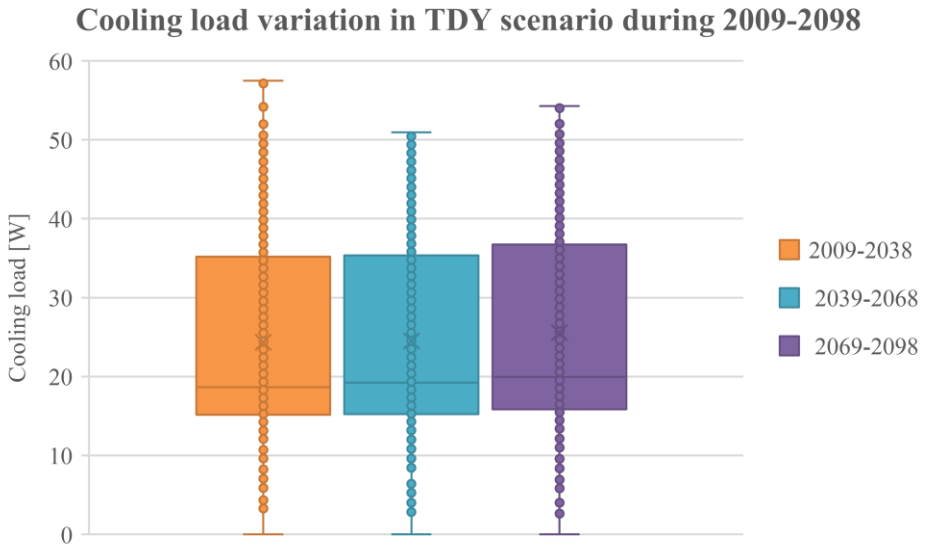

Figure 47: Cooling load variation of the IKDC in TDY scenario during 2009-2098.

Cooling demand and cooling load variations of the IKDC in TDY, ECY and EWY scenarios during 2009-2038 are showed in figure 48 and figure 49 respectively. Both cooling demand and cooling load in TDY scenario all have the value between other two scenarios. Also, same as heating load simulation, the series called Triple in figure 49 is a combination of cooling load result in TDY, ECY and EWY scenarios. The similar result Triple series has as TDY series indicates that TDY scenario has its representativeness for the future cooling energy consumption variations in the IKDC.

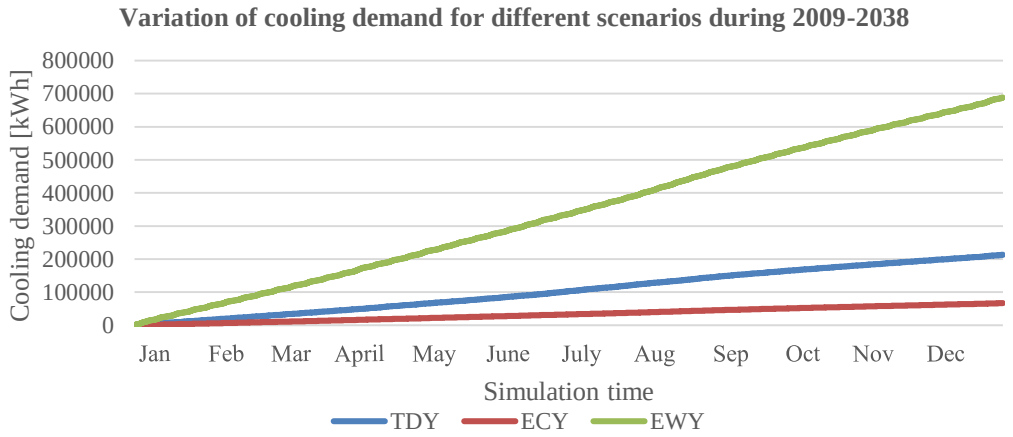

Figure 48: Cooling demand variation of the IKDC in TDY, ECY, and EWY scenarios during 2009-2038.

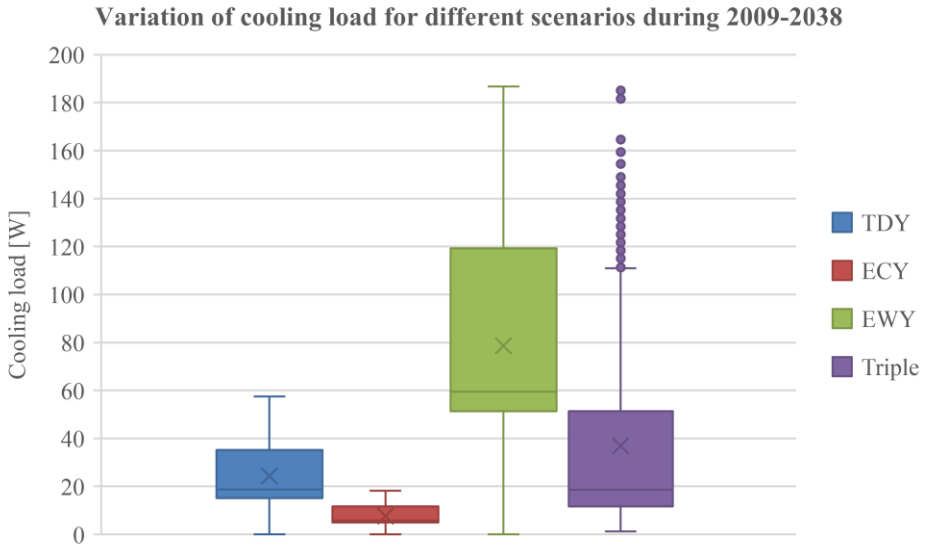

Figure 49: Cooling load variation of the IKDC in TDY, ECY, and EWY scenarios during 2009-2038.

The cooling energy simulation results received from IDA ICE for M-huset under typical downscale year (TDY) are showed in figure 50. It indicates that the annual cooling demand increased by 16% from the first 30 year' periods (2009-2038) to the second 30 years' period (2039-2068). 2% increase from the second 30 year' periods (2038-2069) to the third 30 year' periods (2069-2098). Same as cooling load variations in the IKDC, cooling load in M-huset also has an increasing trend as time goes by in TDY scenario, see figure 51.

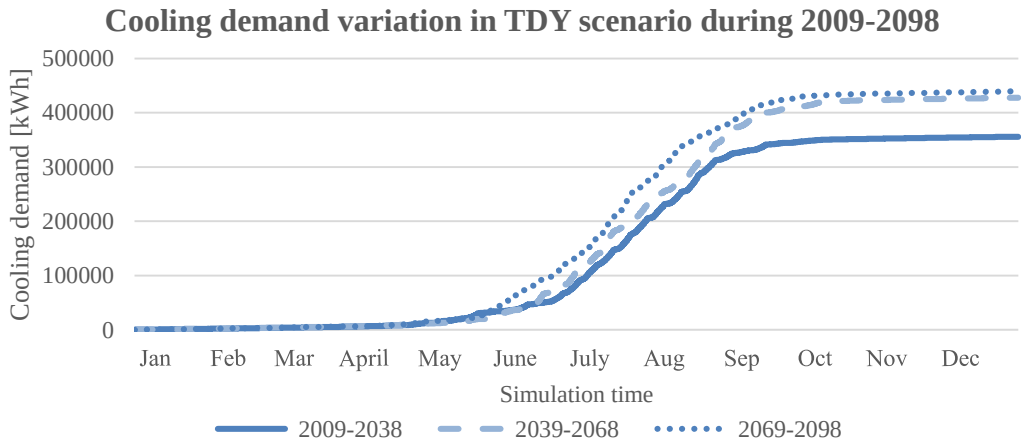

Figure 50: Cooling demand variation of M-huset in TDY scenario during 2009-2098.

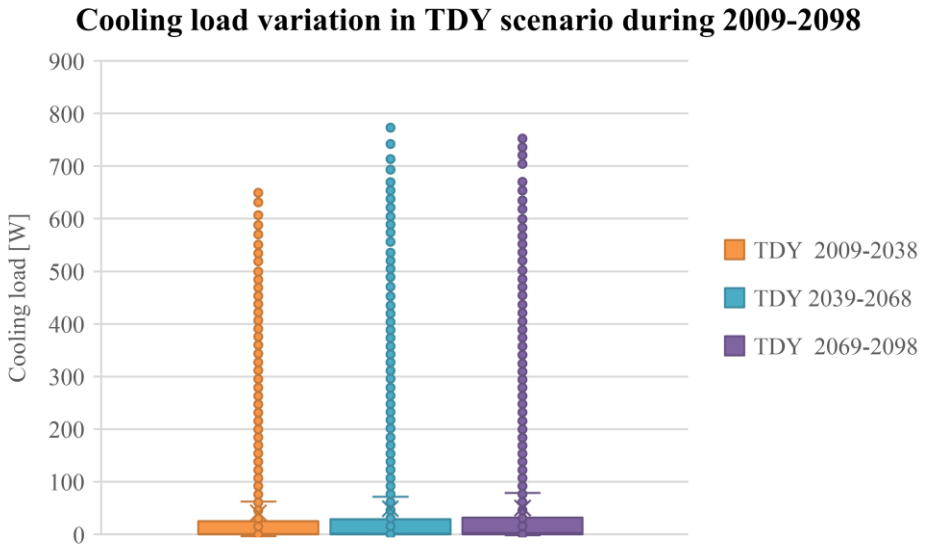

Figure 51: Cooling load variation of M-huset in TDY scenario during 2009-2098.

Cooling demand and cooling load variations of M-huset in TDY, ECY and EWY scenarios during 2009-2038 are showed in figure 52 and figure 53 respectively. Both cooling demand and cooling load in TDY scenario all have the value between other two scenarios. Also, same as heating load simulation, the series called Triple in figure 53 is a combination of cooling load result in TDY, ECY and EWY scenarios. The similar result Triple series has as TDY series indicates that TDY scenario has its representativeness for the future cooling energy consumption variations in M-huset as well.

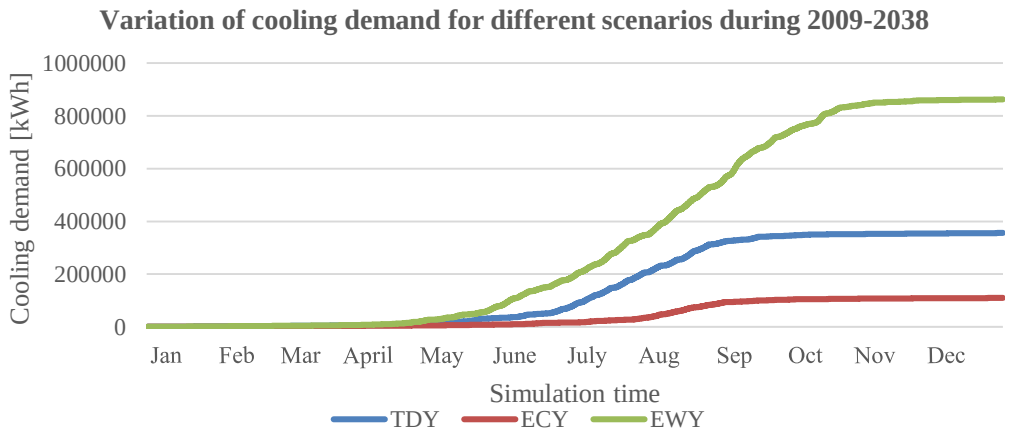

Figure 52: Cooling demand variation of M-huset in TDY, ECY, and EWY scenarios during 2009-2038.

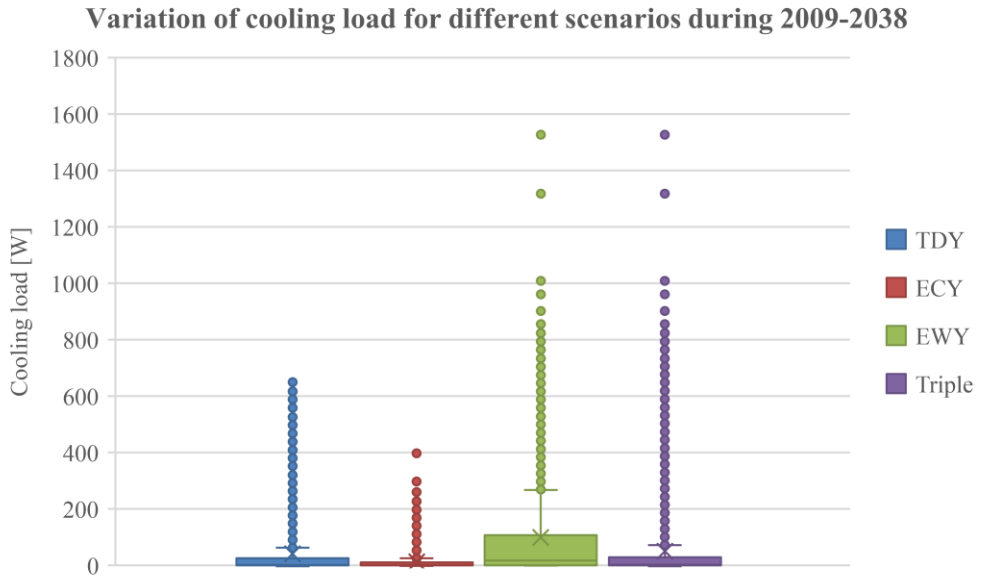

Figure 53: Cooling load variation of M-huset in TDY, ECY, and EWY scenarios during 2009-2038.

4.2 Renewable energy potential assessment

Results of assessing the potential of adding Solar, Wind, and shallow geothermal energy resource in the campus of Lund university are performed in this chapter.

4.2.1 Current climate scenarios

4.2.1.1 Solar energy

The annual solar radiation of six typical buildings inside the LTH campus are showed in figure 54-59. Six buildings are A-huset, M-huset, V-huset, E-huset, the IKDC and the Kemicentrum. Red area refers to a high annual solar radiation. Blue area, on the contrary, represents low annual solar radiation.

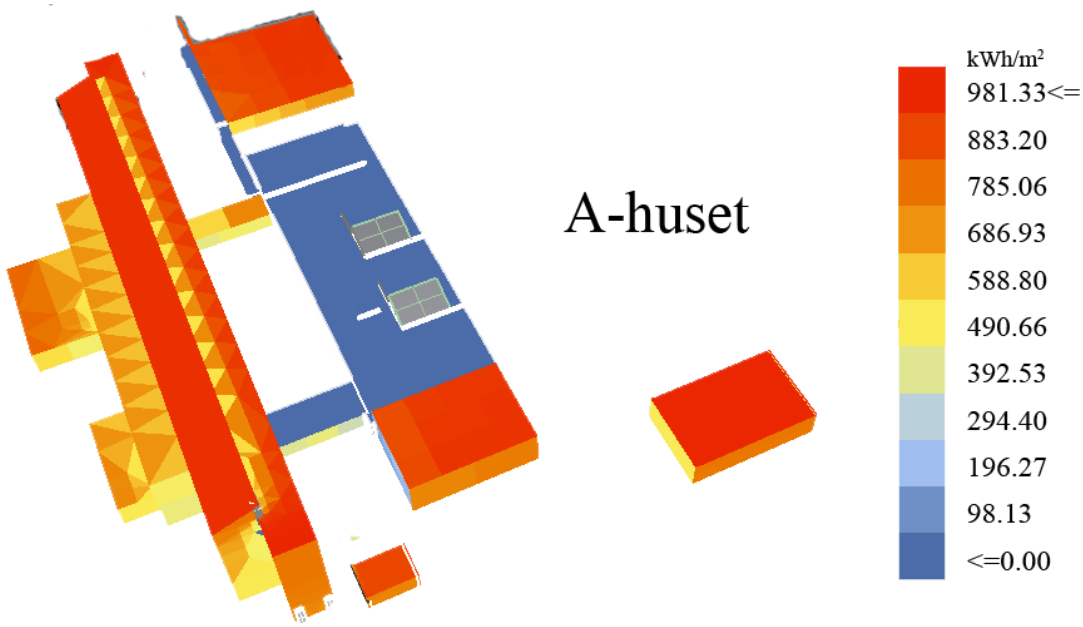

Figure 54: Annual solar radiation of A-huset.

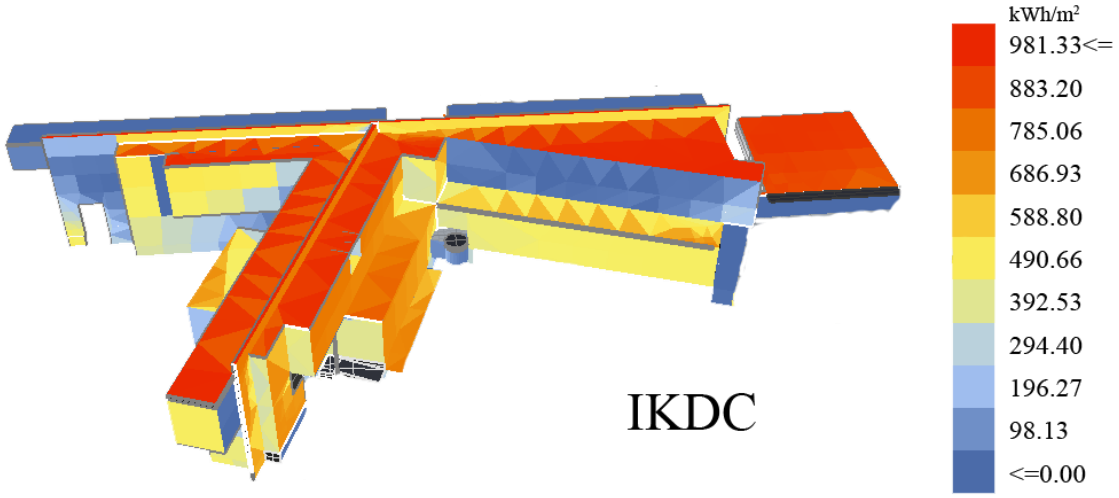

Figure 55: Annual solar radiation of IKDC.

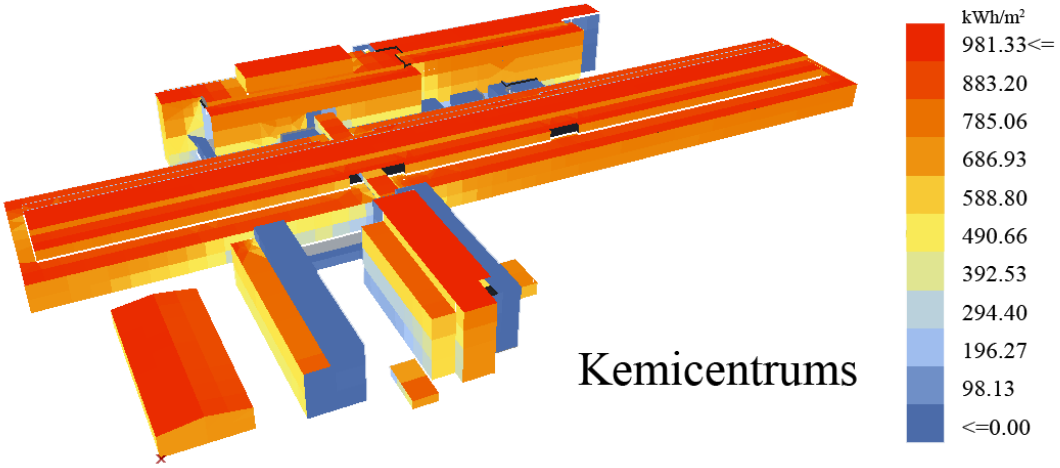

Figure 56: Annual solar radiation of Kemicentrums.

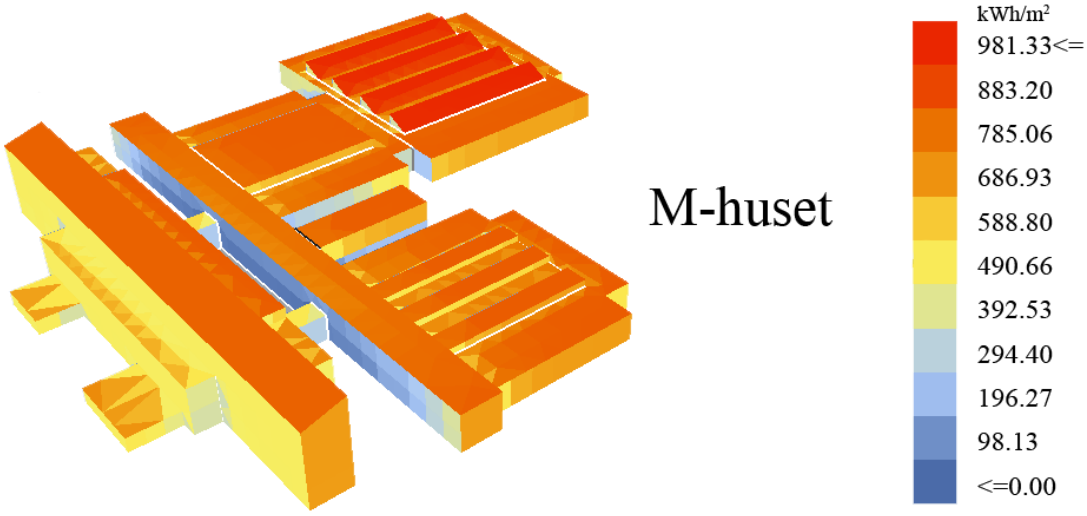

Figure 57: Annual solar radiation of M-huset.

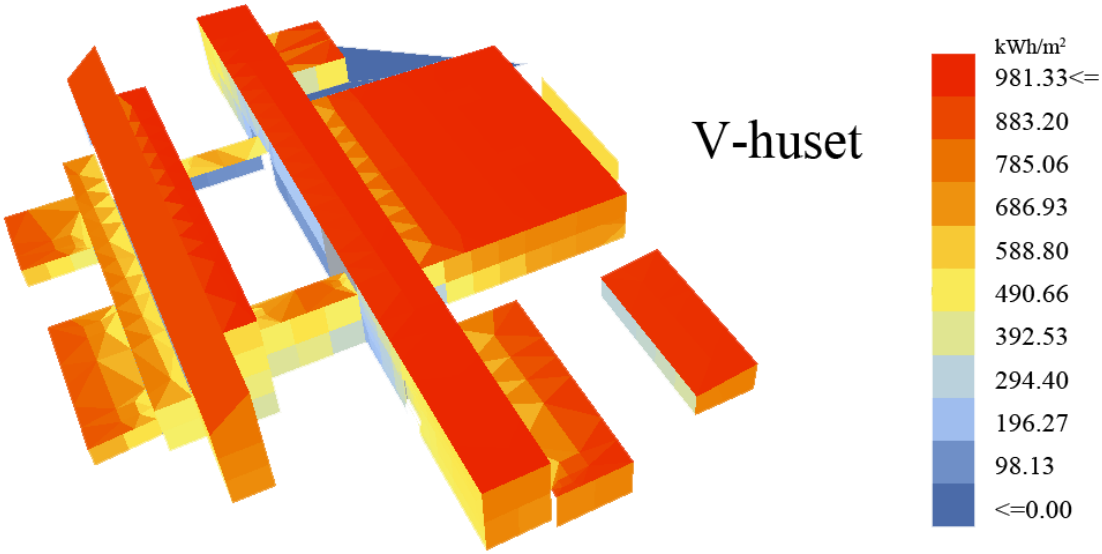

Figure 58: Annual solar radiation of V-huset.

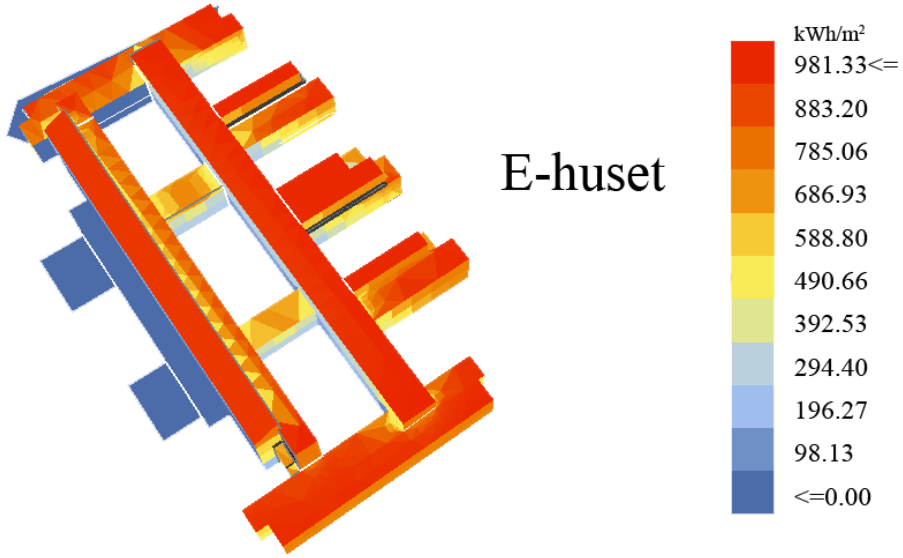

Figure 59: Annual solar radiation of E-huset.

Local measured data of total solar radiation in Lund in 2015 was provided by Akademiska Hus. As it is only valid for one year, solar radiation data for Lund from Energy plus default weather file were taken into comparison to estimate its applicability for solar potential simulation. Comparison are showed in figure 60. Although solar radiation from the measured data has some points which are higher than the data from the software, the majority points are almost same as the data from the software.

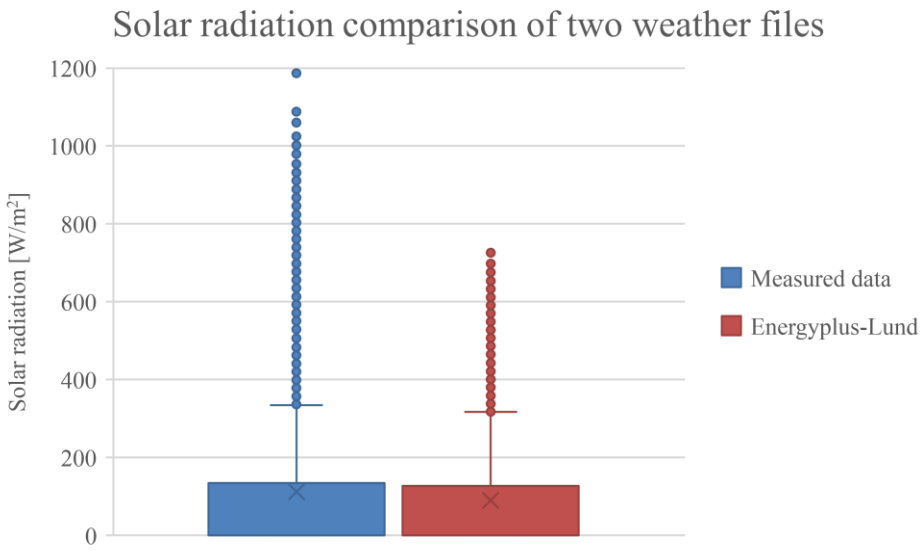

Figure 60: Solar radiation comparison of two weather files.

Figure 61 shows the comparison of measured data received from Akademiska Hus and simulated data from System Advisor Model (SAM) of PV generation in M-huset in 2015. Same type and quantity of PV panels, local measured weather file, and same inverters were applied in SAM. Although the difference between the simulated data and the measured data varies in different month, the accumulated data are almost overlapping curves. Thus, this case is defined as base case for further simulation. The base case has an annual PV generation of 191,445 kWh approximately.

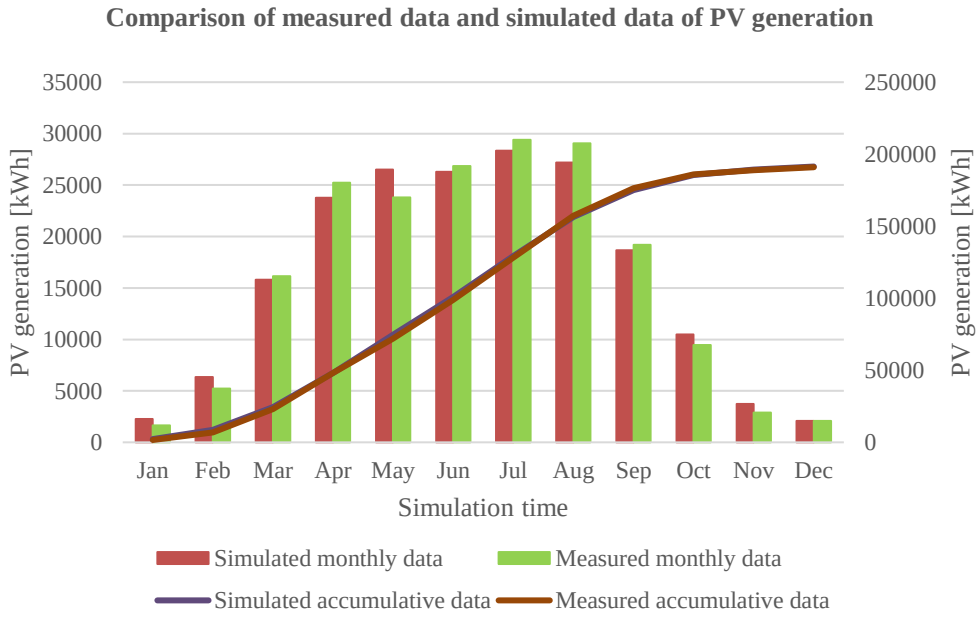

Figure 61: Comparison of measured data and simulated data of PV generation in M-huset in 2015.

Based on the base case simulation and electricity consumption received from IDA ICE, parametric simulations were done for parameters that affects PV generation. Parametric simulations of covering different coverage proportion of electricity consumption in M-huset are showed in figure 62 and figure 63. Information of the adjusted and simulated PV modules for parametric simulations were listed in table 22. Case 1 is the scenario when monthly PV generation equal to monthly electricity consumption in M-huset in May. In this case, electricity consumption in M-huset during May to August could be totally covered by PV panel, which need 7.4 times bigger scale of the PV already installed. Case 2 is the scenario when monthly PV generation equal to monthly electricity consumption in M-huset in December. In this case, electricity consumption in M-huset during the entire year could be totally covered by PV panel. However, it need 94.8 times bigger scale of the PV already installed.

Table 22 Information of parametric simulated PV modules

Case	Nameplate capacity [kWdc]	Number of modules	Total module area [m^2]
Reference	192	648	1029
Case 1	1420	4800	7622
Case 2	18150	61440	97567

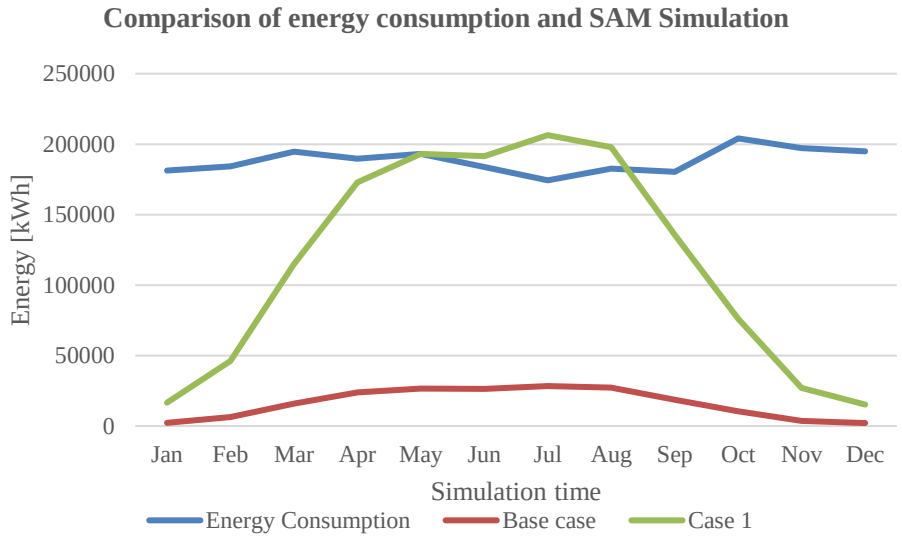

Figure 62: Comparison of different coverage proportion of energy consumption.

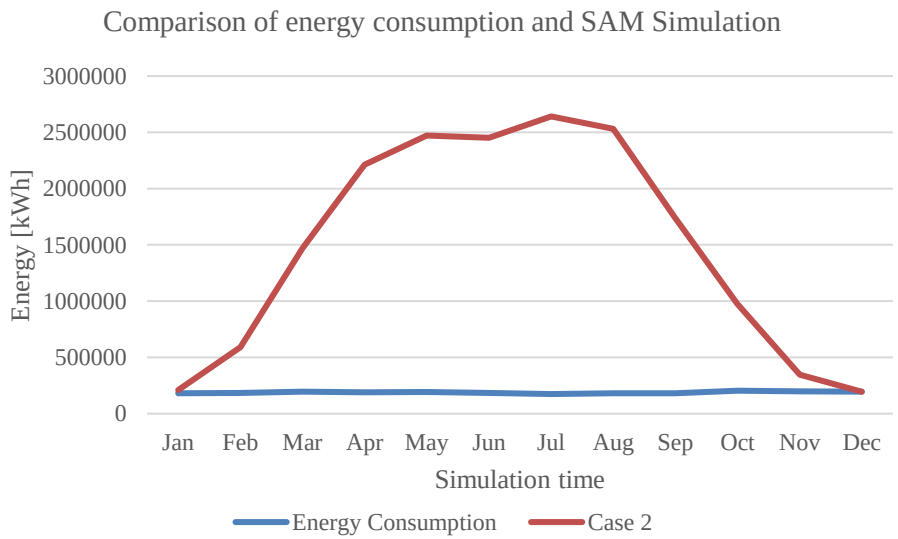

Figure 63: Comparison of different coverage proportion of energy consumption.

Parametric simulations of different PV titled angles are showed in figure 64-66. Different months have different optimal titled angle. From annual electricity generation point of view, 40 degree has the highest output. Meanwhile, parametric simulations of three different PV module types are showed in figure 67. Monocrystalline has the highest efficiency and generation among these three module

types, which has 16% more annual PV generation than polycrystalline and 2.3 times more annual PV generation than Amorphous.

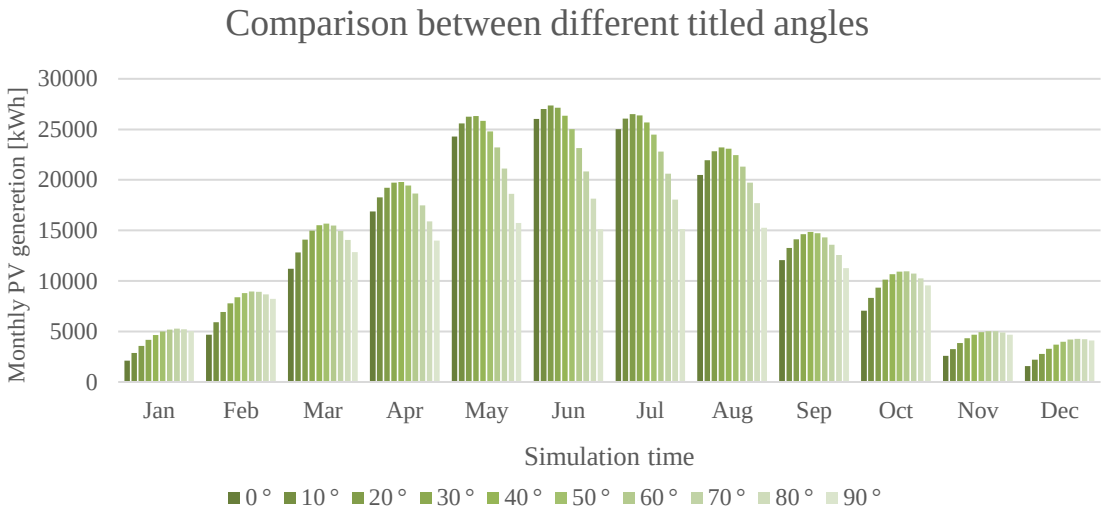

Figure 64: Comparison of different titled angles.

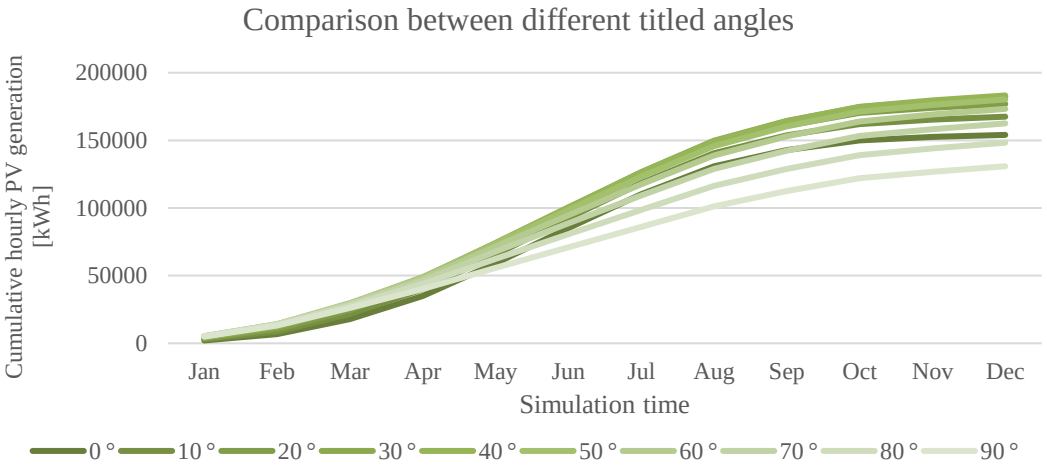

Figure 65: Comparison of different titled angles.

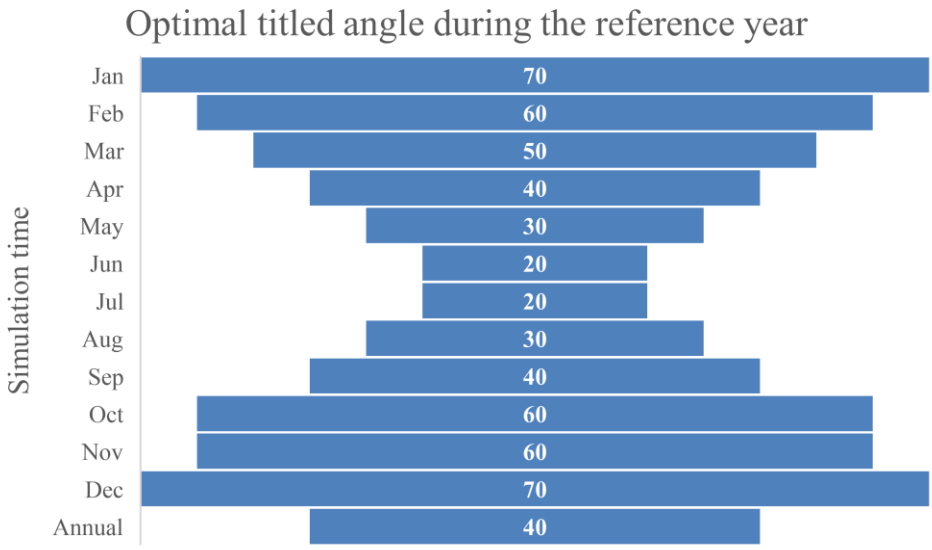

Figure 66: Optimal titled angle during the reference year.

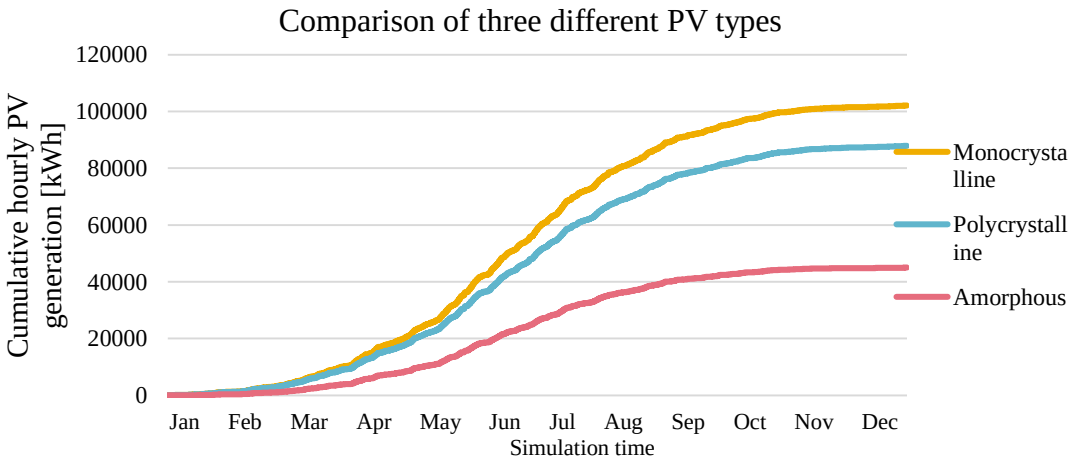

Figure 67: Comparison of three different PV types.

4.2.1.2 Wind energy

Based on Energy plus default weather data for Lund, wind rose generated in ECOTECT weather tool is showed in figure 68. The lightest blocks refer to the most frequent directions, which are gathered in south-westward. Wind speed are mostly varying between 20-40 km/h.

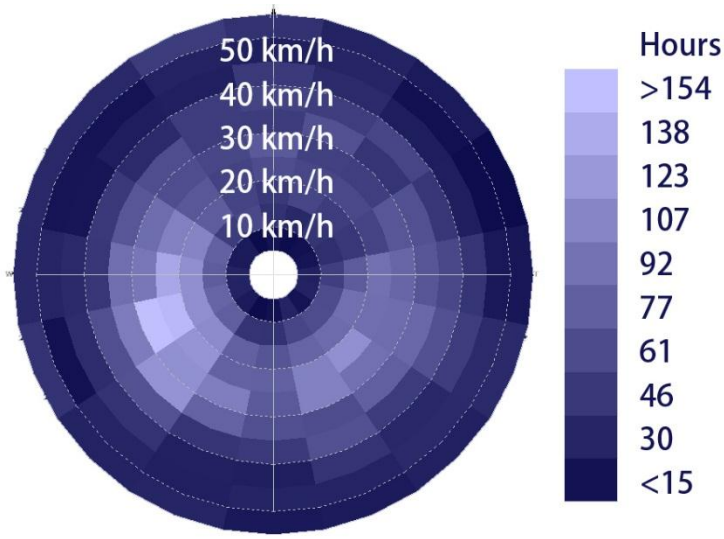

Figure 68: Wind rose in Lund.

More detailed wind class frequency distribution for the same weather data, which generated by WRPLOT View, are showed in figure 69. It is obvious that maximum ratio appears in the interval when wind speed is between 5.7 to 8.8 m/s. After it is the interval when wind speed is between 3.6 to 5.7 m/s. The time when wind speed is between 3.6 to 8.8 m/s is more than 50 percent in this case.

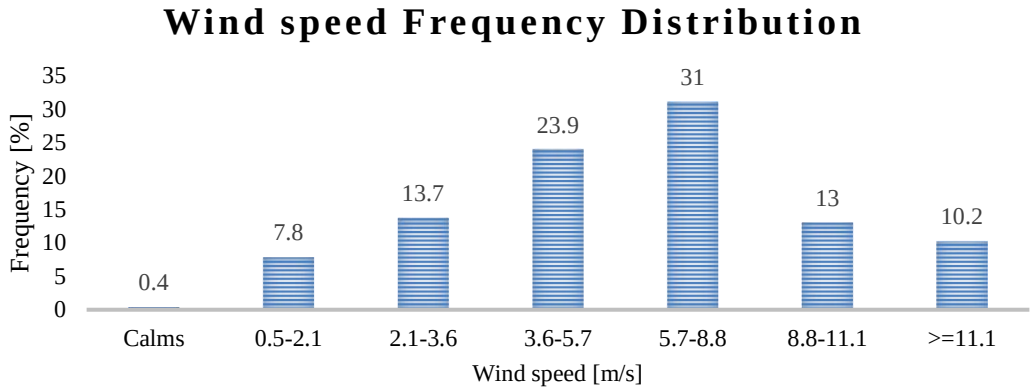

Figure 69: Wind class frequency distribution.

Based on building models and setted wind speed in the air as 10 m/s in Autodesk Flow design, the variation of wind speed in the LTH campus from top view and vertical side view are showed in figure 70 and figure 71. From top view, it is clear that buildings in north side of the campus has higher speed than south side.

Meanwhile, from vertical side view, wind speed at roof height are almost same as the speed in the air.

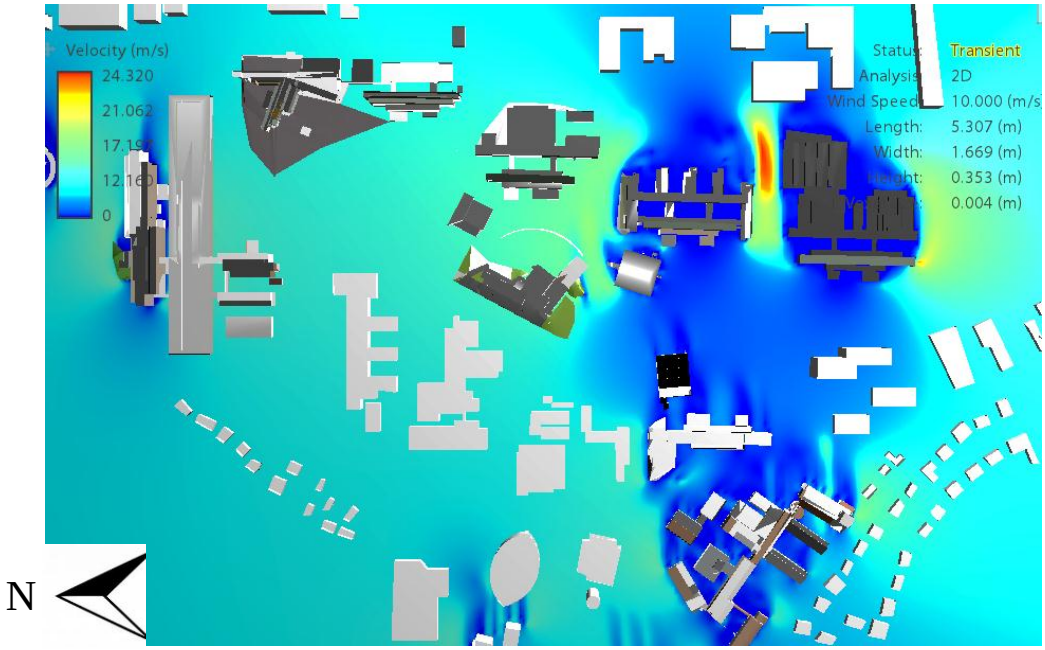

Figure 70: Wind speed in the LTH campus.(top view)

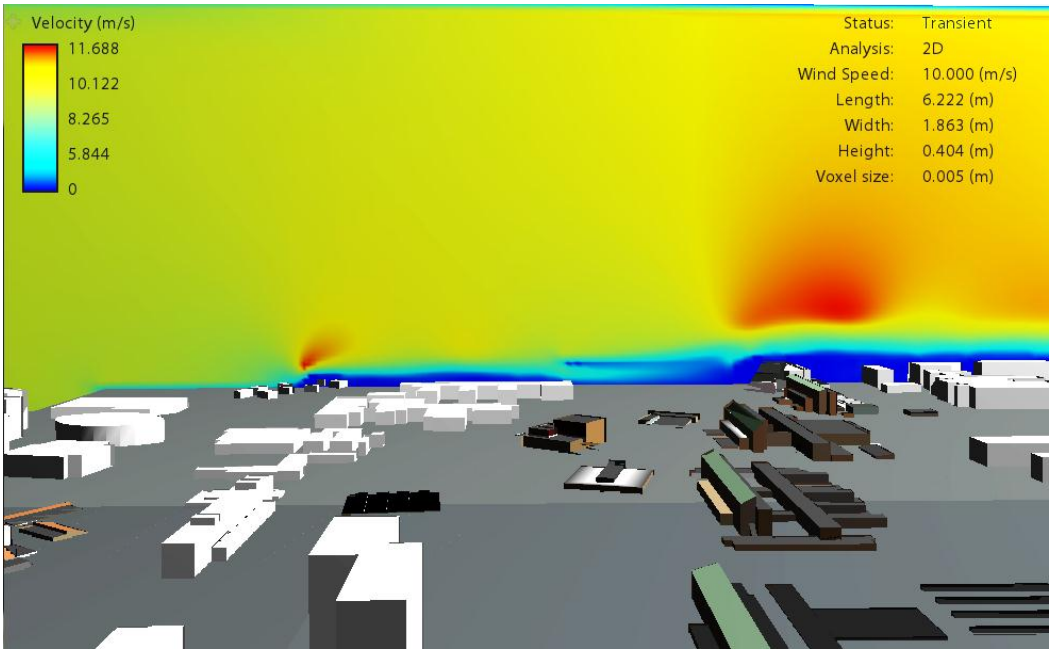

Figure 71: Wind speed in the LTH campus.(Vertical side view)

Relationship between power and wind speed of different wind turbines provided by product catalogue is showed in figure 72. Also, fitting function curve that matches the power and wind speed diagram is showed in figure 73. These two figures have almost same trend and corresponding relation. The higher rated power wind turbine has higher power output when wind speed varies. Except the Aeolos V-10 kW, it has poorer performance than Aeolos V-5 kW when wind speed is less than 10.5 m/s or so. Besides, Aeolos V-10kW have the same or even higher power output with Aeolos H-10 kW when wind speed is more than 15 m/s.

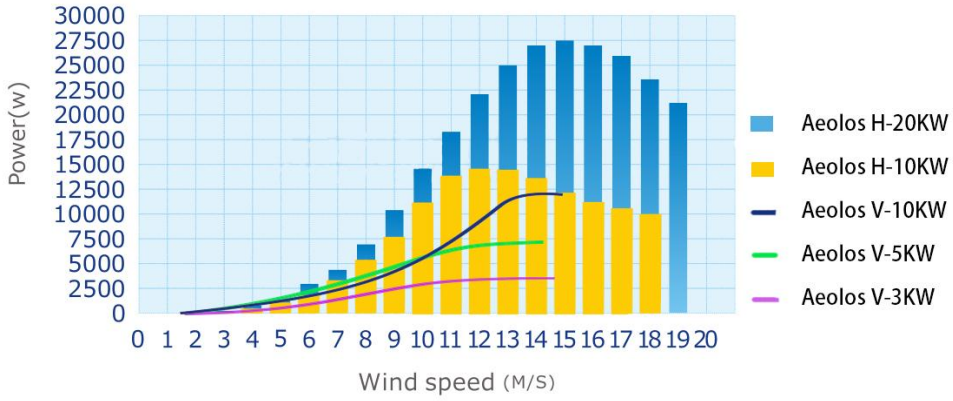

Figure 72: Relationship between power and wind speed of different wind turbines provided by product catalogue.

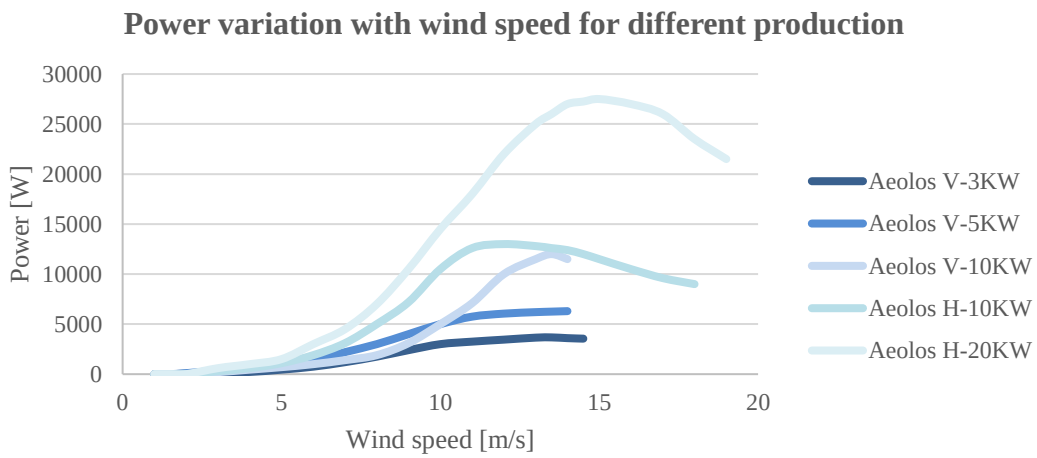

Figure 73: Relationship between power and wind speed of different wind turbines based on fitting function.

Annual energy generation by wind turbine is showed in figure 74. Same comparative result as power output. Single wind turbine with rated power of 3 kW could generate 8,426 kWh energy in a year. Wind turbine with rated power of 5 kW could almost generate double energy than rated power of 3 kW, same result for 10 kW and 20 kW. Besides, with same rated power, wind turbine with horizontal blades could generate more energy than wind turbine with vertical blades. Noticeable, Aeolos V-10 kW has lower annual energy generation than Aeolos V-5 kW. Meanwhile, power output of different wind turbines is showed in figure 75. The interquartile range of power output rised as rated power increased. However, most percentage of power output of Aeolos V-10 kW is lower than Aeolos V-5 kW.

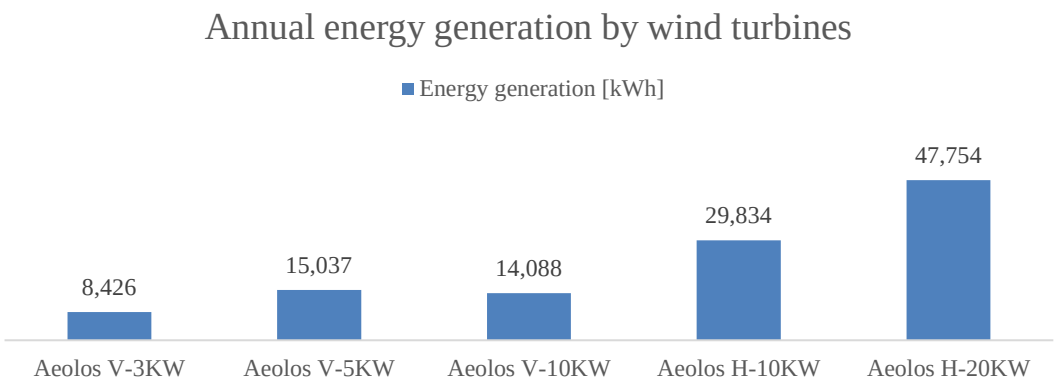

Figure 74: Annual energy generation by different wind turbines at the height of 18 meters.

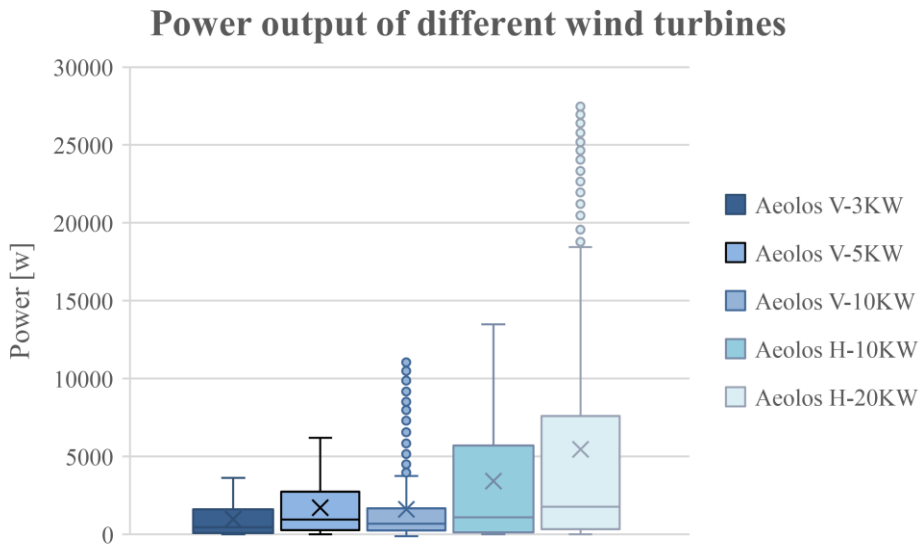

Figure 75: Boxplot of Power output of different wind turbines.

Noise level of Aeolos H-10KW provided by product catalog is showed in figure 76. When wind speed is under 7 m/s, even 10m from tower could gain an acceptable noise level. On the contrary, it could be a bit nosiy if people is 10 m from tower, as noise level would be more than 45 dB(A). For people working in 50 m from tower, the noise is always acceptable.

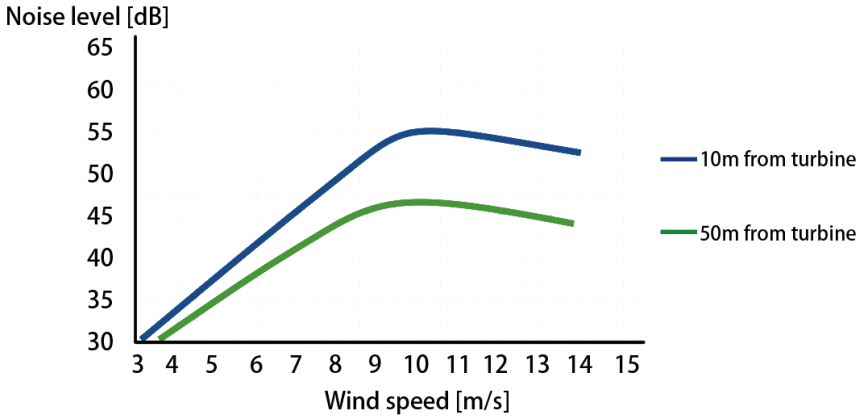

Figure 76: Noise level of Aeolos H-10KW provided by product catalogue.

4.2.1.3 Shallow geothermal energy

Parametric simulations were done based on the parameters that would affect shallow geothermal potential Q_{BHE} in G.POT method. Variations of shallow geothermal potential when varying thermal conductivity of the ground are showed in figure 77. The higher thermal conductivity of the ground is, the higher shallow geothermal potential. Variations of shallow geothermal potential when varying thermal capacity of the ground are showed in figure 78. The higher thermal capacity of the ground is, the higher shallow geothermal potential. Variations of shallow geothermal potential when varying borehole length are showed in figure 79. The longer borehole is, the higher shallow geothermal potential. Variations of shallow geothermal potential when varying borehole radius are showed in figure 80. The bigger borehole radius is, the higher shallow geothermal potential. Variations of shallow geothermal potential when varying length of heating/cooling season are showed in figure 81. The longer length of heating/cooling season is, the higher shallow geothermal potential. Variations of shallow geothermal potential when varying operating time are showed in figure 82. The shorter operating time is, the higher shallow geothermal potential.

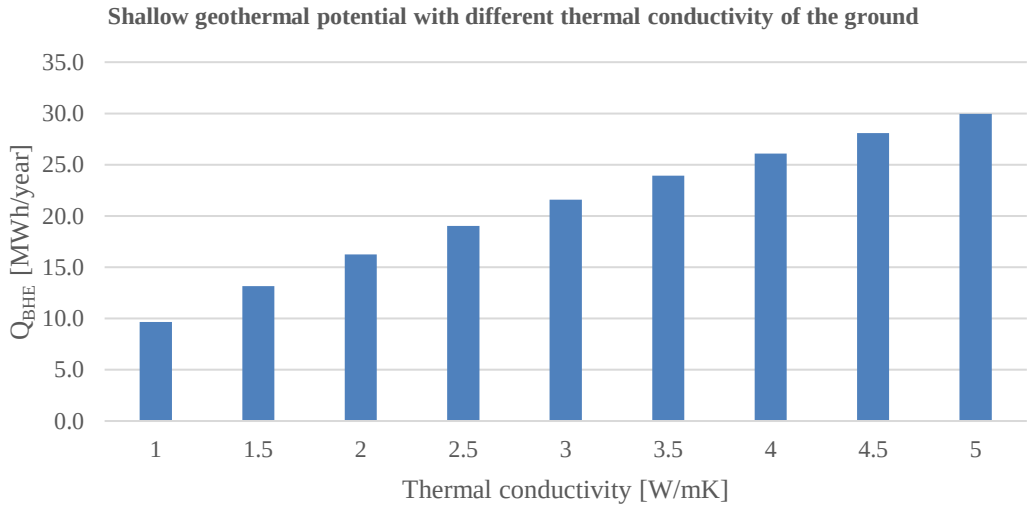

Figure 77: Parametric simulation result of varying thermal conductivity of the ground.

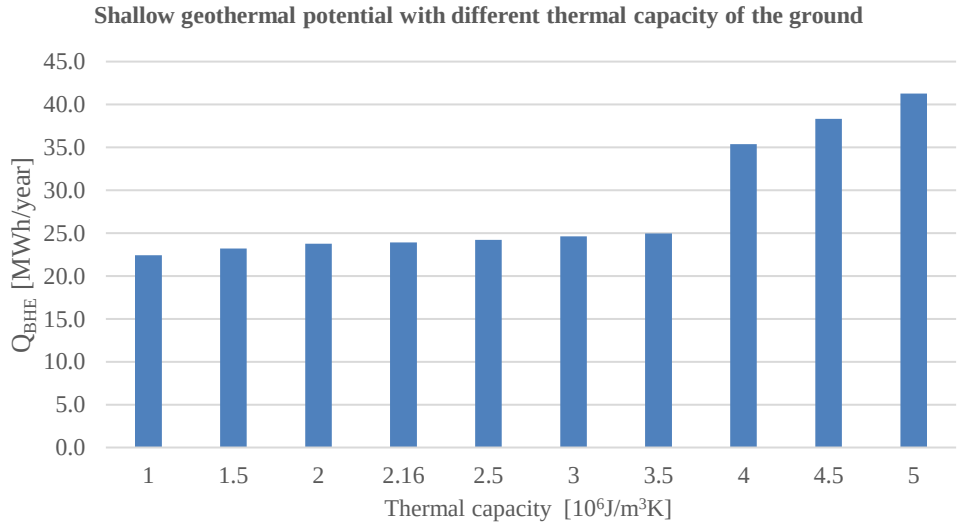

Figure 78: Parametric simulation result of varying thermal capacity of the ground.

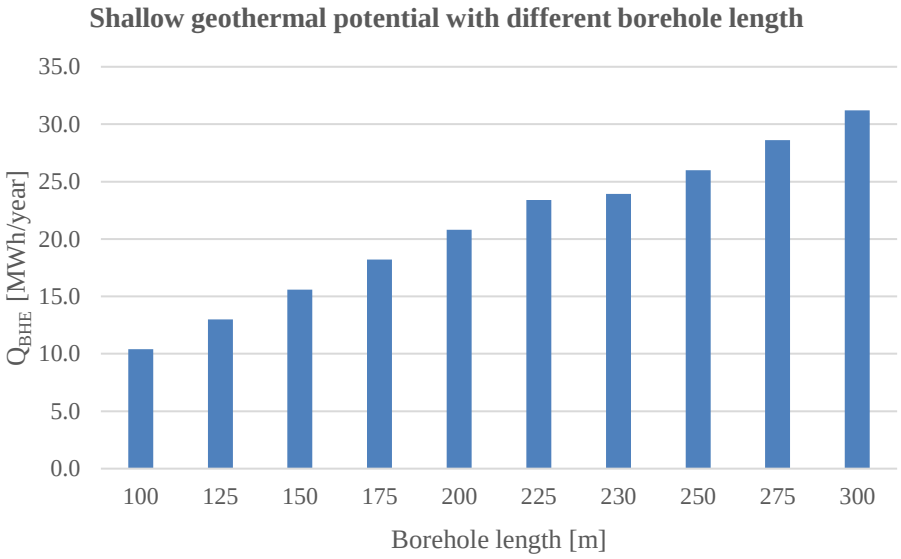

Figure 79: Parametric simulation result of varying borehole length.

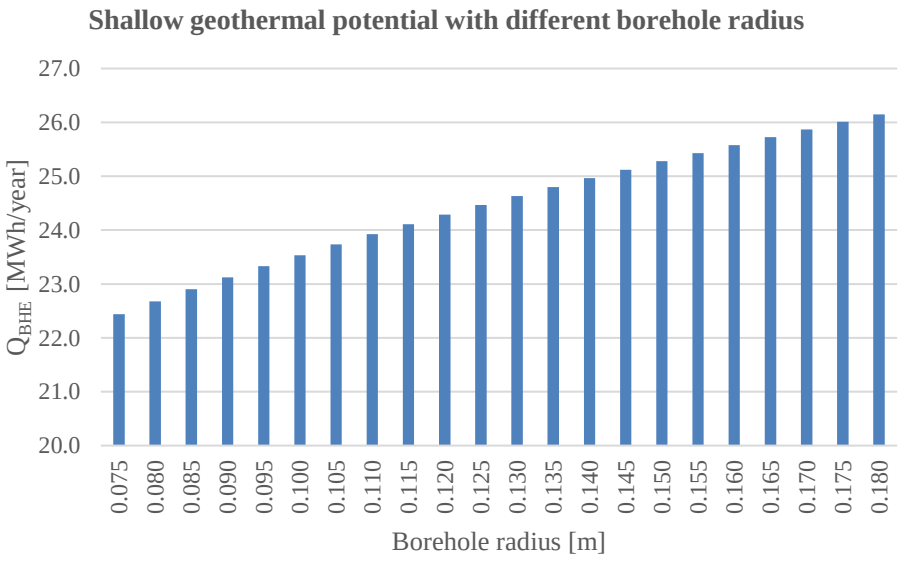

Figure 80: Parametric simulation result of varying borehole radius.

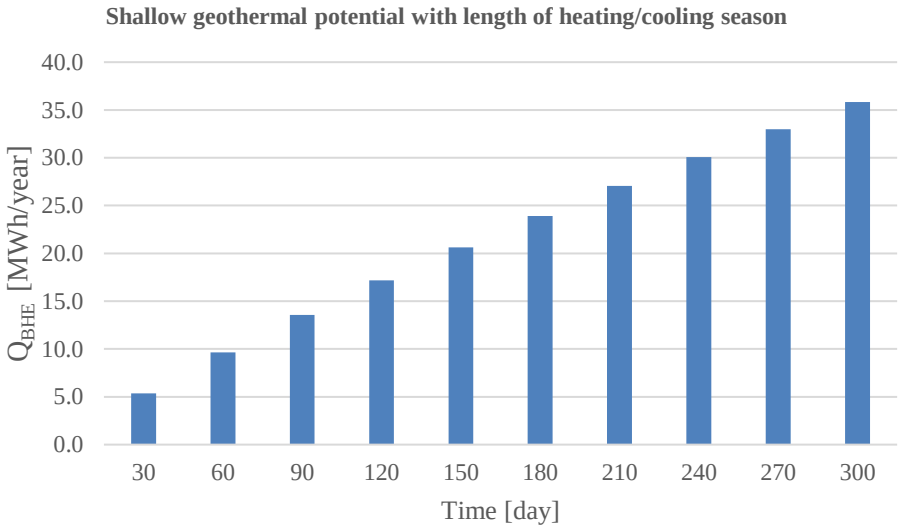

Figure 81: Parametric simulation result of varying length of heating/cooling season.

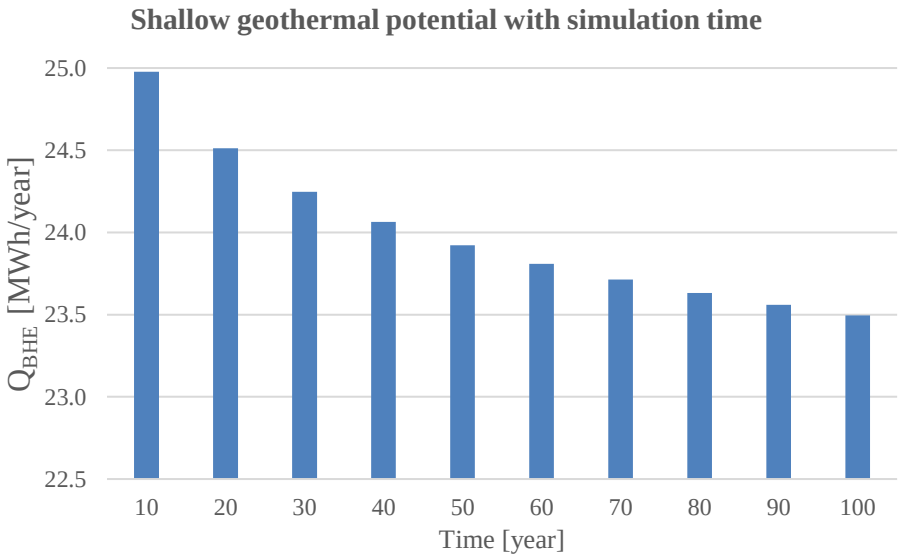

Figure 82: Parametric simulation result of varying length of operating time.

4.2.2 Future climate scenarios

For future climate scenario, weather files for typical downscale year (TDY), extremely cold year (ECY), and extremely warm year (EWY) for period 2009-2038, 2039-2068 and 2069-2098 were applied for solar energy and wind energy simulations.

4.2.2.1 Solar energy

The PV generation simulation results received from System Advisor Model (SAM) under typical downscale year (TDY), extremely cold year (ECY), and extremely warm year (EWY) are showed in figure 83-85. It indicates that monthly PV generation, annual PV generation, and PV power all are varied from time to time, no certain trend were found.

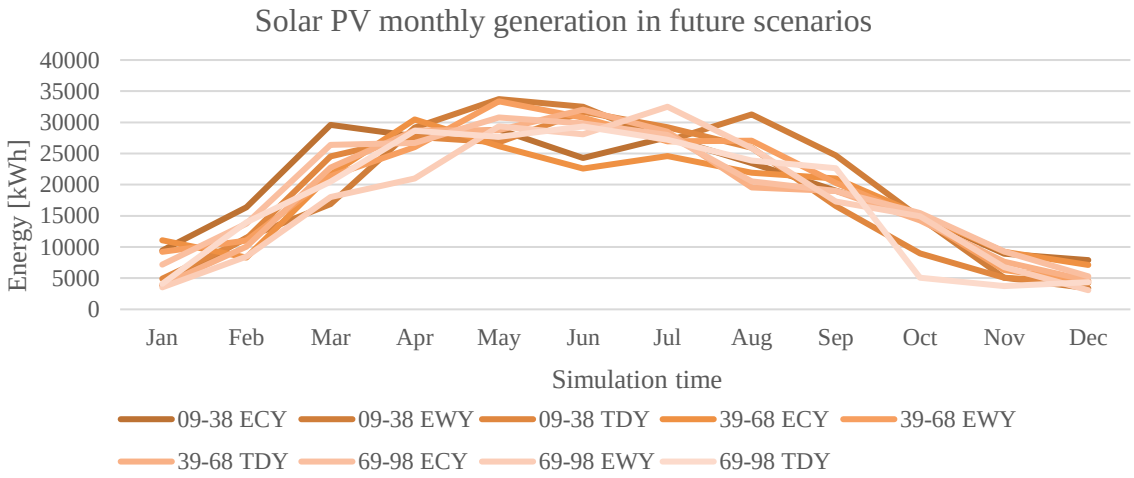

Figure 83: Monthly PV generation in TDY scenario for 2009-2098.

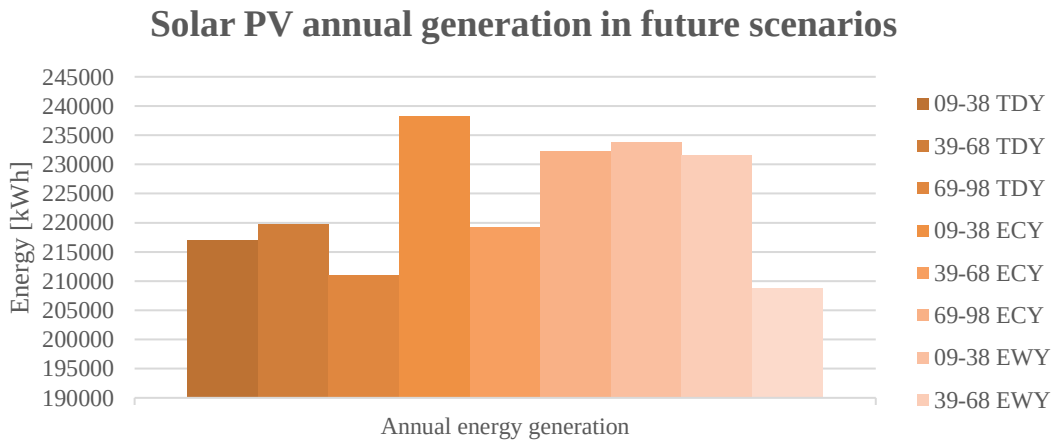

Figure 84: Annual PV generation in TDY scenario for 2009-2098.

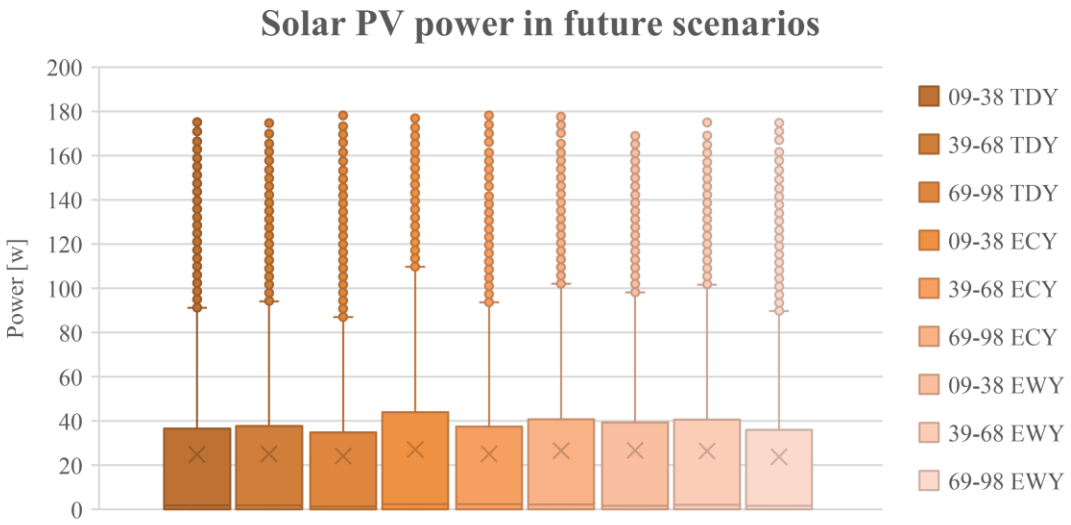

Figure 85: PV power in future scenario for 2009-2098.

4.2.2.2 Wind energy

The wind speed variations gathered from weather file under typical downscale year (TDY), extremely cold year (ECY), and extremely warm year (EWY) are showed for 2009-2098 are showed in figure 86. Also, same as energy consumption simulation, the series called Triple showed in figure 87. It is a combination of wind speed variation result in TDY, ECY and EWY scenarios. It indicates that the interquartile range of wind speed has decreased into a lower interval with the passage of time.

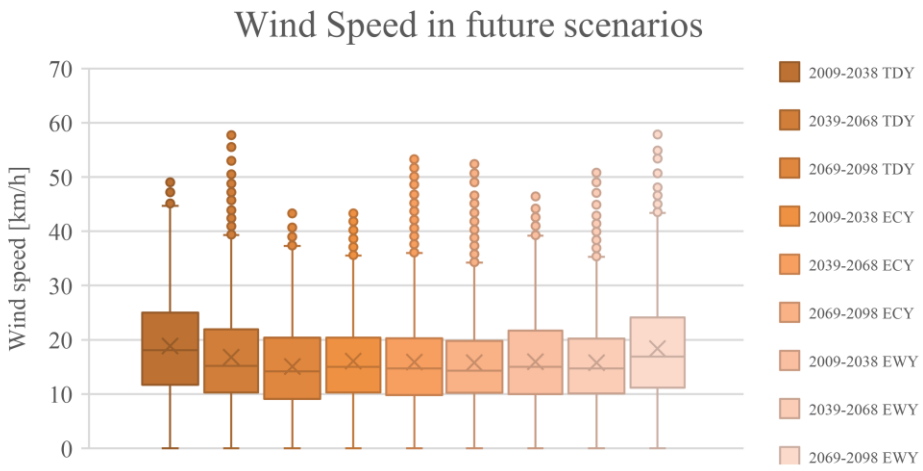

Figure 86: Wind speed variations in future scenarios for 2009-2098.

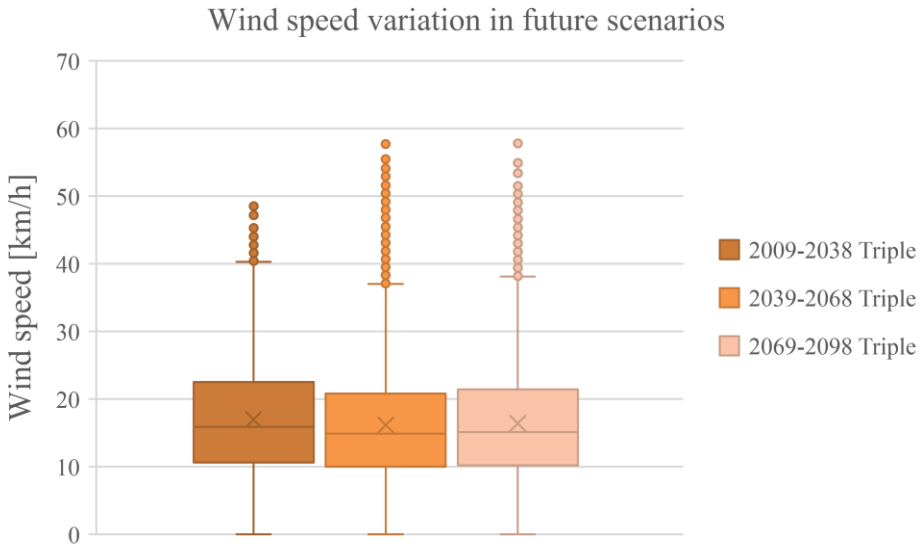

Figure 87: Wind speed variations in future scenarios for 2009-2098.

Comparison of wind class frequency distribution in TDY scenario for 2009-2098, which generated by WRPLOT View, are showed in figure 88. It is obvious that maximum ratio appears in the interval when wind speed is between 5.7 to 8.8 m/s in reference year and period 2009-2038. However, after 2038, the interval when wind speed is between 3.6 to 5.7 m/s become the most likely interval. Also, strong wind situation decreased as time goes by.

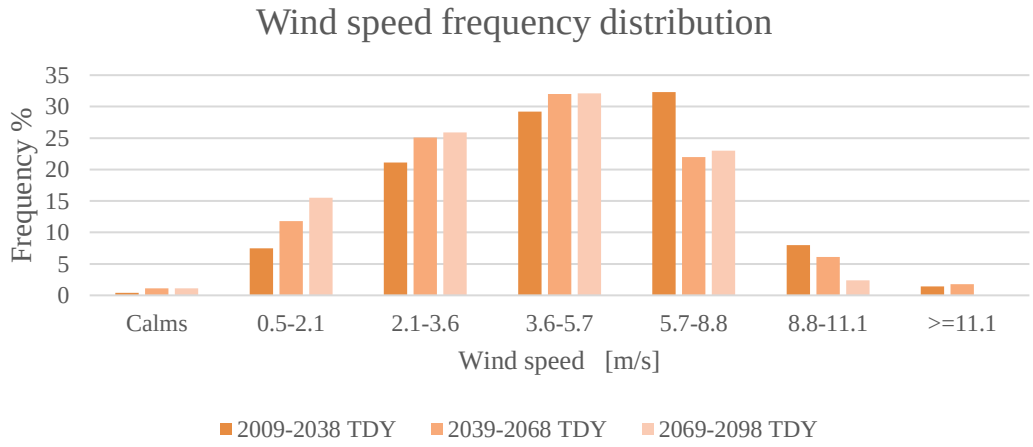

Figure 88: Comparison of wind class frequency distribution in TDY weather data for different periods.

4.3 Life cycle cost

This section shows the result of life cycle cost result on PV panels, wind turbines, adding wall insulation materials and changing windows. Figure 89 is the result of parametric study for different energy price growth rates, discount interest rates, and inflation rates based on PV life cycle cost simulation. A higher energy growth rate, resulted in a higher payback time. On the contrary, both higher interest rates and inflation, the payback time would be longer.

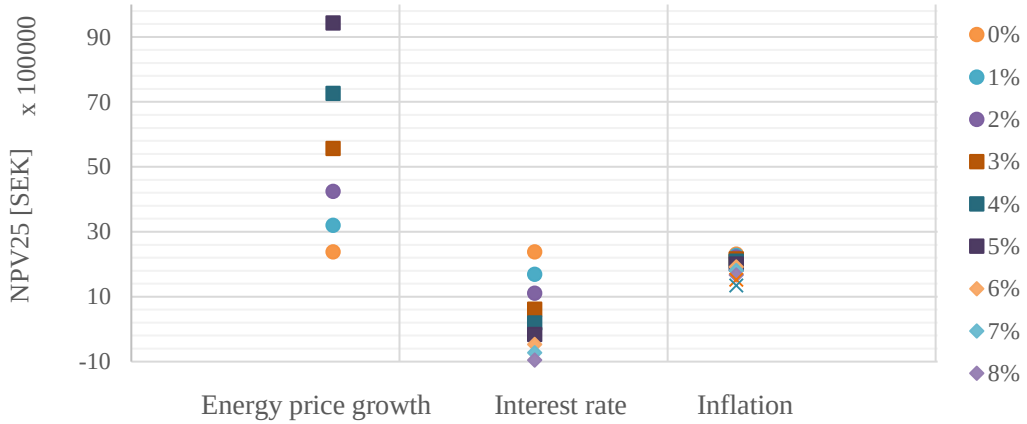

Figure 89: Different scenarios expressed in kSEK for the NPV of the pv system.

In figure 90, two scenarios are showed. The scenario where the inverters break down after ten and twenty years and not change for a new one is the option that first paid back investments, approximately in 15 years. The scenario where the inverters changes every ten years also could be pay back investment in 16 years.

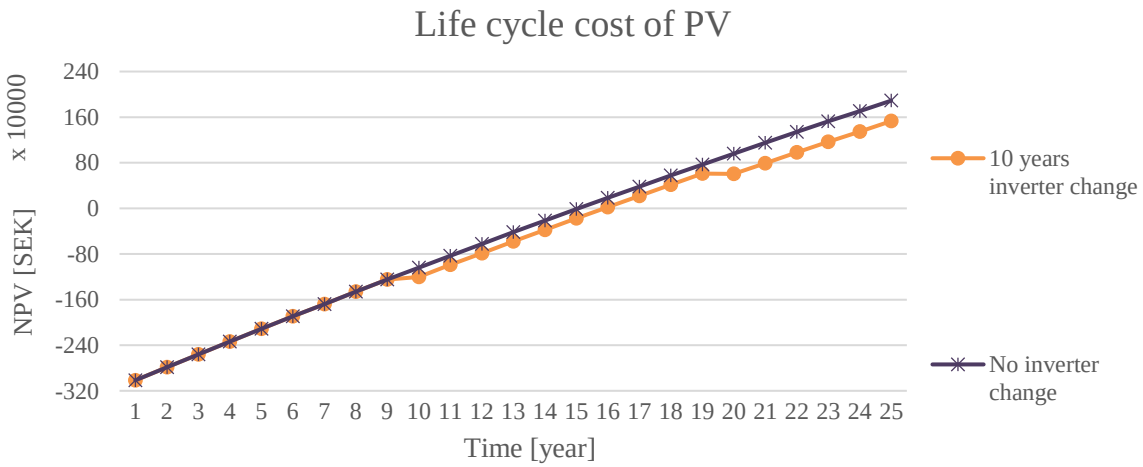

Figure 90: Different scenarios for implementing inverter change in the LCC calculations.

In figure 91, life cycle cost of different wind turbines is showed. Smaller wind turbine has longer payback time, for the biggest size in this study as Aeolos H-20 KW would be payback in 5 years and the smallest size as Aeolos V-3 KW would be payback in 7 years.

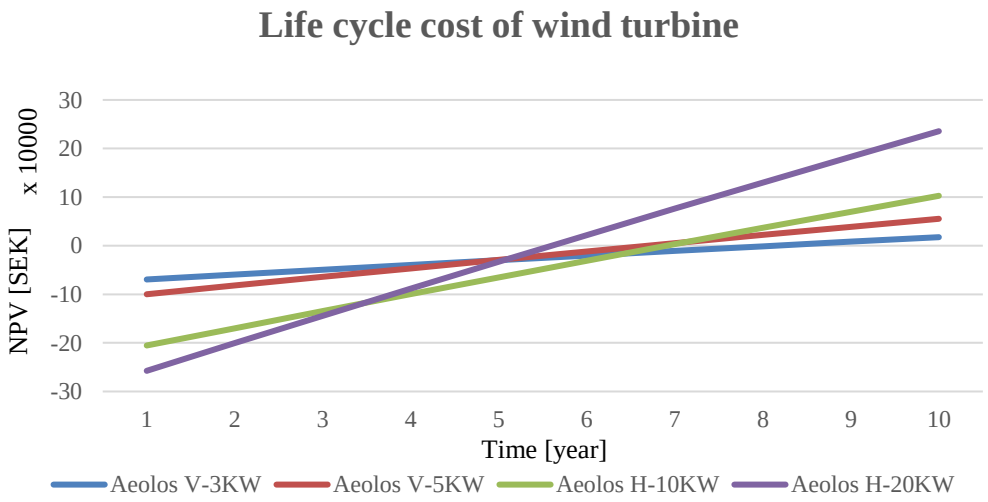

Figure 91: Life cycle cost of different wind turbines.

LCC study result of wall insulation change and window change are showed in figure 92 and figure 93. High initial investment with slightly energy saving payback make it would not be paid back in near future for both changes of wall and window.

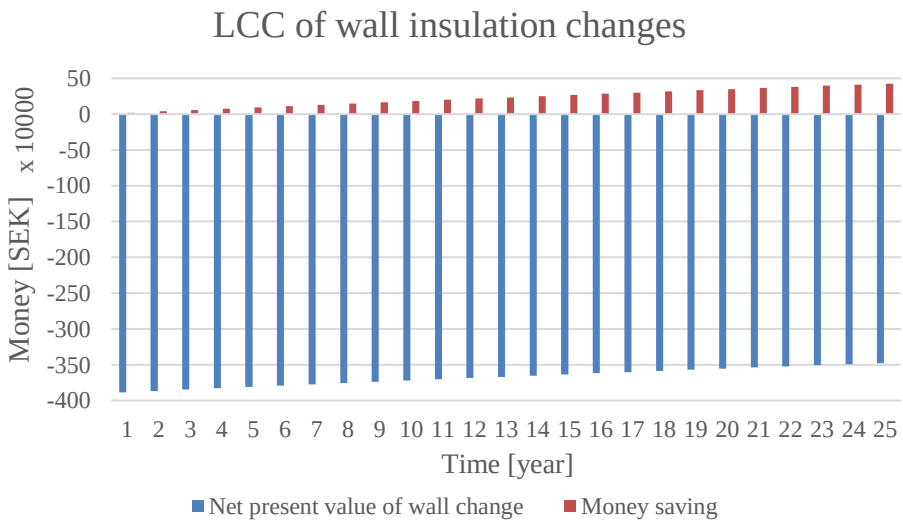

Figure 92: LCC study of wall insulation changes.

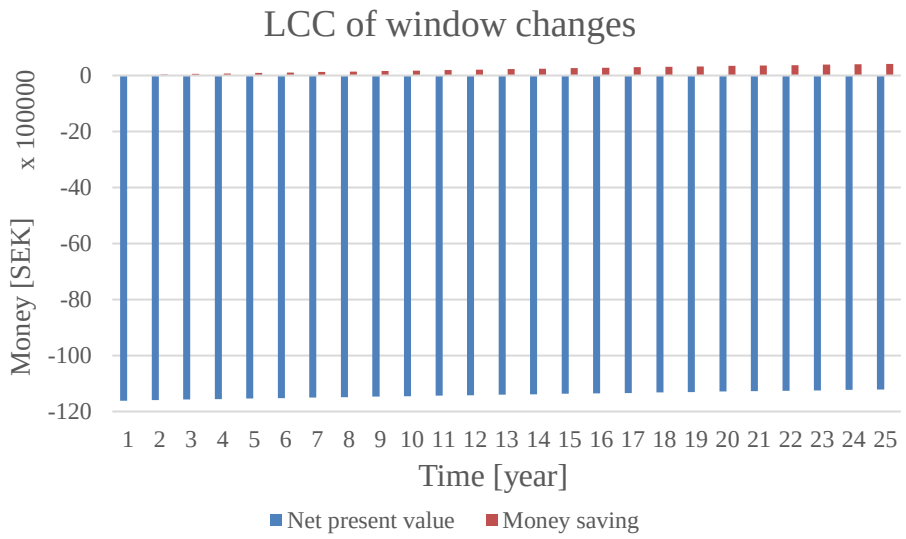

Figure 93: LCC study of window changes.

4.4 Life cycle assessment

Variation of environmental impact of acidification potential in LCA study of wall insulation in different thickness is showed in figure 94. Thickness of 150 mm have the lowest emission. Variation of environmental impact of climate change in LCA study of wall insulation in different thickness is showed in figure 95. Thickness of 150 mm have the lowest emission. Variation of environmental impact of depletion of abiotic resources - elements, ultimate reserves in LCA study of wall insulation in different thickness is showed in figure 96. Thickness of 350 mm have the lowest emission. Variation of environmental impact of depletion of abiotic resources - fossil fuels in LCA study of wall insulation in different thickness is showed in figure 97. Thickness of 150 mm have the lowest emission. Variation of environmental impact of eutrophication in LCA study of wall insulation in different thickness is showed in figure 98. Thickness of 150 mm have the lowest emission. Variation of environmental impact of human toxicity in LCA study of wall insulation in different thickness is showed in figure 99. Thickness of 350 mm have the lowest emission. Variation of environmental impact of ozone layer depletion in LCA study of wall insulation in different thickness is showed in figure 100. Thickness of 250 mm have the lowest emission. Variation of environmental impact of photochemical oxidation in LCA study of wall insulation in different thickness is showed in figure 101. Thickness of 350 mm have the lowest emission. Variation of environmental impact of freshwater aquatic ecotoxicity in LCA study of wall insulation in different thickness is showed in figure 102. Thickness of 350 mm have the lowest emission. Variation of environmental impact of marine aquatic ecotoxicity in LCA study of

wall insulation in different thickness is showed in figure 103. Thickness of 50 mm have the lowest emission. Variation of environmental impact of terrestrial ecotoxicity in LCA study of wall insulation in different thickness is showed in figure 104. Thickness of 350 mm have the lowest emission.

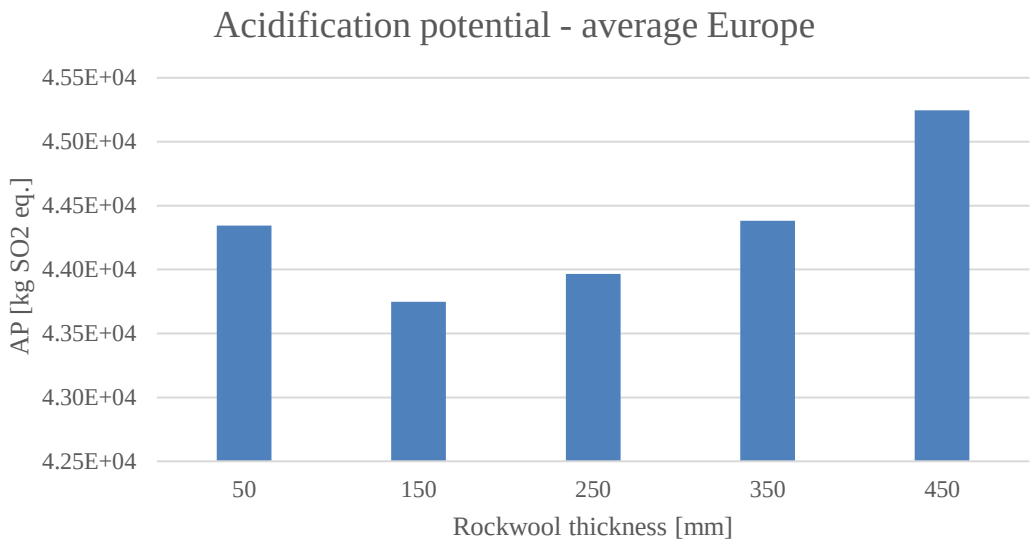

Figure 94: Environmental impact of acidification potential in LCA study of wall insulation in different thickness.

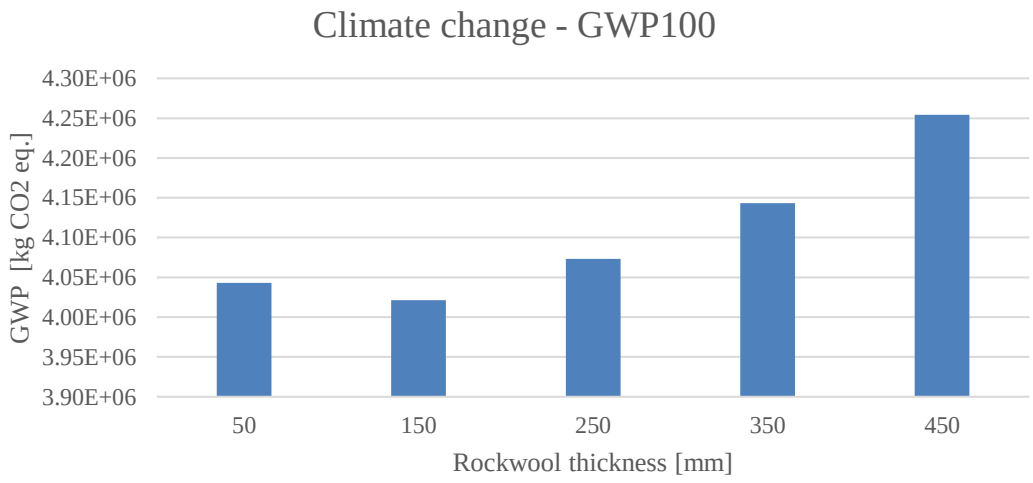

Figure 95: Environmental impact of climate change in LCA study of wall insulation in different thickness.

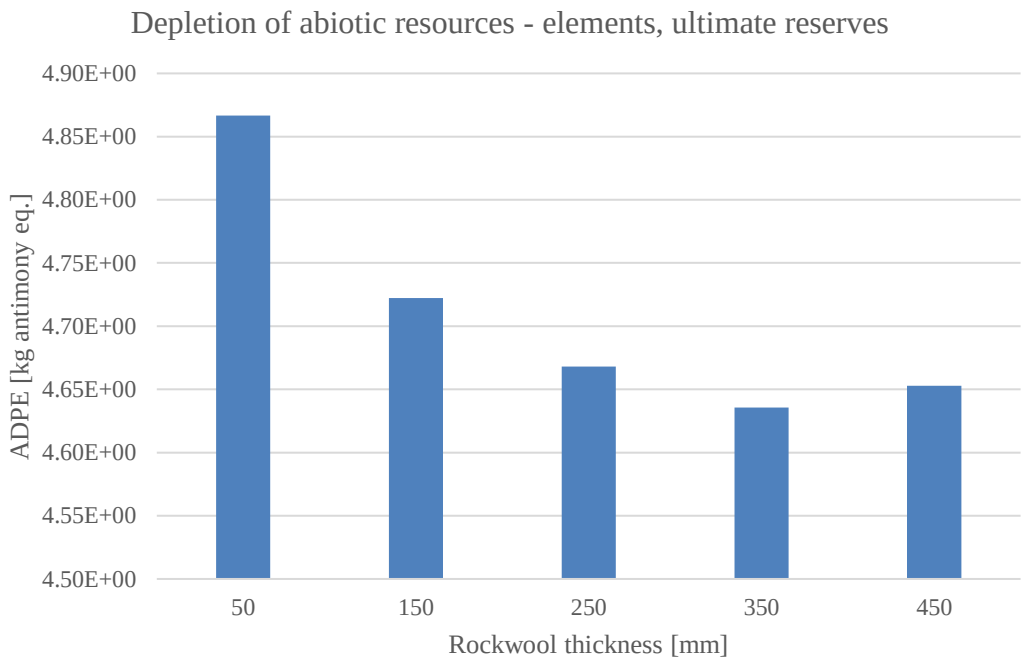

Figure 96: Environmental impact of depletion of abiotic resources - elements, ultimate reserves in LCA study of wall insulation in different thickness.

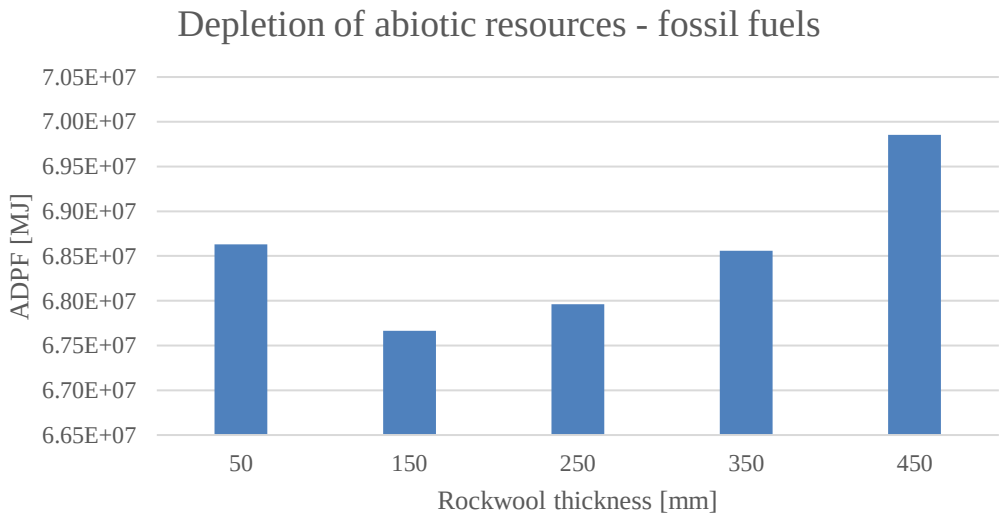

Figure 97: Environmental impact of depletion of abiotic resources - fossil fuels in LCA study of wall insulation in different thickness.

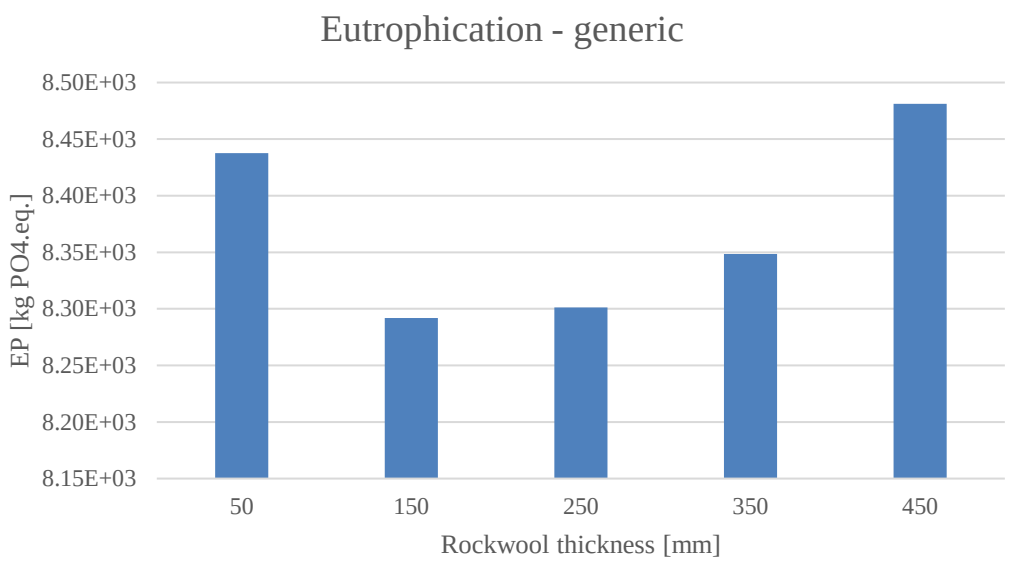

Figure 98: Environmental impact of eutrophication in LCA study of wall insulation in different thickness.

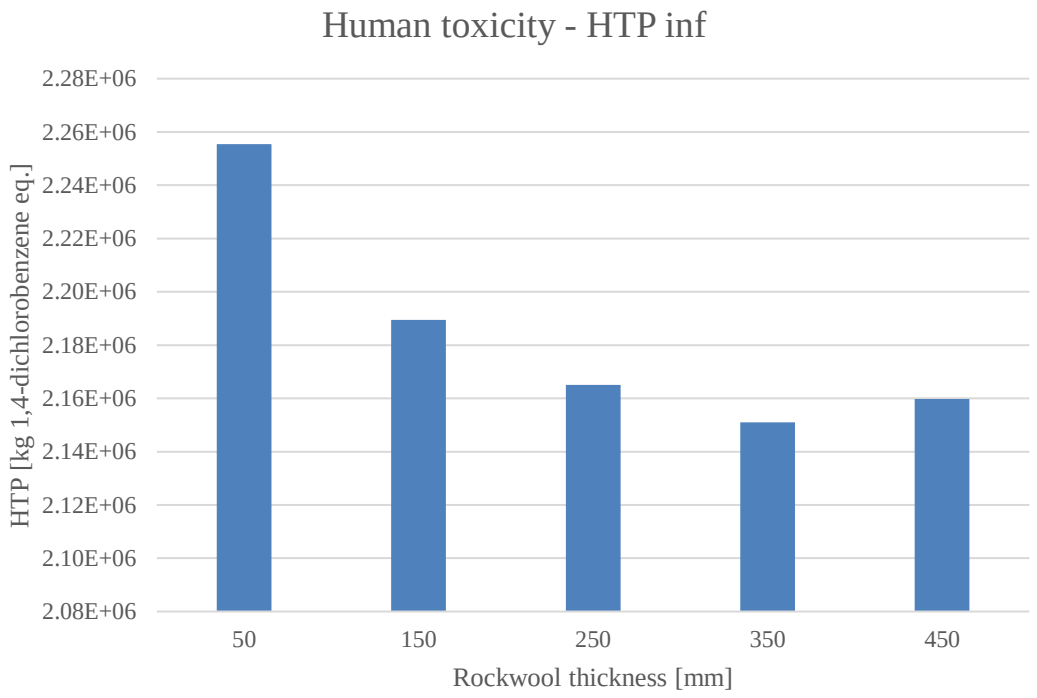

Figure 99: Environmental impact of human toxicity in LCA study of wall insulation in different thickness.

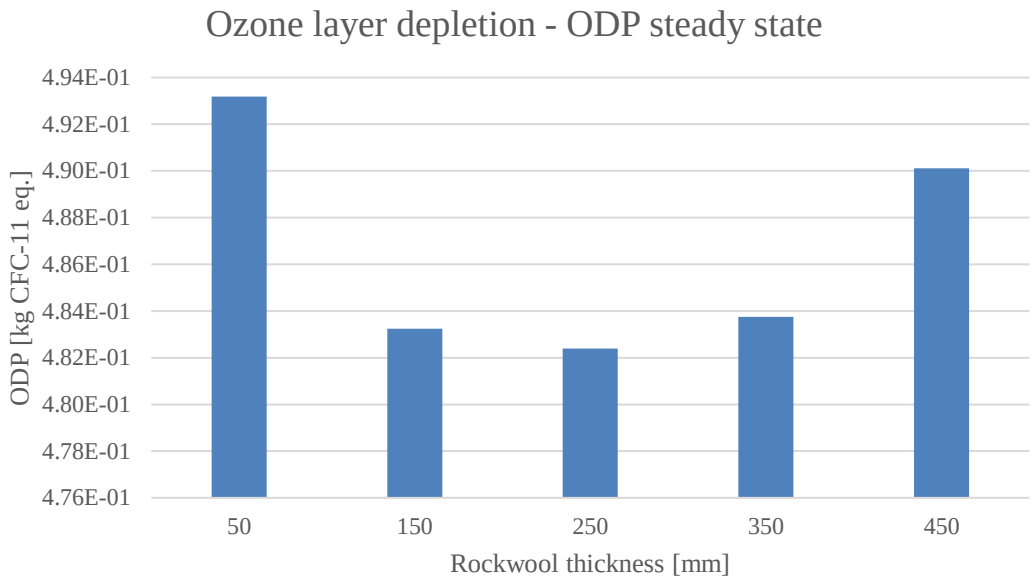

Figure 100: Environmental impact of ozone layer depletion in LCA study of wall insulation in different thickness.

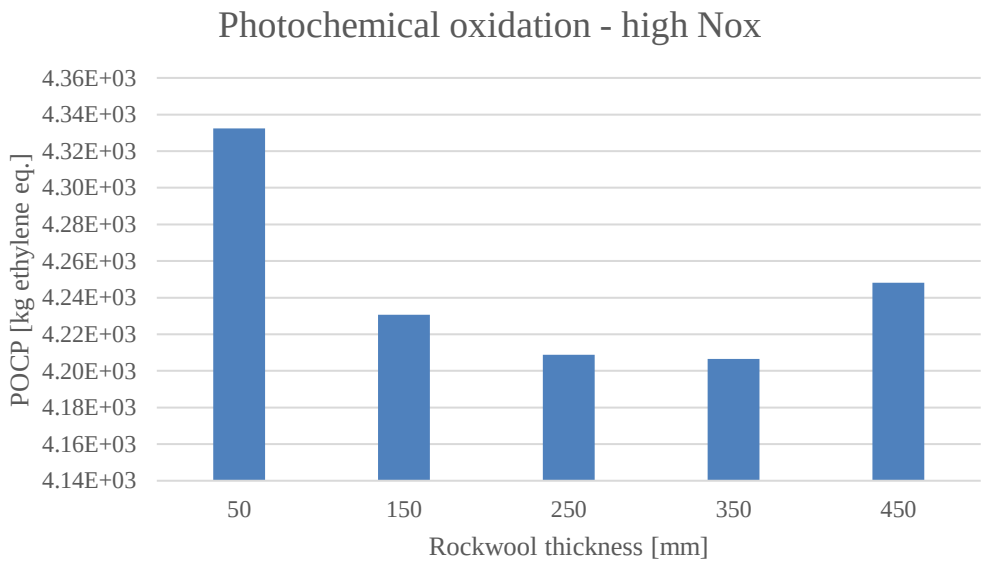

Figure 101: Environmental impact of photochemical oxidation in LCA study of wall insulation in different thickness.

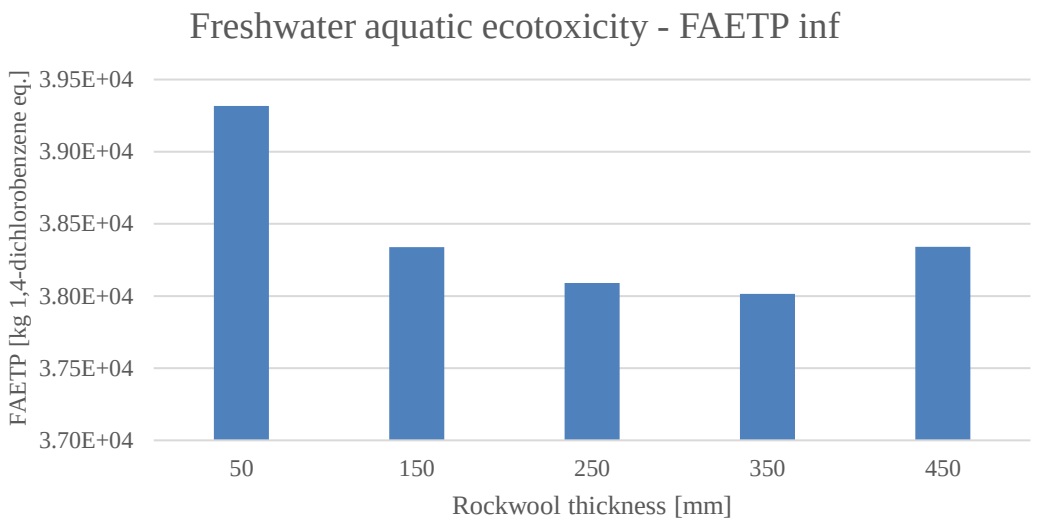

Figure 102: Environmental impact of Freshwater aquatic ecotoxicity in LCA study of wall insulation in different thickness.

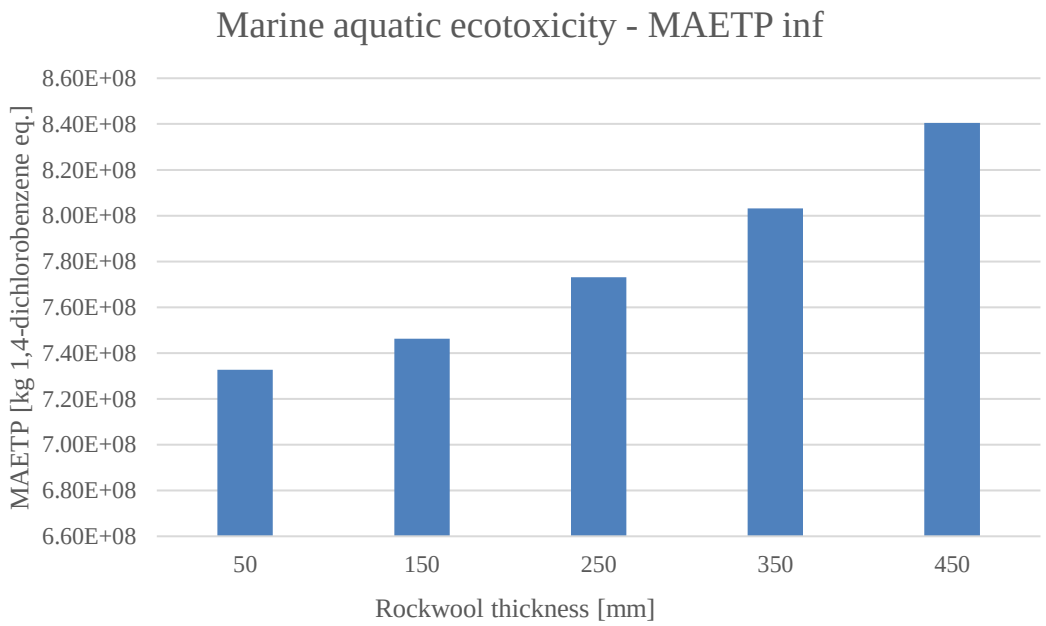

Figure 103: Environmental impact of marine aquatic ecotoxicity in LCA study of wall insulation in different thickness.

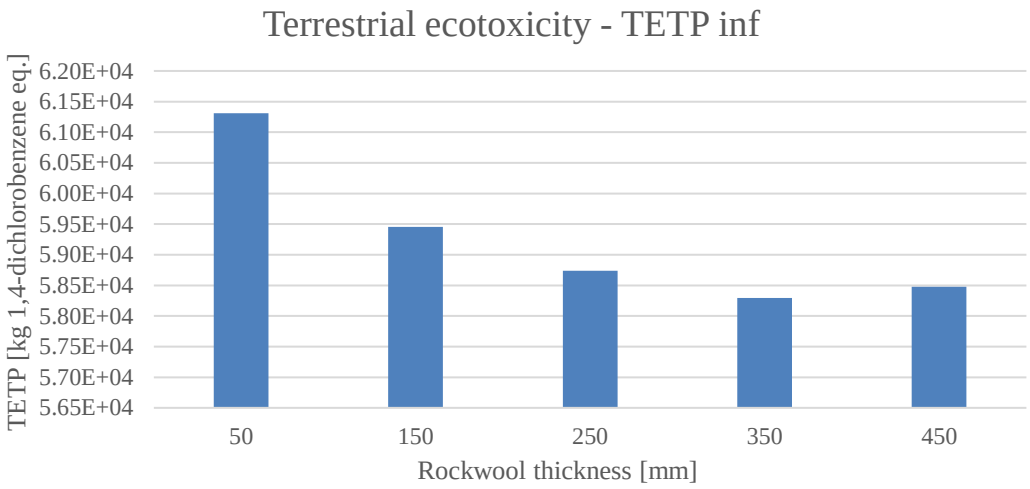

Figure 104: Environmental impact of terrestrial ecotoxicity in LCA study of wall insulation in different thickness.

To sum up all result above, optimal Rockwool thickness for 11 types of environmental impacts is showed in figure 105. Thickness of 350mm is optimal for 5 types of environmental impacts and thickness of 150mm is optimal for 4 types of environmental impacts.

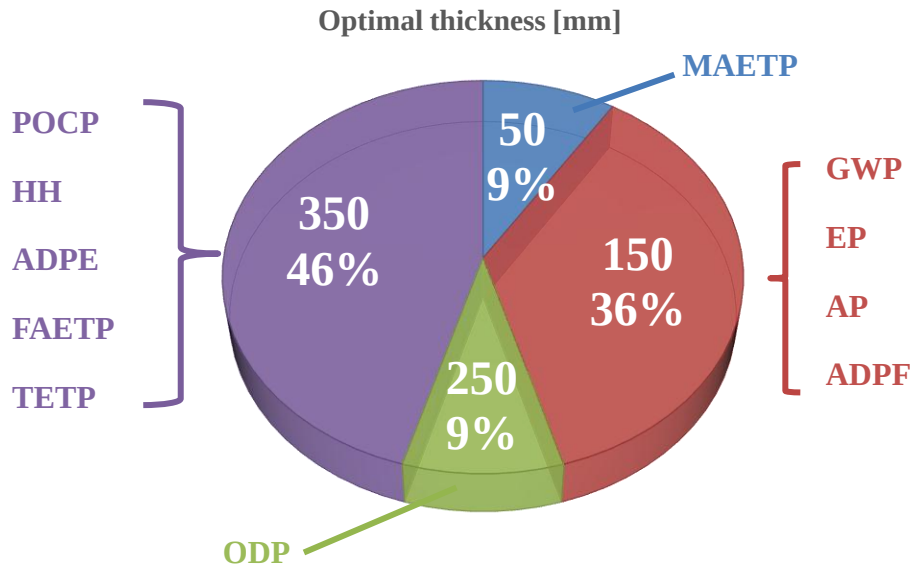

Figure 105: Optimal Rockwool thickness for 11 types of environmental impacts.

For comparison purposes, the results of all above mentained impacts have also been normalized to shadow cost. Figure 106 below shows the total shadow cost for environmental impact. The results showed that thickness of 150mm would result in the lowest shadow cost of approximately 1.15 million SEK during the 50-year period from the LCA. Thickness of 250mm has the value which is 0.4% higher than thickness of 150mm has.

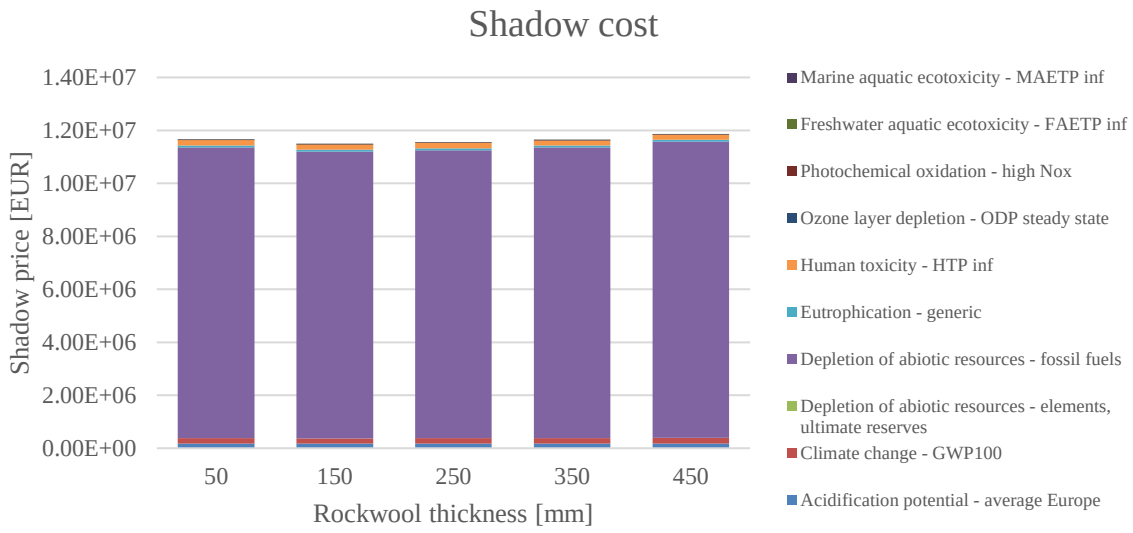

Figure 106: Shadow cost for environmental impact in LCA study of wall insulation in different thickness.

5 Discussion

5.1 Energy performance

5.1.1 Energy consumption variation

In energy consumption calculation part, energy performance of the IKDC and M-huset in current climate and future climate were estimated. In current climate, as the IKDC was built almost 40 years later than M-huset and it has big glazed windows outside the restaurant and corridors, better thermal insulation and higher solar radiation lead to a 20% lower heating demand and 10% lower electricity demand but two times higher cooling demand per unit area than M-huset. For future climate scenario, weather files for typical downscale year (TDY), extremely cold year (ECY), extremely warm year (EWY), as well as a series called "Triple" which is a combination of energy consumption result in TDY, ECY and EWY scenarios were applied for simulations during period 2009-2038, 2039-2068 and 2069-2098. The similar results "Triple" series and TDY series had indicates that TDY scenario has its representativeness for the future energy consumption variations. For both buildings, results all indicate that heating and cooling consumption in future scenarios would reduce and increase respectively, which may due to the global warming effect. After 90 years, the heating energy consumption would decrease by 9% from today for modern building with good insulation like the IKDC, and 38% for old building with weak insulation as M-huset. Meanwhile, the cooling demand would increase by 14% for modern building with good insulation like the IKDC and almost twice higher for old building with weak insulation as M-huset. Energy saving and environment protection are of great urgency.

5.1.2 Energy saving

In parametric simulation of energy saving part, several retrofitting measures for energy saving were applied to M-huset, including adding insulation material to old walls, changing windows and frames, adjusting heating and cooling set point, applying high-efficient heat recovery system, and adding shading device.

Renovating building envelope is always the most common measure that would be taken for energy saving in old buildings. Putting the influence on energy saving first, adding insulation material to old walls have significant effect on decrease heating demand as the annual heating demand could reduce by 16% when applying it to M-huset. However, it would increase cooling demand by 4.8 % as well, which may lead to an overheating problem in future. From economic point of view, the investment of retrofitting walls is hard to payback even in 200 years. Meanwhile, using new

windows and frames have slight effect on energy saving compared with other measures as the annual heating demand reduced by 9%. Same as adding insulation material to old walls, changing windows also need a hefty amount of investment and would be hard to payback in near future. Moreover, if building envelope renovating is applied, it need a slightly long time for construction which may affect the daily operation of the building. Thus, renovating building envelope is not a recommended method if the fund is shortage.

Besides, it is important to consider the thickness of new materials when renovating building envelope. As two flows presenting different insulation materials and yearly energy consumption were considered in LCA study, the effect on environment would be decided by both parameters. The effect on environment from the energy consumption is more important than the effect from the material itself when slight amount of material was applied. This is indicated by LCA results of the case corresponding to "50 mm" insulation. Due to the fact that the energy consumption is very high when 50 mm insulation was used, this case showed the highest values for all impact categories except for marine aquatic ecotoxicity. Then, with the thickness of the insulation material increasing, the values for all environmental impact categories except marine aquatic ecotoxicity showed a decreasing trend. For acidification potential, climate change, eutrophication, and depletion of abiotic resources - fossil fuels, case "150 mm" is the optimal one as it has the lowest values; For Ozone layer depletion, thickness of 250 mm is the best choice. Starting from "350mm", some categories like human toxicity, Freshwater aquatic ecotoxicity, photochemical oxidation, terrestrial ecotoxicity, and depletion of abiotic resources-elements, ultimate reserves of impacts show different results. Thickness of 350 mm becomes the optimal one, as the amount of material determines trend to a higher extent than energy. Overall, 150 mm and 350 mm are better than other thickness. However, thickness of 150 mm insulation of rock wool is not thick enough for cold climate in Lund and energy consumption is much higher than the wall with 350 mm insulation. Whereas, thickness of 350 mm has slightly high negative effect on acidification potential, climate change, and eutrophication which are environmental problem frequently concerned by the whole society spanning group differences. Take all aspects into account, thickness of 250 mm would be recommended in this LCA study for adding insulation materials to old walls in M-huset, as it is thick enough for cold climate and for total shadow value it is only 0.4% higher than the thickness of 150 mm.

Adjusting HVAC system is another common measure that would be taken for energy saving in old buildings. Adjusting heating and cooling set point, simply operations like reducing 1℃ heating set point and increasing 1℃ cooling set point, the heating consumption and cooling consumption would reduce by 20% and 28% respectively. To find optimal temperature for heating and cooling set point for the

building, it is needed to run parametric simulations for real cases. However, real situation of heating and cooling set point or HVAC settings in M-huset and the IKDC are not provided, parametric study of optimal temperature for heating and cooling set point has not be done in this study. Moreover, applying high-efficient heat recovery also have considerable influence on energy savings, as improving 20% heat recovery rate would decreasing heating consumption by 21%. However, applying high-efficient need investment in innovative technology and waiting for developments. If the AHU used now is from old ages, it is recommended to changing to a new AHU for energy saving. Whereas, same as heating and cooling set point, the AHU information for M-huset and IKDC were not provided for this paper.

For the overheating problem that may occur in future climate, adding more shading device would be a good measure as after adding more shading device on walls in south and west side in M-huset, the annual cooling consumption would decrease by 20%. If fund is enough, installing the movable shading device would have even better performance on energy saving.

5.2 Renewable energy potential assessment

5.2.1 Solar energy

Plenty of roofs and several walls on the buildings in LTH campus like A-huset, M-huset, V-huset, E-huset, IKDC, Kemicentrums and so on, green areas, and parking lots all have enough solar potential to install PV panels as the annual solar radiation are over 800 kWh/m^2. However, for building protection and visual appearance, visible roofs and walls are not suitable for PV installations. Besides, due to some new land use plan like metro project would appear in Lund in the far future, parking lots and green areas have the possibility of reprofiling. Thus, invisible roofs are the only and best choice for PV installations. Moreover, LTH campus has its own grid connections, the electricity would never be overproduced as the extra part could be delivered to wherever it is needed. Thus, it is hard to give an optimal proposal of the quantity of PV panels is needed to satisfy the demand. However, from the result of parametric simulation covering different coverage proportion of energy consumption in M-huset, some advices could be draw. The energy consumption in M-huset during May to August could be totally covered by PV panel with 7 times bigger scale of the PV already installed, which is possible as M-huset still have plenty of unused roof area. But to cover energy consumption in M-huset during the entire year by PV panel, 93 times bigger scale of the PV already installed would be needed, which is impossible as area limitation. Also, it indicates that energy consumptions in summer is easy to cover but the energy consumption in winter is hard to reach. Meanwhile, the day time is short and the solar radiation is weak in winter in Sweden.

Thus, from energy saving and money saving point of view, it would be suggested to install enough PV panels to cover summer energy consumption if space allowed. Technological innovation of higher generation in winter in future is long-cherished.

Besides, the PV module materials has considerable influence on PV generations. In the parametric simulations of three different PV module types, Monocrystalline has the highest efficiency and generation among these three module types, which has 16% more annual PV generation than polycrystalline and 2.3 times more annual PV generation than Amorphous. However, the digital model used to assess three different module types was proposed in 2012, innovative technology has rapidly developed. The mentioned technologies in literature review like Copper Indium di-Selenide (CIS), Hetero-junction with Intrinsic Thin layer (HIT), Cadmium telluride (CdTe) and concentrator would have superior performance. Local climate is also an important parameter affects the performance of PV modules.

Moreover, the inclined angle of the PV modules also has noteworthy influence on PV generations as different months have different optimal titled angle. From the annual electricity generation point of view, 40 degrees inclination shows the highest annual energy output. However, with the technology developed, movable PV modules which could change inclined angles following seasons is become popular. The performance of movable PV modules would be even better than the fixed 40 degrees PV modules.

To explain the result that PV power, monthly PV generation and annual PV generation are varied from time to time in future scenarios, a logical reason would be that the solar radiation variations are random changes, which are not based on an established or cycled rule. This on the contrary shows the stability and sustainability of PV systems as it would not have a great extent influence by future climate change.

From an economic point of view, investment in PV panels is possible to be paid back in 15 years without inverter change and 16 years with inverter changes every ten years approximately. Also, higher energy price together with the technology development of PV efficiency, the payback time would be shorter in future. However, inverter changes and other unmentioned cost would make the payback time slightly longer. After all, investment in PV panels is worth from both economic profit and environment protection point of view.

5.2.2 Wind energy

According to the analysis, for more than 50% of time the wind speed is between 3.6 to 8.8 m/s in the reference year, which would play a decisive role when accessing wind potential. When applying local wind speed to wind turbine generations, the result is slightly higher than the production category suggested value, which means

local wind condition has enough potential to install wind turbines. For future climate, as the interquartile range of wind speed would change to a lower interval as time goes by, the power generation of wind turbine would decrease in future. Thus, wind turbine technique need quick development to face the undesirable weather condition in future.

Vertical wind turbine Aeolos V-10 KW shares the same shape and size with Aeolos V-5KW but doubled rated power. However, Aeolos V-10 KW performs poorer than Aeolos V-5 KW when wind speed is less than 10.5 m/s, which speed interval is the major wind speed variation during the year. The reason why the incomprehensible situation appears may concern about the operating principle of vertical wind turbine.

5.2.3 Shallow geothermal energy

G.POT method is a preliminary but useful method to assessing shallow geothermal potential. Although real geographical condition inside campus is unknown, estimation of the assumed geographical condition based on literature and geothermal report of the south Sweden showed a strong application potential of ground source heat pump. The excellent performance of the already installed ground source heat pump system inside campus is a strong evidence. For the affecting parameters of shallow geothermal potential in G.POT method, parametric study shows that higher thermal conductivity of the ground, higher thermal capacity of the ground, longer borehole, longer heating or cooling season, bigger borehole radius, and shorter simulation time would lead to a higher shallow geothermal potential. However, numbers of other unmentioned parameters would also affect geothermal potential. Detailed ground source heat pump system would be needed for further research.

5.3 Limitation

Hourly realistic data received from Academic Hus, such as heating, cooling and electricity consumption, PV generation, solar radiation and so on, was not recorded for complete 8760 hours. Some hours in some days was missing. By using the data in the day before the missing day, the missing data was generated by linear interpolation. Some admissible errors would arise when hourly data was needed to do comparison between realistic data and simulation results due to the uncertainties in measuring and recording data.

For IDA ICE calculations, a lot of input data like heating and cooling set points, supply air temperature etc. were set based on logical assumptions. Only conclusive results like heating and cooling consumption, and total electricity consumption were adjusted with the realistic measured data. However, various uncertain parameters would have positive or negative effect on the conclusive results. The unknown

counteraction may make the simulation model be slightly different with the real buildings.

For solar energy assessment, the effect of snow was not considered, since no detailed data of snow coverage rate in Lund was found. However, snow is inescapable and would have negative effect on PV generation. Also, when doing LCC study, the investment costs tanks, piping system, transportation, labor and maintenance were not taken into consideration for this study, which would extend the payback time.

For wind turbine, although horizontal blade wind turbine has high efficiency and less environmental burden, it is not available to be used in a narrow building blocks due to land limitation. Vertical blade wind turbine has low noise and small size, while the electricity generation is not large enough to satisfy the whole energy consumption for campus buildings.

For shallow geothermal energy assessment, as G.POT method is a simplified model and there is no specific or certain modelled ground source heat pump system were designed in this paper, few potential affecting parameters were not taken into consideration. Thus, if detailed estimations are needed, design an integrated system would be the first step.

6 Conclusion

Regarding to assessing the potential of applying energy saving measures, adding insulation material to old walls, adjusting heating and cooling set point in HVAC system, applying high-efficient heat recovery system and adding shading devices all have considerable effect on energy savings. It is also important to consider environmental protection and economic profits together with local climatic condition when choosing retrofitting methods for buildings. For example, when adding insulation material to M-huset in Lund, the thickness of 250mm rock wool would be recommended in case study as it has lower environment burden and suitable energy saving for cold climate. Meanwhile, adding insulation material to old walls and using new windows and frames would need a hefty amount of investment and hard to be paid back in near future.

From assessing the potential of adding renewable energy resources perspective, the campus of Lund University has enough potential to applying solar, wind and shallow geothermal energy resources by installing PV panels, small-scale wind turbines and ground source heat pump. Through parametric simulations of renewable energy resource applications, several conclusions also have been drawn. For solar energy, PV module materials like monocrystalline has the highest efficiency and generation than polycrystalline and amorphous. Moreover, when the PV modules are fixed, 40 degrees of inclination shows the highest annual power generation. Besides, as LTH campus has its own grid connections, it is hard to give an optimal proposal of the quantity of PV panels to satisfy the demand. However, from coverage proportion of view, covering energy consumptions in summer would be recommended, as to cover the electricity consumption in M-huset, only seven times bigger scale of the PV already installed would be need. Whereas, the energy consumption in winter is hard to reach for space limitation as to cover energy consumption in M-huset during the entire year by PV panel, 93 times bigger scale of the PV already installed would be needed. For wind energy, big scale and horizontal blade wind turbines has higher efficiency, shorter investment payback time, and lower environmental burden than small-scale and vertical blade wind turbines. However, space limitation and acoustic pollution makes the small-scale wind turbines become the optimal choice when applying wind energy inside the campus. For shallow geothermal energy, G.POT method is a preliminary but useful method to assess the potential of application. Although local ground condition is hard to change, deeper and bigger boreholes would lead to a higher shallow geothermal potential.

Moreover, for future climatic condition, heating and cooling energy consumption would reduce and increase respectively, which follows the phenomenon of global warming. Besides, future climatic condition would not have huge or certain influence on renewable energy applications. Although majority of wind speed would

slightly lower down in future, no certain variation trend was find for solar energy and shallow geothermal energy in this thesis.

7 Further Research

For energy saving, further research could be focus on the the innovative retrofitting techniques with building automation and control or artificial intelligence, such as air quality control sensor, occupancy sensor, heating or cooling autocontrol device, movable shading device and so on.

For renewable energy resource, only solar, wind and shallow geothermal energy were discussed in this thesis. Other renewable energy resourece like biomass, hytro, tidal energy and so on are also deserved to do research. Other method to use renewable energy is also worth to be researched. For example, for solar energy, not only solar PV systems but also the solar thermal, concentrated solar power, solar heating, solar refrigeration and so on are worth for further research. Also, some solar technology combined systems like producing heating, cooling and electricity together are good options to do researches in future. Besides, Other PV materials like CdTe, CIS, HIT, a-3j-Si are needed to be taken into further research. Moreover, technology developments of the application of renewable energy resource is urgently needed. Such as improving energy generation efficiency, solving the problem of noises.

8 Summary

Several problems concern about energy are frequently discussed in recent decades, such as the shortage of traditional energy resource, the increase of energy price and the destruction of living environment by energy conversion. Besides, with the rapid growing demand of housing, the energy consumptions of buildings increase dramatically, which is equivalent to approximately 48% of total energy use in Sweden. Meanwhile, traditional energy resources like coal and oil are still the main resources to produce both thermal energy and electricity. Moreover, since Sweden is located in high latitudes with extreme cold climatic condition, more heating energy consumption would be needed to keep a satisfied indoor environment. Phenomenon above lead sustainable development of energy become a preferential task in Sweden.

Under current circumstances, applying energy saving measures and using renewable energy resource are two of the best choices. The main objective of the study is to assess the potential of applying energy saving measures and adding renewable energy resources for both current and future climatic conditions in the campus of Lund University in Sweden. The scope of this project is to investigate the energy performance of two object buildings for current and future climatic conditions as well as considering the potential of applying possible retrofitting techniques. The two buildings are the IKDC and M-huset, both are a part of the LTH in Lund. M-huset was built in 1960s and it was regarded as a representative of old construction in this study. The IKDC was built in 2002 and it was considered as a typical modern construction for comparison with M-huset. Besides, the potential assessment of adding renewable energy resources performing for the whole buildings in the LTH campus is also investigated for current and future climatic conditions. Also, the study of Life Cycle Cost and Life Cycle Assessment were carried out for long-term economic profit and environmental protection point of view.

Five phases were carried out in this study. First, literature review phase was done for energy saving techniques, renewable energy resource applications, life cycle cost and life cycle assessment. Second, heating and cooling energy consumption calculations towards two object buildings were performed for both current and future climatic conditions in IDA ICA. Future climatic conditions were simulated based on the TDY, ECY and EMY weather file for the period of 2009-2038, 2039-2068, and 2069-2098. Third, energy saving measures were applied and simulated for M-huset as a representative. Then, the potential of adding solar energy, wind energy and shallow geothermal energy for whole buildings inside the LTH campus were investigated through Rhinoceros, System Advisor Model, Autodesk Flow Design, WRPLOT View, and G.POT method, which were also estimated for both current

and future climatic conditions. Last but not least, the economic profit and environmental feasibility were estimated through life cycle cost and life cycle assessment for building retrofitting measures and renewable energy applications.

From the masses of results, several valuable conclusions were drawn. For applying energy saving measures perspective, results show that adding insulation material to old walls, adjusting heating and cooling set point, applying high-efficient heat recovery system, and adding shading device would have significant effect on decreasing heating or cooling energy consumption. It is also important to consider environmental protection and economic profits together with local climatic condition when choosing retrofitting methods for buildings.

From assessing the potential of adding renewable energy resources perspective, the campus of Lund University has enough potential to apply solar, wind and shallow geothermal energy resources by installing PV panels, small-scale wind turbines and ground source heat pump. For solar energy, PV module materials like monocrystalline has the highest efficiency and generation than polycrystalline and amorphous. Moreover, 40 degrees inclination of PV modules shows the highest annual power generation when modules are fixed. Besides, to cover the electricity consumption in M-huset only seven times bigger scale of the PV already installed would be need, which indicates it is possible since M-huset still have plenty of available roof areas. Whereas, the energy consumption in winter is hard to reach for space limitation. For wind energy, big scale and horizontal blade wind turbines have higher efficiency, shorter investment payback time, and lower environmental burden than small-scale and vertical blade wind turbines. However, space limitation and acoustic pollution makes the small-scale wind turbines become the optimal choice when applying wind energy inside the campus. For shallow geothermal energy, G.POT method is a preliminary but useful method to assess the potential. Although local ground condition is hard to change, deeper and bigger boreholes would lead to a higher shallow geothermal potential.

For future climatic condition, heating and cooling energy consumption would reduce and increase respectively, which indicates the same phenomenon as the trend of global warming. Besides, future climatic condition would not have huge or certain influence on renewable energy applications. Although majority of wind speed would slightly lower down in future, no certain variation trend was find for solar energy and shallow geothermal energy in this thesis.

9 Reference

Akademiskahus, 2017
http://www.akademiskahus.se/ Date: 02.05.2017

Anshelm, K.; Qvarnström, P. *Arkitekt Klas Anshelm: samlade arbeten*. Stockholm. 1998.

Atzeri, A.; Cappelletti, F.; Gasparella, A. *Internal Versus External Shading Devices Performance in Office Buildings.* Energy Procedia, 2014, 45, 463–472.

Atanasiu, B., Despret, C., Economidou, M., Maio, J., Ingeborg, N., & Raph, O. *Europe's buildings under the microscope-a country by country review on the energy performance of the buildings.* Buildings Performance Institute Europe (BPIE), October 2011.

AutoCAD, 2017
https://www.autodesk.com.cn/products/autocad/overview Date: 02.05.2017

Autodesk Flow Design, 2017
https://www.autodesk.com/education/free-software/flow-design Date: 02.05.2017

Baharwani, Vishakha; Meena, Neetu; Sharma, Arvind; Stephen, Richie B; Mohanty, Parimita. *Comparative Performance Assessment of different Solar PV Module Technologies*. In: International Journal of Innovations in Engineering and Technology, Vol 5, Iss 1 (2015); SN Education Society, 2015.

Beck, W.; Dolmans, D.; Dutoo, G.; Hall, A.; Seppänen, O. *Solar Shading—How to Integrate Solar Shading in Sustainable Buildings*, 1st ed.; REHVA: Brussels, Belgium, 2010.

Berggren, B., & Wall, M. *Thermal bridges in passive houses and nearly zero-energy buildings.* In 4th Nordic Passive House Conference, 2011.

Bilal, B. Ould; Ndongo, M.; Kebe, C.M.F.; Sambou, V.; Ndiaye, P.A. *Feasibility study of wind energy potential for electricity generation in the northwestern coast of Senegal.* In: Proceedings of TerraGreen 13 international conference 2013 – advancements in renewable energy and clean environment; 2013. p. 1119–29.

Bjelm, L. and Schärnell, L.: *Large heat pump plants for district heating utilizing geothermal energy. Lund Institute of Technology*, Dept. Of Engineering Geology

and Stal Laval Turbin AB, Finspång. International symposium on Geothermal Energy. Portland, USA,1983.

Boer, K.W. *Cadmium sulfide enhances solar cell efficiency.* Energy Conversion and Management 2011; 52:426–30.

Boverket, *Regelsamling för byggande, BBR, 2015 (Swedish),* 20/ 02 /2016. [Online]. Available: http://www.boverket.se/globalassets/publikationer/dokument/2015/regelsamling-for-byggande-bbr-2015.pdf.

Carletti, Cristina; Sciurpi, Fabio; Pierangioli, Leone. *The Energy Upgrading of Existing Buildings: Window and Shading Device Typologies for Energy Efficiency Refurbishment.* In: Sustainability, Vol 6, Iss 8, Pp 5354-5377 (2014); MDPI AG, 2014.

Carneiro, C. *Extraction of urban environmental quality indicators using LiDAR-based Digital Surface Models.* E´cole Polytechnique Fe´de´rale de Lausanne, PhD thesis. 2011.

Carr, A. J; Pryor, T.L; *A comparison of the performance of different PV module types in temperate climates*; Solar Energy, 2004, 76, 285–294.

Carslaw, HG.; Jaeger, JC. *Conduction of heat in solids.* Cambridge, UK.1959.

Casasso, Alessandro; Sethi, Rajandrea. *G.POT: A quantitative method for the assessment and mapping of the shallow geothermal potential. In Energy.* 1 July 2016 106:765-773

Casasso, Alessandro; Sethi, Rajandrea. *Modelling thermal recycling occurring in groundwater heat pumps (GWHPs)*, Renew. Energy, 2015, 77, 86-93.

Casasso, Alessandro; Sethi, Rajandrea. *Efficiency of closed loop geothermal heat pumps: a sensitivity analysis*, Renew. Energy, 2014, 62, 737-746.

CDIT. *Technology manual of offshore wind power.* CDIT; 2001 [in Japanese].

CEN. *The European Standard EN 15251*. Brussel, 2007

Chevalerias, Marie. *Assessing environmental impact of building materials using the Dutch approach-The case of the Triodos bank office building using BREEAM.NL*. Master Thesis in Energy-efficient and Environmental Buildings Faculty of Engineering of Lund University, 2015.7

Claesson, J.; Eskilson, P.; *Conductive heat extraction to a deep borehole: thermal* analyses and dimensioning rules. In Energy. 1988. 13(6):509-527

Compagnon, R. *Solar and daylight availability in the urban fabric.* Energy and Buildings. 2004. 36(4), 321-328.

Cuce, Erdem. *Role of airtightness in energy loss from windows: Experimental results from in-situ tests.* In Energy & Buildings. 15th March 2017. 139:449-455

Dahmouni, AW.; Salah, MB.; Askri, F.; Kerkeni, C.; Nasrallah, SB. *Wind energy in the Gulf of Tunis, Tunisia.* Renew Sustain Energy Rev 2010;14(4):1303–11.

De Bruyn, S. et al. *Shadow Price Handbook, Valuation and weighting of emissions and environmental impacts.* Delft: CE Delft. .2010

Duffie, J.A.; Beckman, W.A. *Solar engineering of thermal processes.* 2: a upplagan. John Whiley & Sons, Inc. 2013

Durisch, W.; Bitnar, B.; Mayer, J-C.; Kiess, H.; Lam, K-hang.; Close, J. *Efficiency model for photovoltaic modules and demonstration of its application to energy yield estimation.* In Solar Energy Materials & Solar Cells. 2007. 91:79-84.

Elhadidy, MA; Shaahid, SM. Parametric study of hybrid (wind+solar+diesel) power generating systems. Renew Energy 2000; 21:129–39.

Ellabban, Omar; Abu-Rub, Haitham; Blaabjerg, Frede. *Renewable energy resources: Current status, future prospects and their enabling technology.* Renewable and Sustainable Energy Reviews. 2014. 39.: 748–764.

Emmi, G.; Zarrella, A.; DeCarli, M.; Galgaro, A. *An analysis of solar assisted ground source heat pumps in cold climates*, Energy Conversion and Management, 2015.vol. 106, pp. 660–675.

Energiforsk. *European district heating price series.* Report 2016:316. ISBN 978-91-7673-316-5. Could be download from: www.energiforsk.se

Energimyndigheten. *Läget på elmarknaden Vecka 9 år 2017.*
Could be download from: www.energimyndigheten.se

Energy in Sweden 2015. Swedish Energy Agency ET015:19. December 2015. energy-in-sweden-till-webben.pdf .

European Commission. *ILCD Handbook (International Reference Life Cycle Data System), Analysis of existing Environmental Impact Assessment methodologies for use in Life Cycle Assessment*. European Commission, DG-JRC. 2010.

Fridleifsson, I.B. *Geothermal energy for the benefit of the people.* In Renew. Sustain. Energy Rev. 5, 2001, 299–312.

Frischknecht, R.; Itten, R.; Wyss, F.; Blanc, I.; Heath, G.; Raugei, M.; Sinha, P.; Wade, A.; *Life cycle assessment of future photovoltaic electricity production from residential-scale systems operated in Europe*, Subtask 2.0 "LCA", IEA-PVPS Task 12. 2014.

Fu, P.; Rich, P.M. *Design and implementation of the solar analyst: an ArcView extension for modeling solar radiation at landscape scales.* In: Proc. IX Annual ESRI User Conference. 1999.

Gehlin, Signhild; Andersson, Olof. *Geothermal Energy Use, Country Update for Sweden.* European Geothermal Congress 2016, Strasbourg, France, 19-24 Sep 2016.

Grasshopper, 2017
http://www.grasshopper3d.com/ Dated: 02/05/2017

Greening, Benjamin; Azapagic, Adisa. *Environmental impacts of micro-wind turbines and their potential to contribute to UK climate change targets.* In Energy. 15 September 2013. 59:454-466

Guezuraga, B.; Zauner, R.; Polz, W. *Life Cycle Assessment of Two Different 2 MW Class Wind Turbine.* Renewable Energy, 2011, 37, 37-44. http://dx.doi.org/10.1016/j.renene.2011.05.008

Haapala, K.R.; Prempreeda, P. *Comparative life cycle assessment of 2.0 MW wind turbines*, Int. J. Sustainable Manufacturing, Vol. 3, No. 2, 2014. pp.170–185.

Higgins, P.; Foley, A. *The evolution of offshore wind power in the United Kingdom.* Renew Sustain Energy Rev 2014; 37:599–612.

Hofierka, J.; Su ́ri, M. *The solar radiation model for Open source GIS: implementation and applications.* In: Proceedings of the Open source GIS – GRASS Users Conference. Trento, Italy, 11–13 September 2002.

Hofierka, J.; Kanuk, J. *Assessment of photovoltaic potential in urban areas using open-source solar radiation tools.* Renewable Energy 34, 2009. 2206–2214.

Huld, T.; Gottschalg, R.; Beyer, H. G.; Topic, M. *Mapping the performance of PV modules, effects of module type and data averaging*; Solar Energy 84 (2010) 324–338

IDA ICE, 2017. http://www.equa.se/en/ Date:02/05/2017
IEA. *Technology roadmap—wind energy.* 2013 edition. Paris: IEA; 2013. p.1–53.

Jakubiec, J.A., Reinhart, C.F. *A Method for Predicting City-Wide Electricity Gains from Photovoltaic Panels Based on LiDAR and GIS Data Combined with Hourly Daysim Simulations.* Solar Energy. 2013. 93, 127-143.

Jaramillo, P.; Griffin, W.; Matthews, H. *Comparative life-cycle air emissions of coal, domestic natural gas, LNG, and SNG for electricity generation.* Environ Sci Technol. 2007. 41(17):6290–6296

Jensen, Nickolaj Feldt. *Hygrothermal Analysis of Retrofitted Buildings in the campus of Lund university.* Master thesis in Energy-efficient and Environmental Buildings, Faculty of Engineering, Lund University, 2016.

Ji, W.; You, T.; Bai, S.; Shi, W.; Wang, B. *Effects of ground heat exchanger design parameters on performance of ground-source heat pump systems in cold zone*, Journal of HV&AC, no. 3, pp.113–118, 2015.

Kabir, M.R.; Rooke B.; Dassanayake, M.; Fleck, B.A. *Comparative Life Cycle Energy, Emission, and Economic Analysis of 100 kW Nameplate Wind Power Generation.* Renewable Energy, 2012, 37, 133-141.
http://dx.doi.org/10.1016/j.renene.2011.06.003

Kanters, J; Dubois, M.-C; Wall, M. *Architects' design process in solar-integrated architecture in Sweden.* Architectural Science Review, May 2013, Vol. 56 Issue 2, p141-151,

Kanters, J; Wall, M. *The impact of urban design decisions on net zero energy solar buildings in Sweden.* In: Urban, Planning and Transport Research, Vol 2, Iss 1, Pp 312-332 (2014); Taylor & Francis Group, 2014.

Kanters, J., Wall, M., Kjellsson, E. *The solar map as a knowledge base for solar energy use.* In: Energy Procedia, Proceedings of the 2nd International Conference on Solar Heating and Cooling for Buildings and Industry (SHC 2013). 48:1164-1606; Elsevier, 2014.

Karlsson Björn, Gustafssona Mattias, Rönnelidc Mats, Tryggd Louise, *CO2 emission evaluation of energy conserving measures in buildings connected to a*

district heating system-case study of a multi-dwelling building gin Sweden. Original Research Article: Energy, volume 111, 15 September 2016 pages 341-350.

Kealy, Tony. *Stakeholder outcomes in a wind turbine investment; is the Irish energy policy effective in reducing GHG emissions by promoting small-scale embedded turbines in SME's?* Renewable Energy. February 2017 101:1157-1168

Ko, Dong Hui; Jeong, Shin Taek; Kim, Yoon Chil. *Assessment of wind energy for small-scale wind power in Chuuk State, Micronesia.* Renewable and Sustainable Energy Reviews. December 2015 52:613-622

Koroneos, Christopher J.; Nanaki, Evanthia A. *Environmental impact assessment of a ground source heat pump system in Greece.* Geothermics. Jan 2017, Vol. 65, p1-9. 9p. DOI: 10.1016/j.geothermics.2016.08.005.

Kraftringen, 2012
https://www.kraftringen.se/Privat/solceller/solkartan/ Dated: 2012

Langer, S., Bekö, G., Bloom, E., Widheden, A., & Ekberg, L. *Indoor air quality in passive and conventional new houses in Sweden.* Building and Environment. 2015. 93, 92-100.

Larsson, Anders. *Vindkraft-något det blåser om.* Örebro universitet, instiutionen for naturvetenskap, 2003.

Ladybug, 2017
http://www.grasshopper3d.com/group/ladybug Dated: 02/05/2017

Lee, ME; Kim, G.; Jeong, ST; Ko, DH; Kang, KS. *Assessment of offshore wind energy at Younggwang in Korea.* Renew Sustain Energy Rev 2013; 21:131–41.

Lukac, N; Seme, S; Zlaus, D; Stumberger, G; Zalik, B. *Buildings roofs photovoltaic potential assessment based on LiDAR (Light Detection and Ranging) data*, Energy 2014. 66. 598-609.

Lund, J.W.; Boyd, T.L. *Direct utilization of geothermal energy 2015 worldwide review.* In: Proceedings, World Geothermal Congress 2015, Melbourne, Australia, April 20–25, 2015, p. 31.

Lunds Tekniska Högskolan, 2017
http://www.lth.se/english Dated: 02/05/2017

Makrides, G; Zinsser, B; Norton, M; Georghiou, G.E; Schubert, M; Werner, J.H. *Potential of photovoltaic systems in countries with high solar irradiation*; Renewable and Sustainable Energy Reviews 2010;14,754-62.

Martinez, E.; Sanz, F.; Pellegrini, S.; Jimenez, E.; Blanco, J.; *Life cycle assessment of a multimegawatt wind turbine*. Renew Energy. 2009a. 34(3):667–673

Martinez, E.; Sanz, F.; Pellegrini, S.; Jimenez, E.; Blanco, J.; *Life-cycle assessment of a 2-MW rated power wind turbine: CML method.* In Life Cycle Assess. 2009b. 14(1):52–63

Mata Érika, Sasic Kalagasidis Angela, Johnsson Filip, *Retrofitting measures for energy savings in the Swedish residential building stock – assessing methodology.* In 11th International Conference on Thermal Performance of the Exterior Envelopes of Whole buildings, Building XI; Sheraton Sand Key Resort in Clearwater Beach Clear water; United States; 5 December 2010 through 9 December 2010.

Miguel, AD; Bilbao, J.; Kambezidis, H.; Negro, E. *Diffuse solar irradiation model in the north Mediterranean Belt area.* In Solar Energy. 2001. 70:143-153.

Munir, N.B., Huque, Z. and Kommalapati, R.R. *Impact of Different Parameters on Life Cycle Analysis, Embodied Energy and Environmental Emissions for Wind Turbine System.* Journal of Environmental Protection, 7, 2016. pp 1005-1015. http://dx.doi.org/10.4236/jep.2016.77089

Nik, Vahid M.; Mata, Erika; Sasic Kalagasidis, Angela; Scartezzini, Jean-Louis. *Effective and robust energy retrofitting measures for future climatic conditions—Reduced heating demand of Swedish households.* In Energy & Buildings. 1 June 2016. 121:176-187

Nik, Vahid M. *Making energy simulation easier for future climate – Synthesizing typical and extreme weather data sets out of regional climate models (RCMs).* In Applied Energy. 1st September 2016 177:204-226

Nguyen, H.T., Pearce, J.M., Harrap, R., Barber, G. *The Application of LiDAR to Assessment of Rooftop Solar Photovoltaic Deployment Potential in a Municipal District Unit.* In Sensors (14248220). 2012, Vol. 12 Issue 4, p4534-4558.

Olsen, Stig Irving; Pant, Deepak; Singh, Anoop. *Life Cycle Assessment of Renewable Energy Sources, Series: Green Energy and Technology.* London: Springer. 2013.

Ozdogan Dolcek, Ayse; Ghanekar, Saurabh; Tinjum, James M. *Life cycle assessment and comparison of various ground source heat pump systems and coefficient of performance calculations based on a Wisconsin case study*. A: SEG. "International Symposium on Energy Geotechnics (1st.: 2015: Barcelona)". 1st ed. Barcelona: Universitat Politècnica de Catalunya. Departament d'Enginyeria del Terreny, Cartogràfica i Geofísica, 2015.

Perera, A.T.D.; Wickremasinghe, D.M.I.J.; Mahindarathna, D.V.S.; Attalage, R.A.; Perera, K.K.C.K.; Bartholameuz, E.M. *Sensitivity of internal combustion generator capacity in standalone hybrid energy systems.* In Sustainable Energy and Environmental Protection 2010, Energy. March 2012. 39(1):403-411

Pfeifer, Norbert; Rutzinger, Martin; Höfle, Bernhard; Jochem, Andreas. *Automatic roof plane detection and analysis in airborne LiDAR point clouds for solar potential assessment.* In: Sensors, Vol 9, Iss 7, Pp 5241-5262 (2009); MDPI AG, 2009.

Quansah, David A.; Adaramola, Muyiwa S.; Appiah, George K.; Edwin, Isaac A. *Performance analysis of different grid-connected solar photovoltaic (PV) system technologies with combined capacity of 20 kW located in humid tropical climate.* In International Journal of Hydrogen Energy. 16 February 2017 42(7):4626-4635

Redweik, P; Catita, C; Brito M. *Solar energy potential on roofs and facades in an urban landscape,* Solar Energy 97 (2013) 332-341

Resnick Institute Report. *Critical materials for sustainable energy applications.* California September 2011.
<www.resnick.caltech.edu/learn/docs/ri_criticalmaterials_report.pdf>.

Rhinoceros, 2017
https://www.rhino3d.com/ Dated: 02/05/2017;

Rolland, S.; Auzane, B. *The potential of small and medium wind energy in developing countries.* Alliance for Rural Electrification position paper 2012, pp. 1–11.

Russo, S. Lo.; Gnavi, L.; Roccia, E.; Taddia, G.; Verda, V. *Groundwater Heat Pump (GWHP) system modeling and Thermal Affected Zone (TAZ) prediction reliability: Influence of temporal variations in flow discharge and injection temperature,* In Geothermics. July 2014. 51:103-112

Sahin, AD. *Progress and recent trends in wind energy.* Progress in Energy and Combustion Science 2004; 30:501-543.

Sarbu, I.; Sebarchievici, C. *General review of ground-source heat pump systems for heating and cooling of buildings.* Energy Build. 2014, 70, 441–454.

SCB, *Prisutveckling på energi samt leverantörsbyten, andra kvartalet 2016. Energy prices and switching of suppliers, 2nd quarter 2016.* ISSN 1404-5869 Serie EN - Energi. Utkom den 12 september 2016. (In Swedish).

Sharma, V; Kumar, A; Sastry, O.S; Chandel, S.S; *Performance assessment of different solar photovoltaic technologies under similar outdoor conditions*; Energy 2013,58, 511-518.

Si, Q.; Okumiya, M.; Zhang, X. *Performance evaluation and optimization of anovel solar-round source heat pump system,* Energy and Buildings, 2014. vol. 70, pp. 237–245.

Singh, A; Olsen SI; *Critical analysis of biochemical conversion, sustainability and life cycle assessment of algal biofuels.* Applied Energ. 2011. 88:3548–3555

Singh, A. et al (eds.), *Life Cycle Assessment of Renewable Energy Sources, Green Energy and Technology*, DOI: 10.1007/978-1-4471-5364-1_1 Springer-Verlag London 2013

Sipio, E. Di.; Galgaro, A.; Destro, E.; Teza, G.; Chiesa, S.; Giaretta, A.; Manzella, A. *Subsurface thermal conductivity assessment in Calabria (southern Italy): a regional case study*. In Environmental Earth Sciences, Sep2014, Vol. 72 Issue 5, p1383-1401, 19p.

SketchUp, 2017
https://www.sketchup.com/ Dated: 02/05/2017;

Skoplaki, E.; Palyvos, J.A. *On the temperature dependence of photovoltaic module electrical performance: A review of efficiency/power correlations*; Solar Energy. 2009. 83: 614–624.

Soest, van; Paul, Jan; Sas, Hein; Wit, Gerrit de. *Appels, peren en milieumateregelen. Afweging van milieumaatregelen op basis van kosteneffectiviteit.* 1997. Delft: CE.

Solanki, C. *Solar Photovoltaic: fundamental*, Technologies and Application: Second edition, 2011.

Stevanović, S. *Optimization of Passive Solar Design Strategies: A Review. Renew. Sustain.* Energy Rev. 2013, 25, 177–196. Svensk Geoenergi, No. 1/2014, page 12. www.geoenergicentrum.se (2014).

Svedberg, O. *Klas Anshelm. O. HULTIN, & M. STANNOW (Eds.)*. Arkitektur. 2004.

Svensk Geoenergi, 2014
www.geoenergicentrum.se Dated:2014.

Svensson, Gunilla. *Gunilla Svensson Arktiektkontor AB.* 2017. Avaliable on internet. www.gunillasvensson.se

Swedish Energy Agency: *Energistatistik för småhus, flerbostadshus och lokaler 2014. Summary of energy statistics for dwellings and non-residential premises for 2014.* ES 2015:07 (2015) (In Swedish).

Swedish Energy Agency. *Energy in Sweden 2015*. ET015:19 December 2015. Could be download from www.energimyndigheten.se

Swedish Energy Markets Inspectorate. *The swedish electricity and natural gas market.* Ei R 2016:10. Could be download from www.ei.se

System Advisor Model, 2017
https://sam.nrel.gov/ Dated: 02/05/2017

Thorstensson, Erika. *Small-scale Wind Turbines- Introductory market study for Sweden.* Master thesis in International Project Management, Chalmers university of technology, 2009

Tremeac, B.; Meunier, F. *Life Cycle Analysis of 4.5 MW and 250 W Wind Turbines. Renewable and Sustainable Energy Reviews*, 2009, 13, 2104-2110. http://dx.doi.org/10.1016/j.rser.2009.01.001

Todorov, Mihail. *Implementation of solar energy in urban planning, Analysis of SAFAR n as a solar potential metric & improvement of simulation tools*, Master Thesis in Energy-efficient and Environmental Buildings Faculty of Engineering, Lund University, 2015

Uddin, S.; Kumar, S. *Energy, Emissions and Environmental Impact Analysis of Wind Turbine Using Life Cycle Assessment Technique.* Cleaner Production, 2014, 69, 153-164. http://dx.doi.org/10.1016/j.jclepro.2014.01.073

Udo de Haes, HA.; Heijungs, R. *Life-cycle assessment for energy analysis and management.* In Industrial Energy Analysis and Management: A European Perspective, Applied Energy. 2007. 84(7):817-827.

Van Den Bossche, Nathan; Janssens, Arnold. *Airtightness and water tightness of window frames: Comparison of performance and requirements. Building & Environment.* December 2016, Vol. 110, p129-139. 11p.

Varun; Bhat, IK.; Prakash, R.; *LCA of renewable energy for electricity generation systemsA review*. Renew Sustain Energy Rev. 2009a. 13(5):1067–1073

VDI, *VDI 4640-Thermal Use of Underground*, Blatt 1: Fundamentals, Ap-provals, Environmental Aspects, 2010.

Viebahn, P.; Nitsch, J.; Fischedick, M.; Esken, A.; Schuwer, D.; Supersberger, N.; Zuberbuhler, U.; Edenhofer, O.; *Comparison of carbon capture and storage with renewable energy echnologies regarding structural, economic, and ecological aspects in Germany.* In Greenhouse Gas Control. 2007. 1(1):121–133

Wang, Kuan; Li, Nianping; Peng, Jinqing; He, Yingdong. *Study on the Optimizing Operation of Exhaust Air Heat Recovery and Solar Energy Combined Thermal Compensation System for Ground-Coupled Heat Pump.* International Journal of Photoenergy. 1/1/2017, p1-19. 19p. DOI: 10.1155/2017/6561797.

Weisser, D. *A guide to life-cycle greenhouse gas (GHG) emissions from electric supply technologies.* In Energy. 2007. 32(9):1543–1559

Wong, Man Sing; Zhu, Rui; Liu, Zhizhao; Lu, Lin; Peng, Jinqing; Tang, Zhaoqin; Lo, Chung Ho; Chan, Wai Ki. *Estimation of Hong Kong's solar energy potential using GIS and remote sensing technologies*, In Renewable Energy. December 2016. 99:325-335

WG Environmental Management & Economics. *Life Cycle Assessment of Electricity Generation.* D/2011/12.105/53

Wizelius, T. *Vindkraft I teori och praktik.* Lund: Studentlitteratur. 2007.

Wang, X.; Zheng, M.; Zhang, W.; Zhang, S.; Yang, T. *Experimental study of a solar-assisted ground-coupled heat pump system with solar seasonal thermal storage in severe cold areas*, Energy and Buildings, vol. 42, no. 11, pp. 2104–2110, 2010.

Yang, W.; Chen, Y.; Shi, M.; Spitler, J. D. *Numerical investigation on the underground thermal imbalance of groun dcoupled heat pump operated in cooling-dominated district*, Applied Thermal Engineering, vol. 58, no. 1-2, pp. 626–637, 2013.

Yang, W.; Sun, L.; Chen, Y. *Experimental investigations of the performance of a solar-ground source heat pump system operated in heating modes.* Energy and Buildings, vol. 89, pp. 97–111, 2015.

You, T.; Shi, W.; Wang, B.; Wu, W.; Li, X. *A new ground coupled heat pump system integrated with a multi-mode air-source heat compensator to eliminate thermal imbalance in cold regions*, Energy and Buildings, vol. 107, pp. 103–112, 2015.

Zhu, N.; Hu, P.; Xu, L.; Jiang, Z.; Lei, F. *Recent research and applications of ground source heat pump integrated with thermal energy storage systems: a review*, Applied Thermal Engineering, vol. 71, no. 1, pp. 142–151, 2014.

10 Appendix

Appendix A

Construction detials of the IKDC.

Table 23 External walls

Material	Thermal conductivity [W/m K]	Density [kg/m^3]	Specific heat [J/kg K]	Thickness [m]	U-value [W/m^2 K]
Light insulation	0.036	20	750	0.02	1.38
Concrete (light weight)	0.15	500	1050	0.378	0.371
TotalU-value					0.31

Table 24 Internal walls

Material	Thermal conductivity [W/m K]	Density [kg/m^3]	Specific heat [J/kg K]	Thickness [M]	U-value [W/m^2 K]
Gypsum	0.22	970	1090	0.012	4.453
Concrete (light weight)	0.15	500	1050	0.1	1.195
Gypsum	0.22	970	1090	0.012	4.453
Total U-value					1.057

Table 25 Internal floor/slab

Material	Thermal conductivity [W/m K]	Density [kg/m^3]	Specific heat [J/kg K]	Thickness [m]	U-value [W/m^2 K]
Floor coating	0.17	1200	1400	0.005	5.05
Concrete	0.15	500	1050	0.02	3.29

(Light weight)					
Concrete	1.7	2300	880	0.15	3.87
TotalU-value					2.38

Table 26 Roof

Material	Thermal conductivity [W/m K]	Density [kg/m^3]	Specific heat [J/ kg K)	Thickness [M]	U-value [W/m^2 K]
Gypsum	0.22	970	1090	0.01	4.6
Light weight insulation	0.036	20	750	0.3	0.11
Concrete	1.7	2300	880	0.15	3.87
TotalU-value					0.12

Table 27 External Floor/slab

Material	Thermal conductivity [W/m K]	Density [kg/m^3]	Specific heat [J/ kg K)	Thickness [M]	U-value [W/m^2 K]
Light weight insulation	0.036	20	750	0.044	3.42
Concrete	2.5	2400	1000	0.15	0.14
TotalU-value					0.13

Appendix B

Construction details of M-huset.

Table 28 External walls

Material	Thermal conductivity [W/m K]	Density [kg/m^3]	Specific heat [J/ kg K)	Thickness [M]	U-value [W/m^2 K]
Brick Masonry	0,57	1700	800	0.378	1.2

Table 29 Internal walls

Material	Thermal conductivity [W/m K]	Density [kg/m^3]	Specific heat [J/ kg K)	Thickness [M]	U-value [W/m^2 K]
Gypsum	0.22	970	1090	0.012	4.453
Brick	0.57	1700	840	0.1	2.92
Gypsum	0.22	970	1090	0.012	4.453
Total U-value					2.215

Table 30 Internal floor/slab

Material	Thermal conductivity [W/m K]	Density [kg/m^3]	Specific heat [J/ kg K)	Thickness [M]	U-value [W/m^2 K]
Linolium	0.17	1200	1400	0.003	5.32
Concrete	1.7	2300	880	0.3	2.88
Total U-					2.76

value

Table 31 Roof

Material	Thermal conductivity [W/m K]	Density [kg/m^3]	Specific heat [J/ kg K)	Thickness [M]	U-value [W/m^2 K]
Asphalt paper	0.7	2100	1000	0.01	5.426
Stone wool	0.038	40	840	0.37	0.1
Concrete (High density)	2.5	2400	1000	0.15	4.34
Total U-value					0.13

Table 32 External Floor/slab

Material	Thermal conductivity [W/m K]	Density [kg/m^3]	Specific heat [J/ kg K)	Thickness [M]	U-value [W/m^2 K]
Linoleum	0.17	1200	1400	0.003	5.32
Concrete (High density)	2.5	2400	1000	0.15	4.34
Gravel	0.36	1840	840	0.044	3.42
Total U-value					2.7

Appendix C

Table 33 Schedule (Week day)

Zone	Occupancy Schedule	Lights Schedule	Equipment Schedule	Heating Schedule	Cooling schedule	Ventilation schedule
Classroom	8:00-17:00	8:00-17:00	8:00-17:00	8:00-17:00	8:00-17:00	8:00-17:00
Lecture hall	8:00-17:00	8:00-17:00	8:00-17:00	8:00-17:00	8:00-17:00	8:00-17:00
Hallway	8:00-17:00	8:00-17:00	none	8:00-17:00	8:00-17:00	8:00-17:00
Corridor office	9:00-17:00	9:00-17:00	9:00-17:00	9:00-17:00	9:00-17:00	9:00-17:00
Group room	9:00-20:00	9:00-20:00	9:00-20:00	9:00-20:00	9:00-20:00	9:00-20:00
Workshop	8:00-17:00	8:00-17:00	8:00-17:00	8:00-17:00	8:00-17:00	8:00-17:00
Free study area	7:00-20:00	7:00-20:00	7:00-20:00	7:00-20:00	7:00-20:00	7:00-20:00
Storage	none	9:00-17:00	9:00-17:00	none	none	9:00-17:00
Lab (small)	8:00-17:00	8:00-17:00	8:00-17:00	8:00-17:00	8:00-17:00	8:00-17:00
Lab (middle)	8:00-17:00	8:00-17:00	8:00-17:00	8:00-17:00	8:00-17:00	8:00-17:00
Lab (large)	8:00-17:00	8:00-17:00	8:00-17:00	8:00-17:00	8:00-17:00	8:00-17:00
Fan room	8:00-17:00	8:00-17:00	7:00-17:00	8:00-17:00	8:00-17:00	8:00-17:00

Appendix D

Table 34 Holiday Schedule

Date	Weekday	Holiday Name	Number of days
Jan 1	Sunday	New Year's Day	1
Jan 5	Thursday	Twelfth Night	1
Jan 6	Friday	Epiphany	1
Mar 20	Monday	March equinox	1
Mar 26	Sunday	Daylight Saving Time starts	1
Apr 14	Friday	Good Friday	1
Apr 15	Saturday	Holy Saturday	1
Apr 16	Sunday	Easter Day	1
Apr 17	Monday	Easter Monday	1
Apr 30	Sunday	Walpurgis Night	1
May 1	Monday	May 1st	1
May 25	Thursday	Ascension Day	1
May 28	Sunday	Mother's Day	1
Jun 3	Saturday	Summer shut down	42
Oct 29	Sunday	Daylight Saving Time ends	1
Nov 3	Friday	All Saints' Eve	1
Nov 4	Saturday	All Saints' Day	1
Nov 12	Sunday	Father's Day	1
Dec 21	Thursday	December Solstice	1
Dec 24	Sunday	Christmas Eve	1
Dec 25	Monday	Christmas Day	1
Dec 26	Tuesday	Boxing Day	1
Dec 31	Sunday	New Year's Eve	1

Appendix E

Table 35 Thermal bridges of the IKDC

Thermal bridges	Area or Length	Avg. Heat conductivity [W/m K]	Total [W/K]
External wall / internal slab	2373.47 m	0.005	11.867
External wall / internal wall	444.60 m	0.005	2.223
External wall / internal wall	260.94 m	0.060	15.656
External windows perimeter	2565.86 m	0.020	51.317
External doors perimeter	88.56 m	0.020	1.771
Roof / external walls	665.92 m	0.070	46.615
External slab / external walls	481.90 m	0.080	38.552
Balcony floor / external walls	0.00 m	0.000	0.000
External slab / Internal walls	520.52 m	0.005	2.603
Roof / Internal walls	662.62 m	0.005	3.578
External walls, inner corner	48.39 m	0.000	0.000
Total envelope (incl. roof and ground)	13422.58 m^2	0.000	0.000
Extra losses	-	-	-0.000
Sum	-	-	174.182

Table 36 Thermal bridges for M-huset

Thermal bridges	**Area or Length**	**Avg. Heat conductivity [W/m K]**	**Total [W/K]**
Thermal bridges	Area or Length	Avg. Heat conductivity	Total W/K
External wall / internal slab	5411.49 m	0.025	135.287
External wall / internal wall	420.24 m	0.015	6.304
External wall / internal wall	335.76 m	0.080	26.861
External windows perimeter	5177.32 m	0.030	155.320
External doors perimeter	179.08 m	0.030	5.372
Roof / external walls	1377.97 m	0.090	124.017
External slab / external walls	1102.36 m	0.140	154.331
Balcony floor / external walls	0.00 m	0.000	0.000
External slab / Internal walls	1193.78 m	0.015	17.907
Roof / Internal walls	918.83 m	0.015	13.782
External walls, inner corner	30.79 m	0.000	0.000
Total envelope (incl. roof and ground)	39277.22 m^2	0.000	0.000
Extra losses	-	-	0.001
Sum	-	-	639.182

Appendix F

For extremely cold year (ECY), the annual heating demand decreased by 1.01% from the first 30 year' periods (2009-2038) to the second 30 years' period (2039-2068). 12% decreased from the second 30 year' periods (2038-2069) to the third 30 year' periods (2069-2098). Compared with the reference year the heating demand Increased about 29.3%, see figure 107. Also, heating power per watts have a decreasing trend as year goes by in ECY scenario, see figure 108.

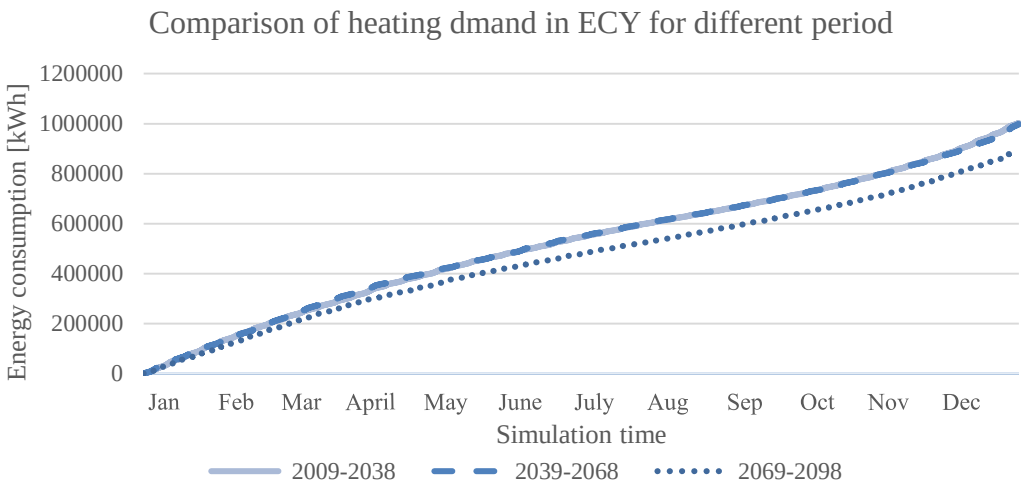

Figure 107: IKDC heating demand (Cumulative value) for ECY during 2009-2098.

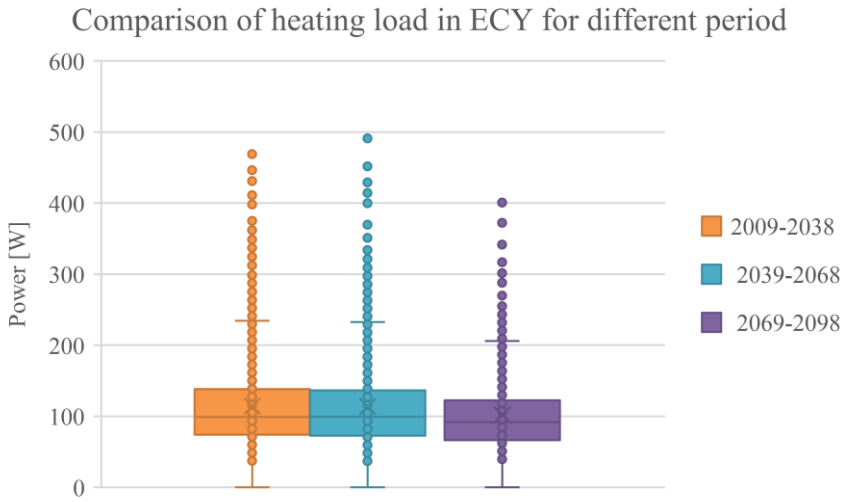

Figure 108: IKDC heating load (BOXPLOT) for ECY during 2009-2098.

For extremely warm year (EWY), the annual heating demand increased by 5% from the first 30 year' periods (2009-2038) to the second 30 years' period (2039-2068).

30% decreased from the second 30 year' periods (2038-2069) to the third 30 year' periods (2069-2098). Compared with the reference year the heating demand decreased about 40%, see figure 109. However, heating power per watts have a increasing trend during 2038-2068 in EWY scenario and decreasing trend appeas in following years, see figure 110.

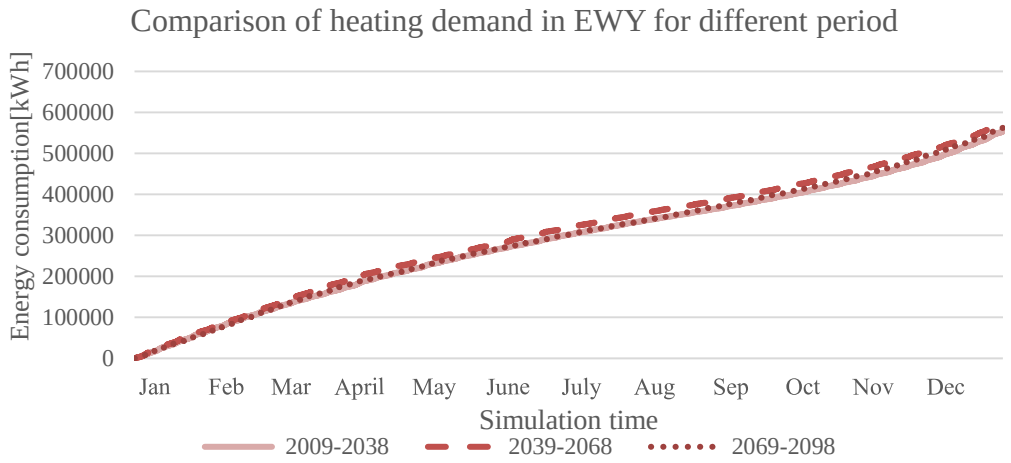

Figure 109: IKDC heating demand (Cumulative value) for EWY during 2009-2098.

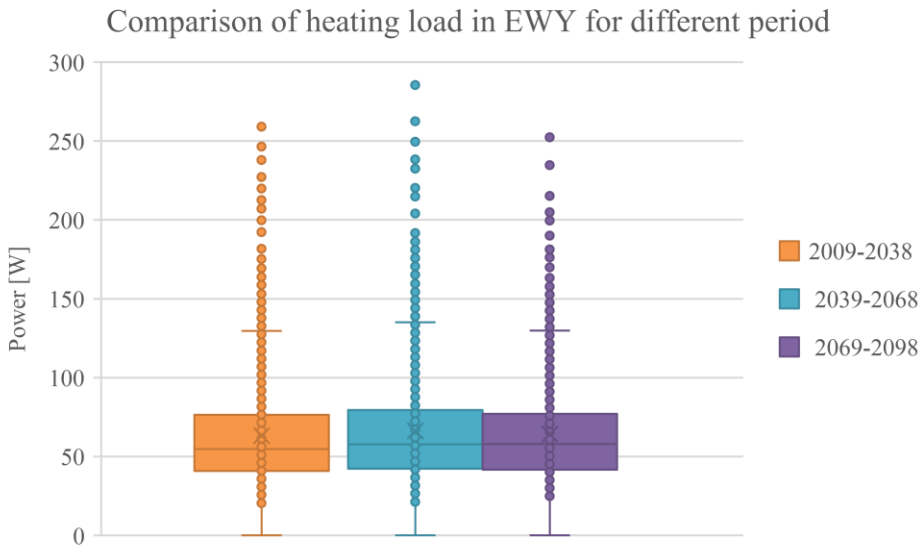

Figure 110 IKDC heating load for EWY during 2009-2098.

For Extremely cold year (ECY), the annual heating demand decreased by 3% from the first 30 year' periods (2009-2038) to the second 30 years' period (2039-2068). 27% decreased from the second 30 year' periods (2038-2069) to the third 30 year' periods (2069-2098). Compared with the reference year the heating demand Increased about 14%, see figure 111. Also, heating power per watts have a decreasing trend as year goes by in ECY scenario, see figure 112.

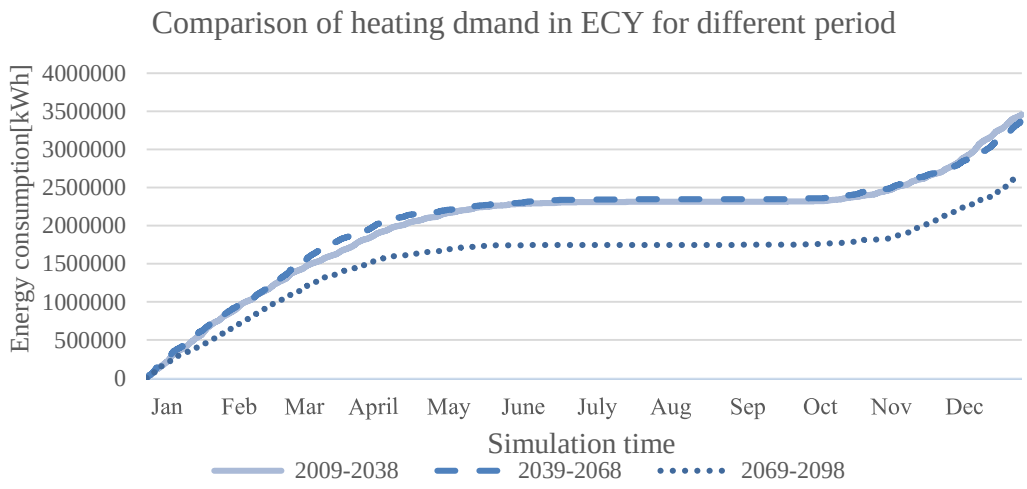

Figure 111: M- huset heating demand (Cumulative value) for ECY during 2009-2098.

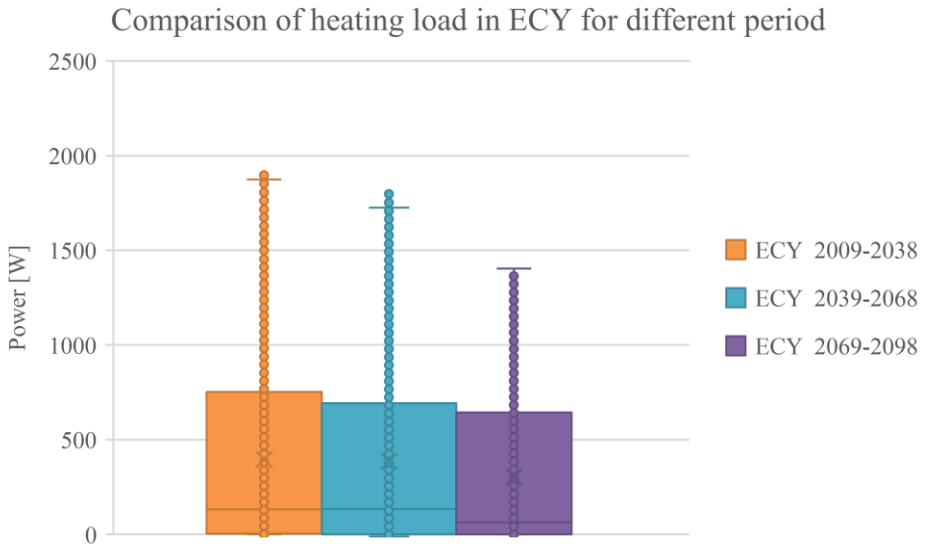

Figure 112: M-huset heating load for ECY during 2009-2098.

For Extremely warm year (EWY) The annual heating demand increased by 8% from the first 30 year' periods (2009-2038) to the second 30 years' period (2039-2068). 31% decreased from the second 30 year' periods (2038-2069) to the third 30 year' periods (2069-2098). Compared with the reference year the heating demand decreased about 200%, see figure 113. However, heating power per watts have a increasing trend during 2038-2068 in EWY scenario and decreasing trend appeas in following years, see figure 114.

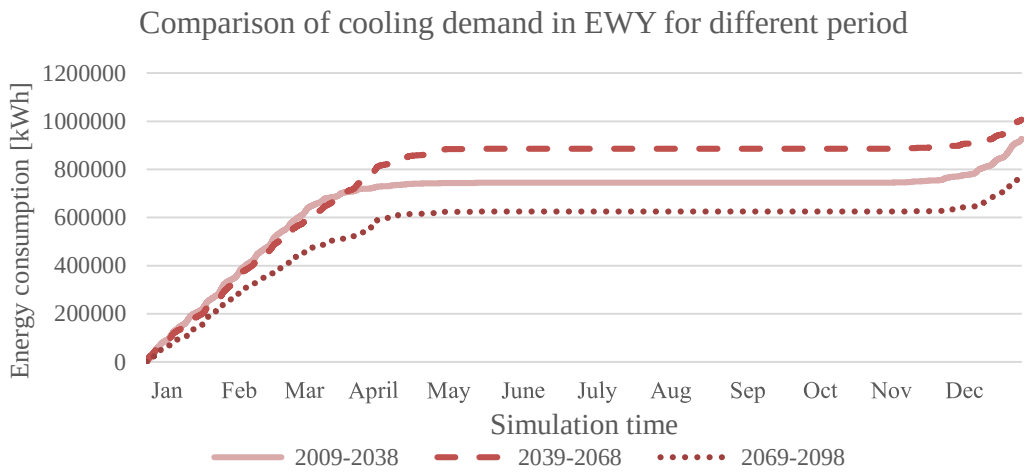

Figure 113: M-huset heating demand (Cumulative value) for EWY during 2009-2098.

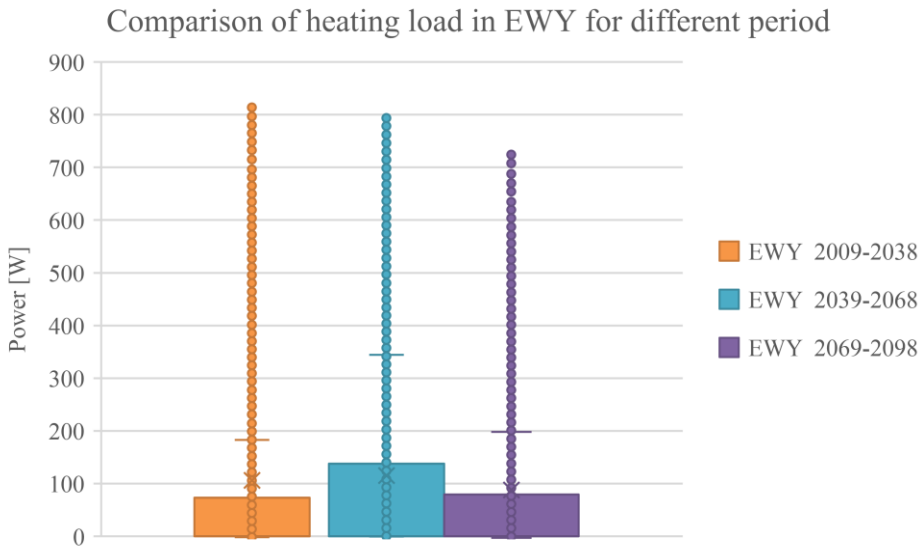

Figure 114: M-huset heating load (BOXPLOT) for EWY during 2009-2098.

For Extremely cold year (ECY) The annual cooling demand increased by 20% from the first 30 year' periods (2009-2038) to the second 30 years' period (2039-2068). 4% increase from the second 30 year' periods (2038-2069) to the third 30 year' periods (2069-2098). Compared with the reference year the cooling demand decreased about 55% (Figure 115 below). However, cooling power per watts have a increasing trend as year goes by in ECY scenario, see figure 116.

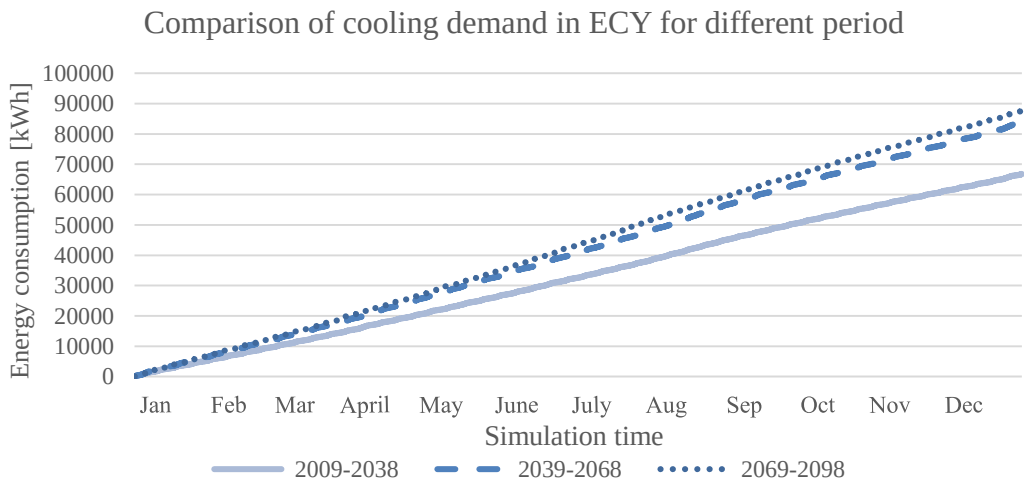

Figure 115: IKDC cooling demand (Cumulative value) for ECY during 2009-2098.

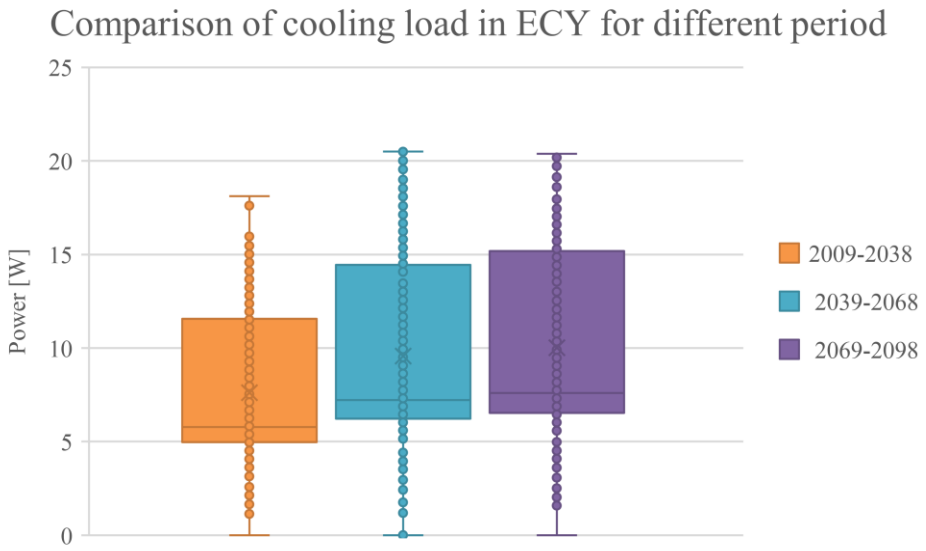

Figure 116: IKDC cooling load (BOXPLOT) for ECY during 2009-2098.

For Extremely warm year (EWY) The annual cooling demand decreased by 2% from the first 30 year' periods (2009-2038) to the second 30 years' period (2039-2068). 5% decreased from the second 30 year' periods (2038-2069) to the third 30 year' periods (2069-2098). Compared with the reference year the cooling demand increased about 220% (Figure 117 below). However, cooling power per watts have a decreasing trend as year goes by in EWY scenario, see figure 118.

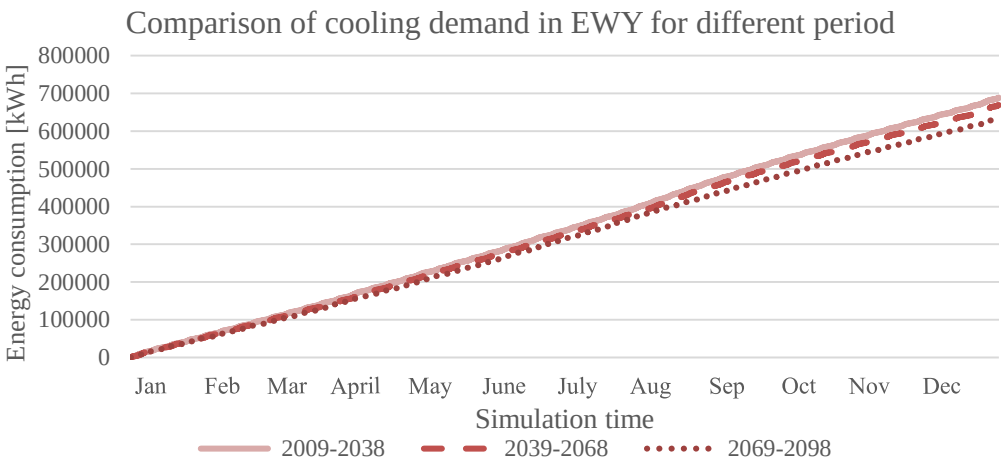

Figure 117: IKDC-building cooling demand (Cumulative value) for EWY during 2009-2098.

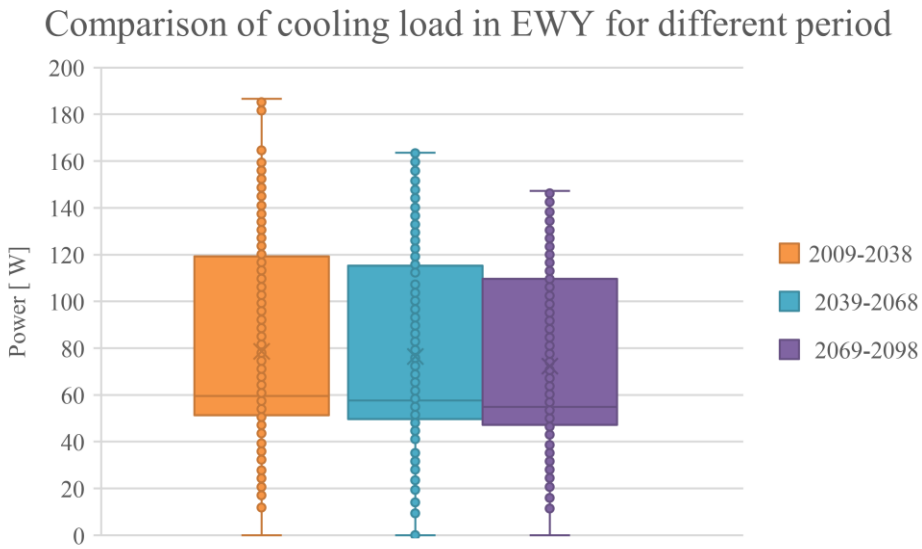

Figure 118: IKDC cooling load (BOXPLOT) for EWY during 2009-2098.

For Extremely cold year (ECY) The annual cooling demand increased by 15% from the first 30 year' periods (2009-2038) to the second 30 years' period (2039-2068). 2% decrease from the second 30 year' periods (2038-2069) to the third 30 year' periods (2069-2098). Compared with the reference year the cooling demand decreased about 40% (Figure 119 below). However, cooling power per watts have a slightly increasing trend as year goes by in ECY scenario, see figure 120.

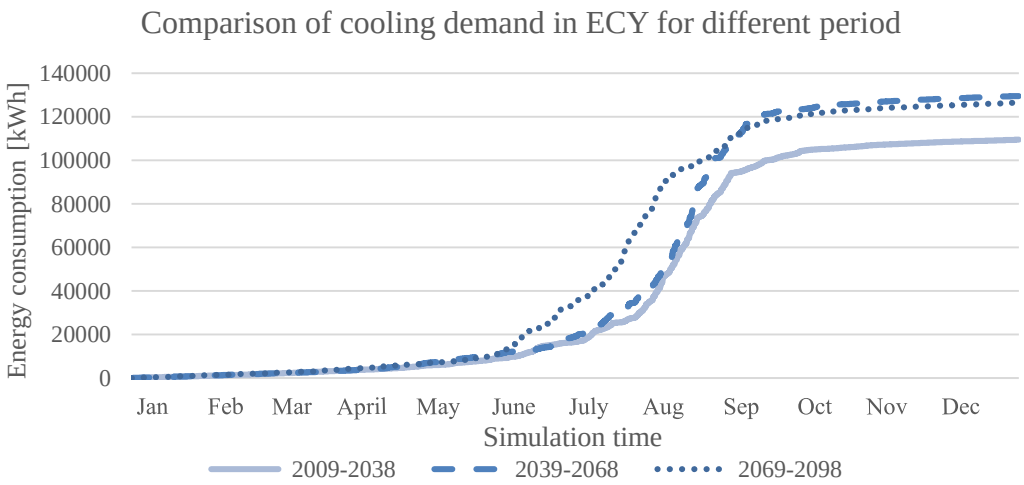

Figure 119: M- huset cooling demand (Cumulative value) for ECY during 2009-2098.

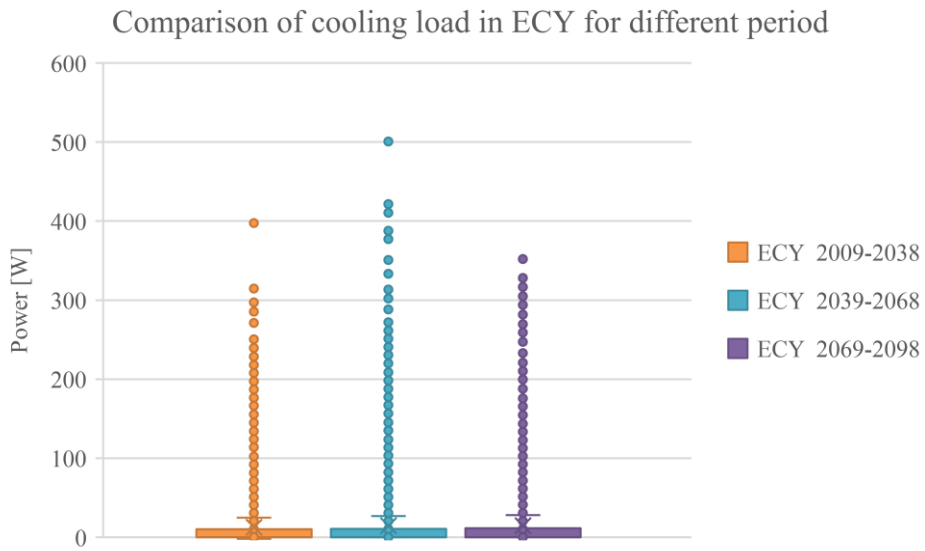

Figure 120: M-huset cooling load (BOXPLOT) for ECY during 2009-2098.

For Extremely warm year (EWY) The annual cooling demand decreased by 2% from the first 30 year' periods (2009-2038) to the second 30 years' period (2039-2068). 6% decreased from the second 30 year' periods (2038-2069) to the third 30 year' periods (2069-2098). Compared with the reference year the cooling demand increased about 220% (Figure 121 below). However, cooling power per watts have a decreasing trend as year goes by in EWY scenario, see figure 122.

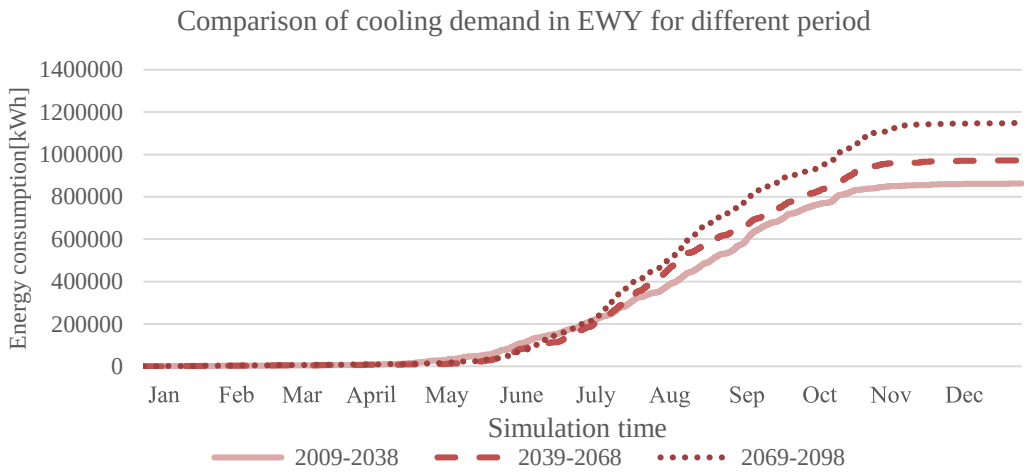

Figure 121: M-huset cooling demand (Cumulative value) for EWY during 2009-2098.

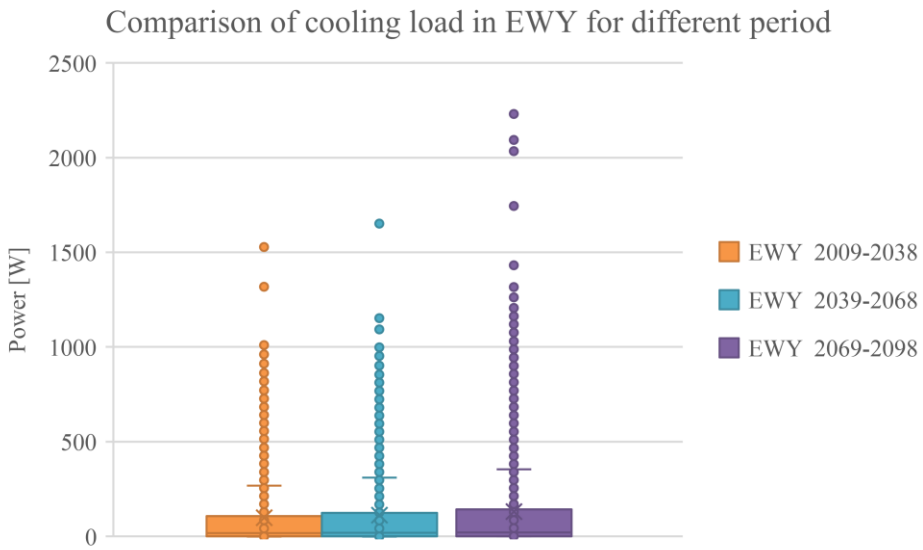

Figure 122: M-huset cooling load (BOXPLOT) for EWY during 2009-2098.

Appendix G

Comparison of PV generation in TDY for different period are showed in figure 123, 124, 125. Although PV power has an increasing trend with time flowing, monthly PV generation and annual PV generation are varied from time to time.

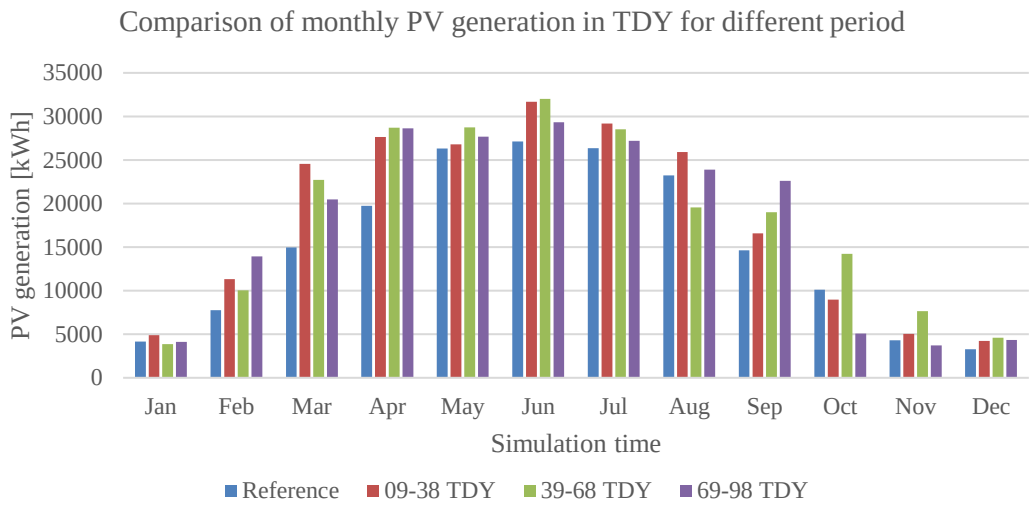

Figure 123: Comparison of monthly PV generation in TDY for different period.

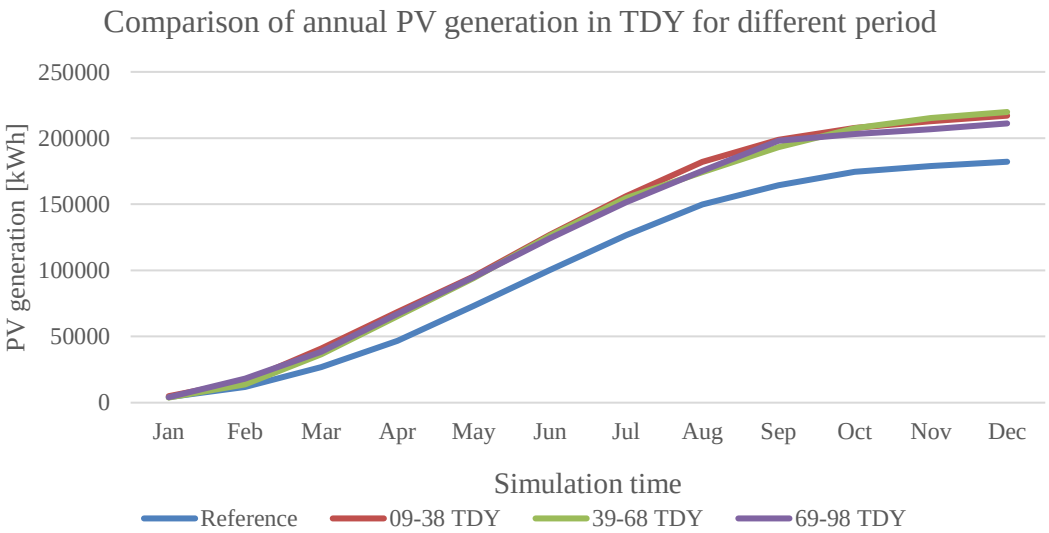

Figure 124: Comparison of annual PV generation in TDY for different period.

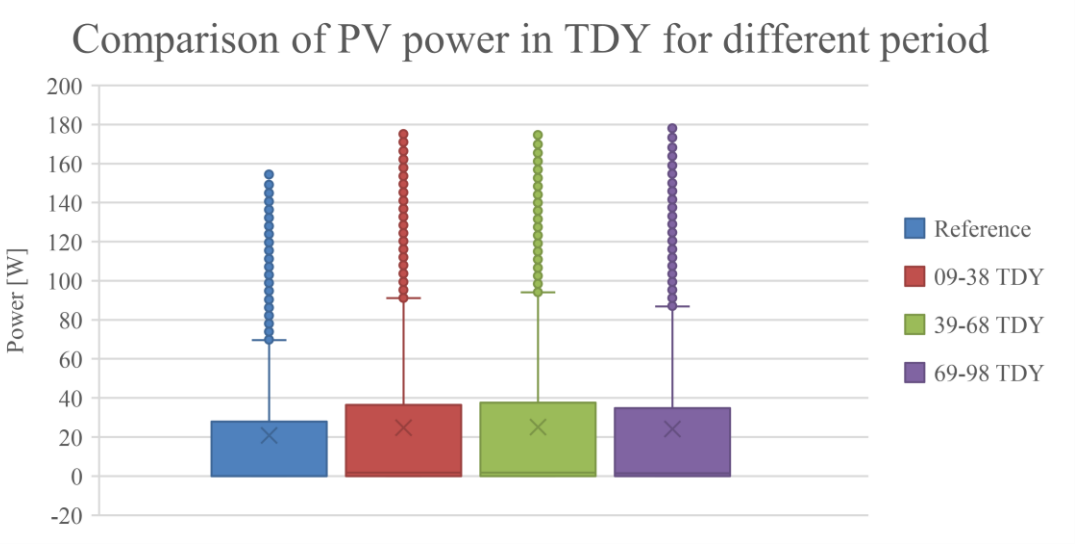

Figure 125: Comparison of PV power in TDY for different period.

Comparison of PV generation in ECY for different period are showed in figure 126, 127, 128. Although annual PV generation has an decresing trend with time flowing, monthly PV generation and PV power are varied from time to time.

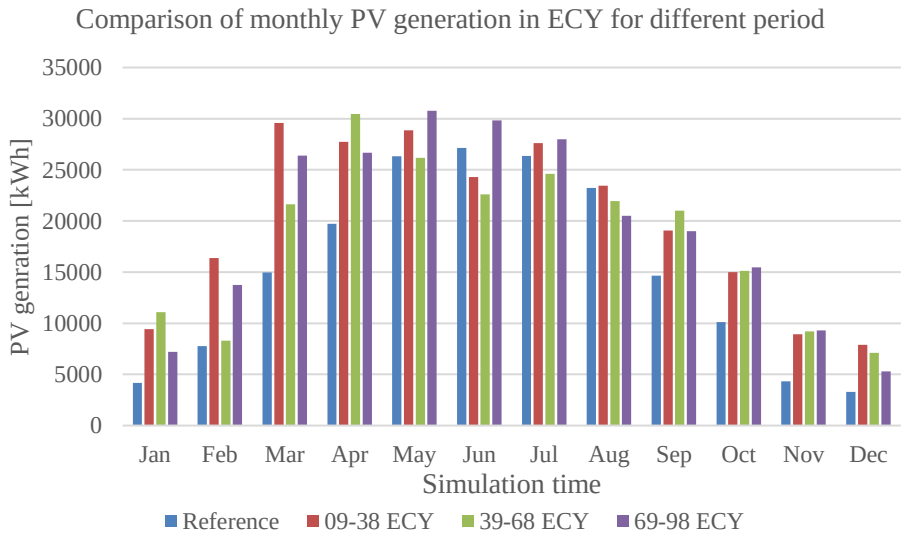

Figure 126: Comparison of monthly PV generation in ECY for different period.

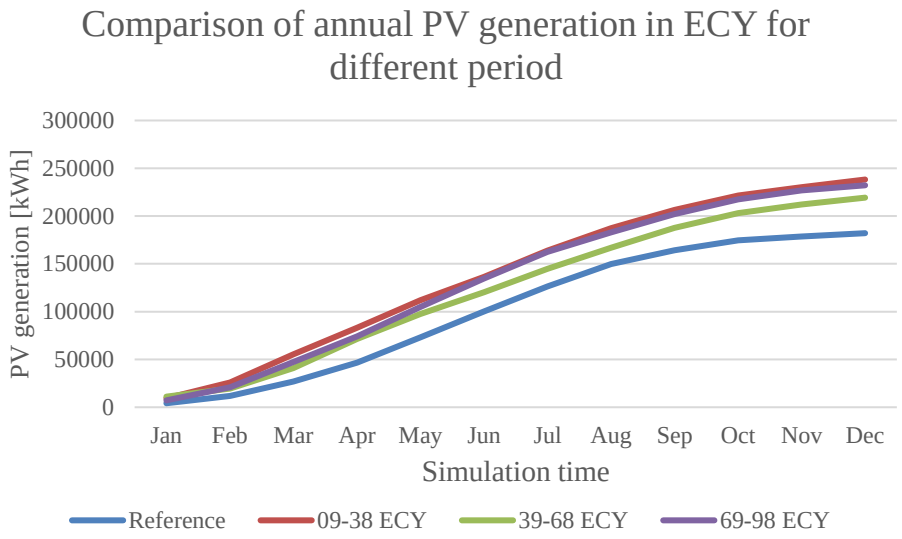

Figure 127: Comparison of annual PV generation in ECY for different period.

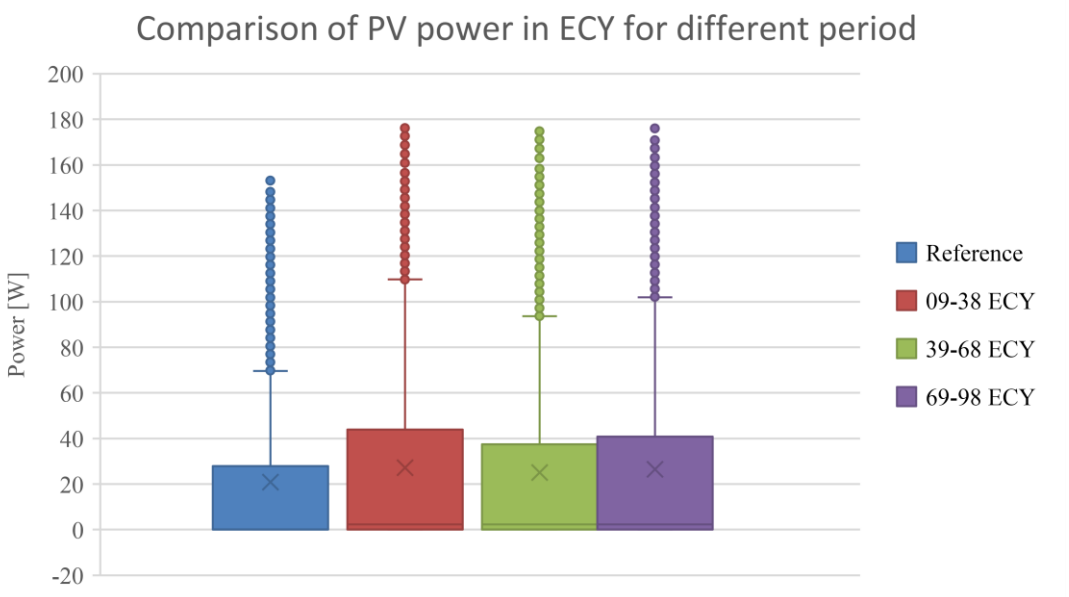

Figure 128: Comparison of PV power in ECY for different period.

Comparison of PV generation in EWY for different period are showed in figure 129, 130, 131. Annual PV generation, monthly PV generation and PV power all varied from time to time.

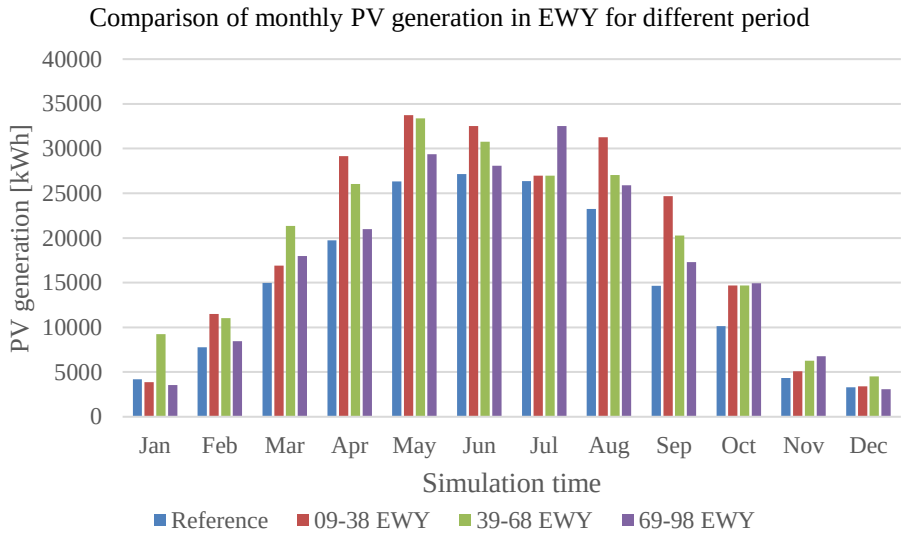

Figure 129: Comparison of monthly PV generation in EWY for different period.

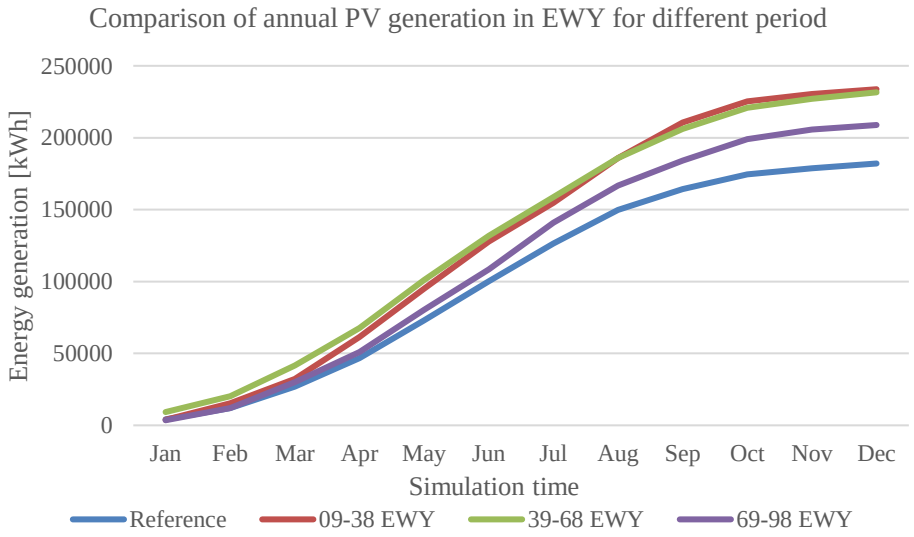

Figure 130: Comparison of annual PV generation in EWY for different period.

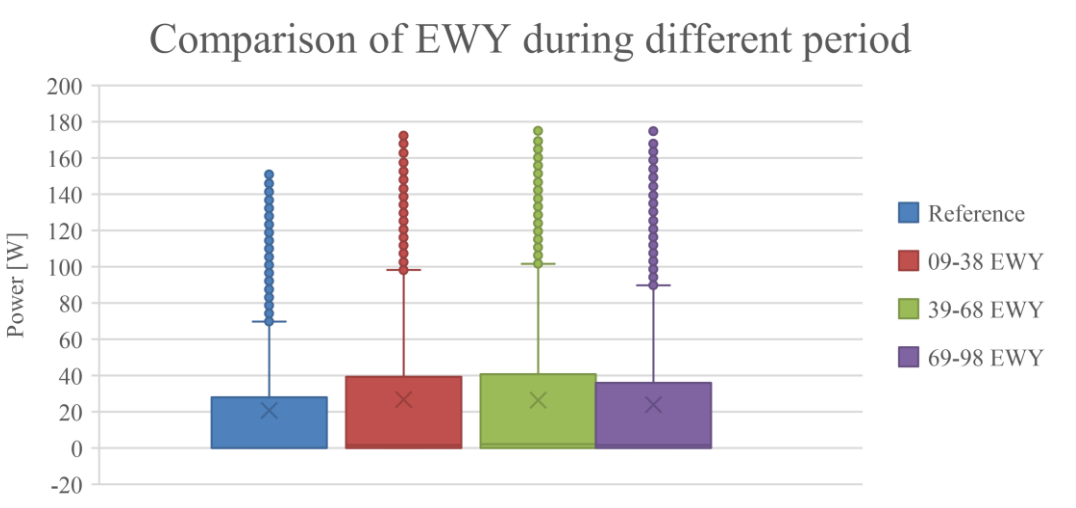

Figure 131: Comparison of PV power in EWY for different period.

Comparison of monthly PV generation, annual PV generation and PV power in TDY, ECY, and EWY for 2009-2038 are showed in figure 132, 133, 134. Although PV power in ECY scenoros has the highest value, monthly PV generation and annual PV generation are varied from time to time.

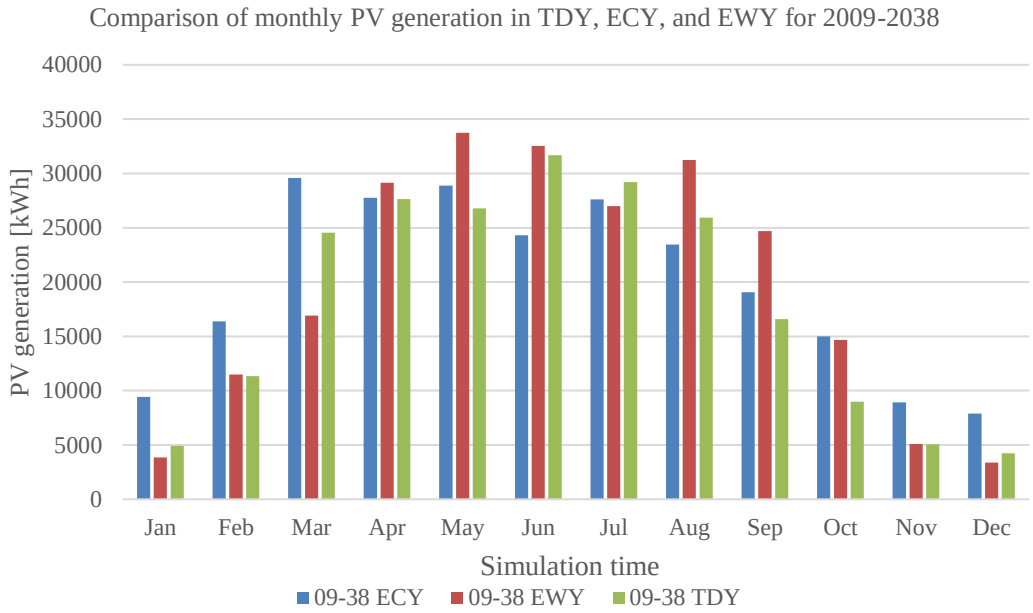

Figure 132: Comparison of monthly PV generation in TDY, ECY, and EWY for 2009-2038.

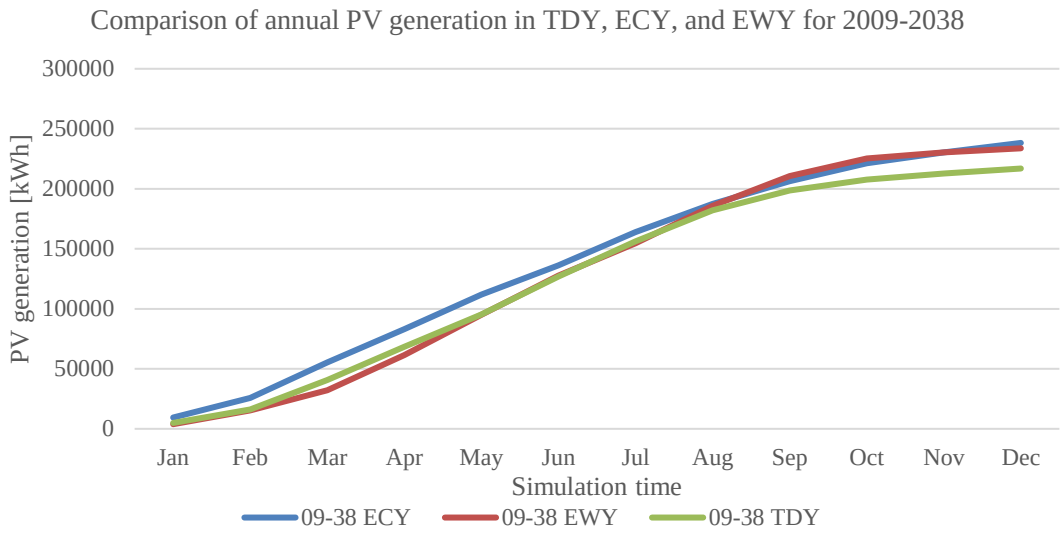

Figure 133: Comparison of annual PV generation in TDY, ECY, and EWY for 2009-2038.

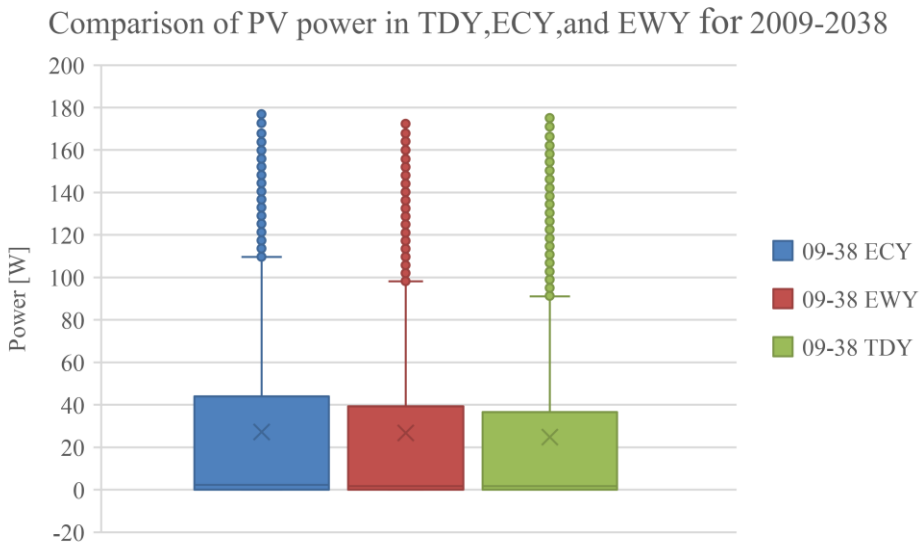

Figure 134 Comparison of PV power in TDY, ECY, and EWY for 2009-2038.

Comparison of monthly PV generation, annual PV generation and PV power in TDY, ECY, and EWY for 2039-2068 are showed in figure 135, 136, 137. Although EWY scenoros has the highest value in PV power and annual PV generation, monthly PV generation is varied from time to time.

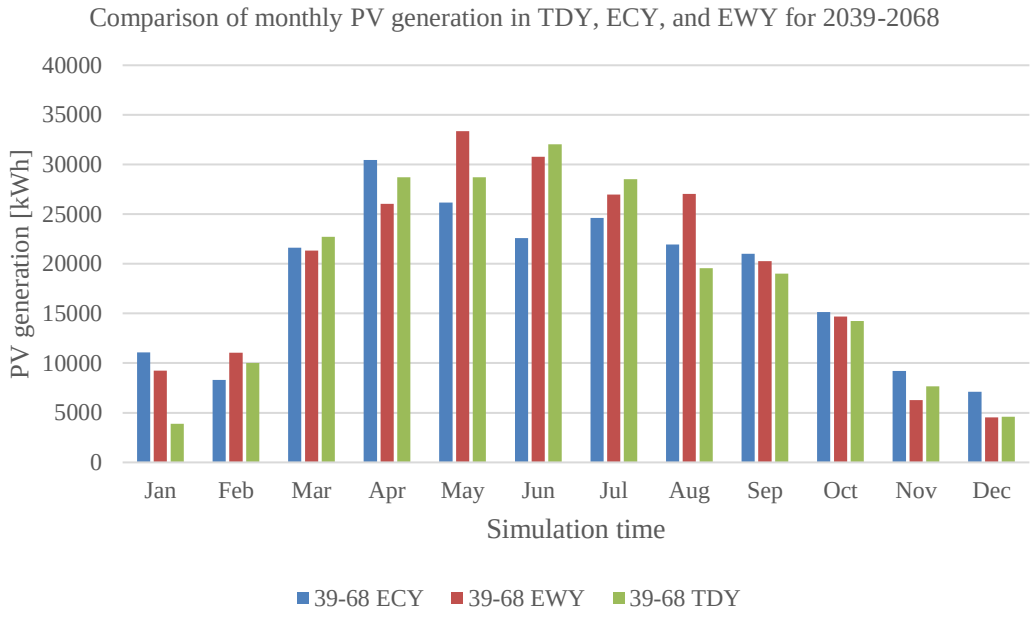

Figure 135: Comparison of monthly PV generation in TDY, ECY, and EWY for 2039-2068.

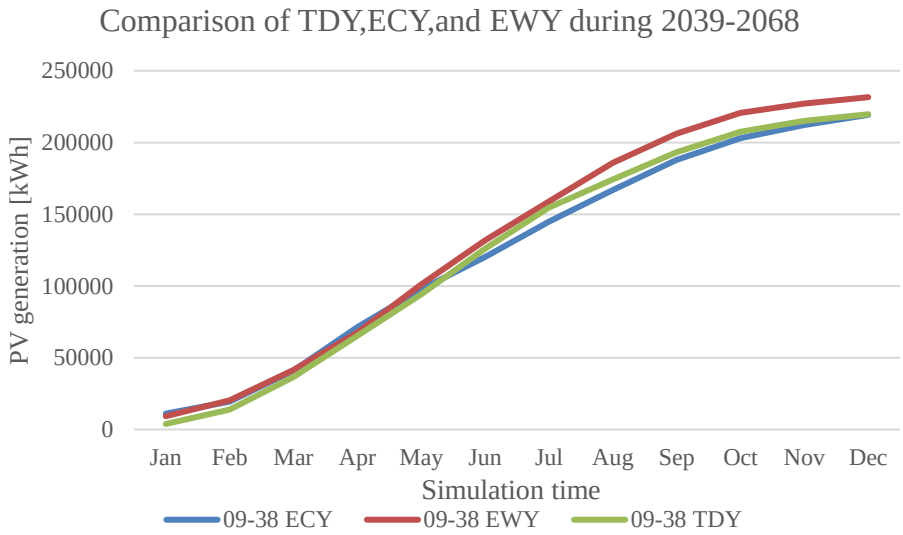

Figure 136: Comparison of annual PV generation in TDY, ECY, and EWY for 2039-2068.

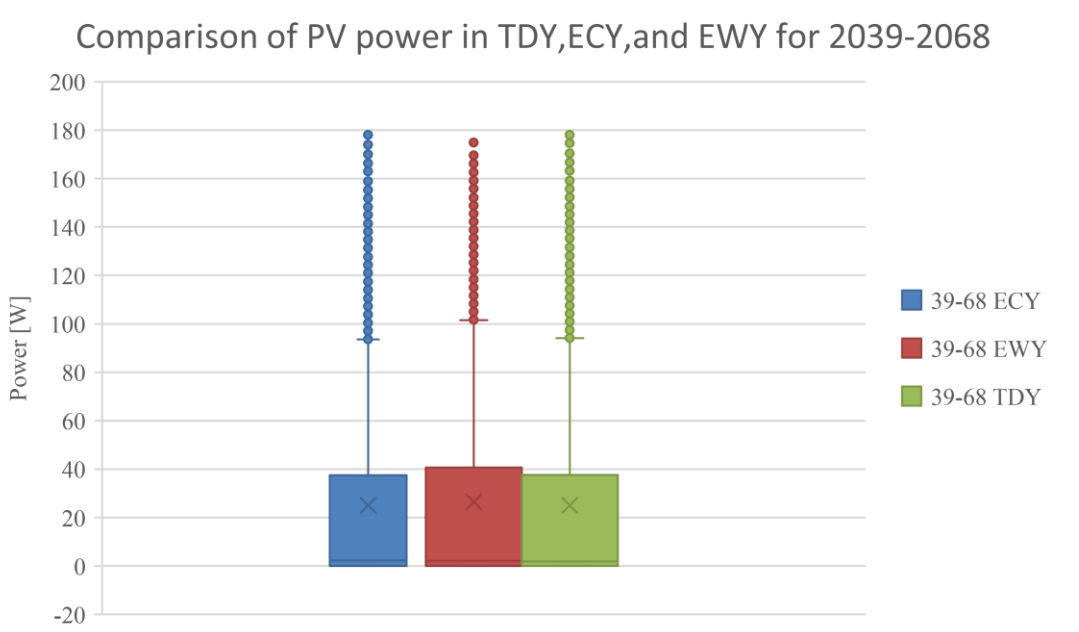

Figure 137 Comparison of PV power in TDY, ECY, and EWY for 2039-2068.

Comparison of monthly PV generation, annual PV generation and PV power in TDY, ECY, and EWY for 2069-2098 are showed in figure 138, 139, 140. Although ECY scenoros has the highest value in PV power and annual PV generation, monthly PV generation is varied from time to time.

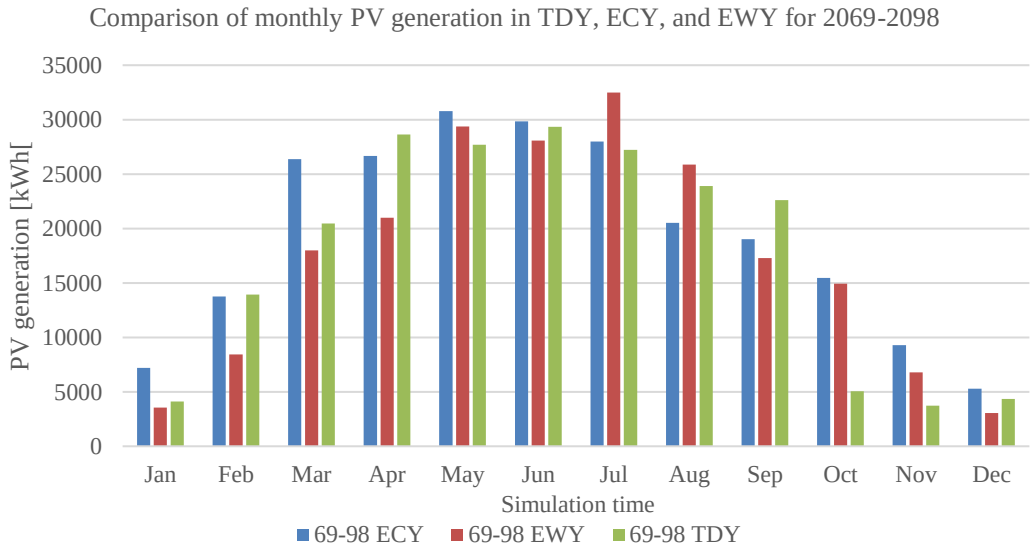

Figure 138: Comparison of monthly PV generation in TDY, ECY, and EWY for 2069-2098.

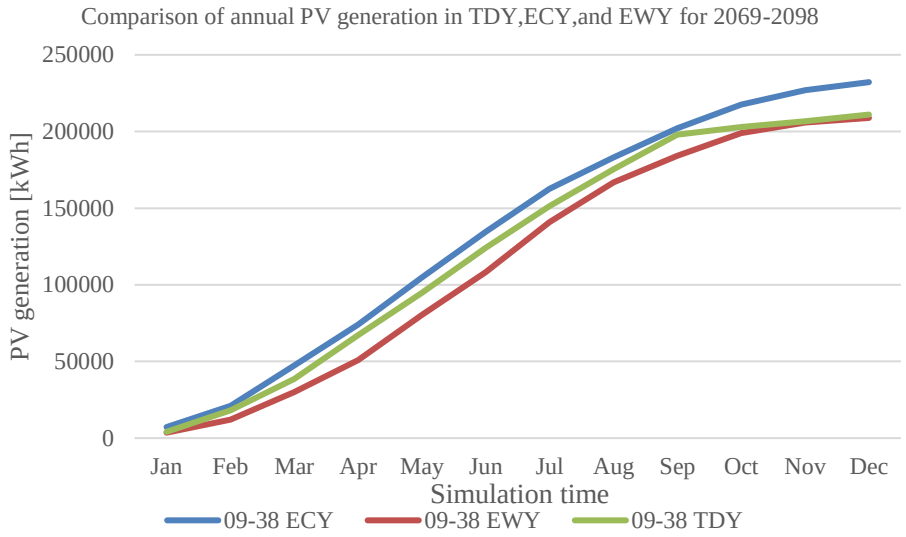

Figure 139: Comparison of annual PV generation in TDY, ECY, and EWY for 2069-2098.

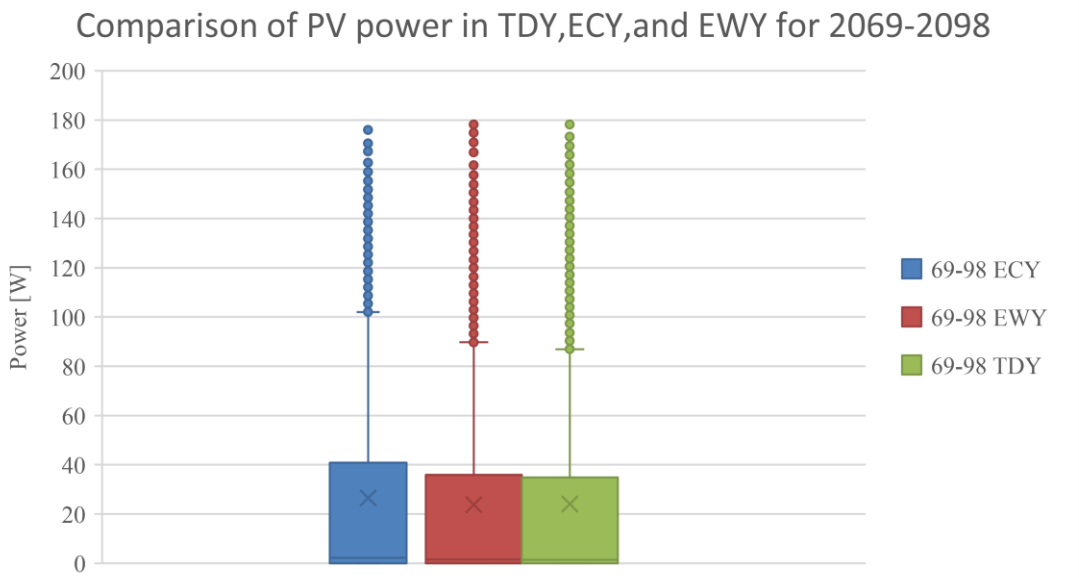

Figure 140: Comparison of PV power in TDY, ECY, and EWY for 2069-2098.

Appendix H

Fitting function with Power- Wind speed diagram.

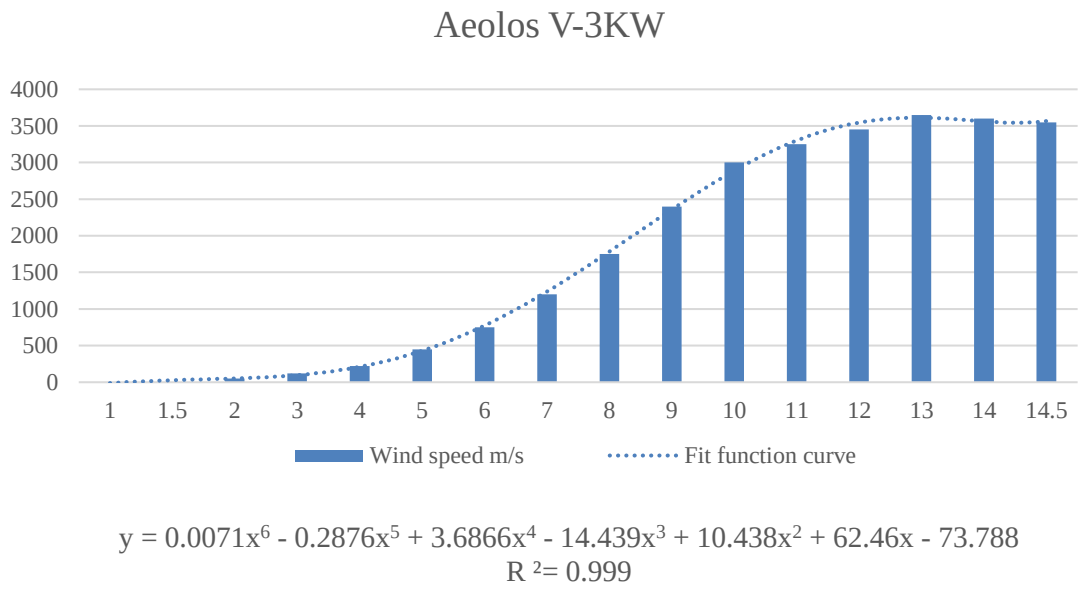

Figure 141: Aeolos V-3KW.

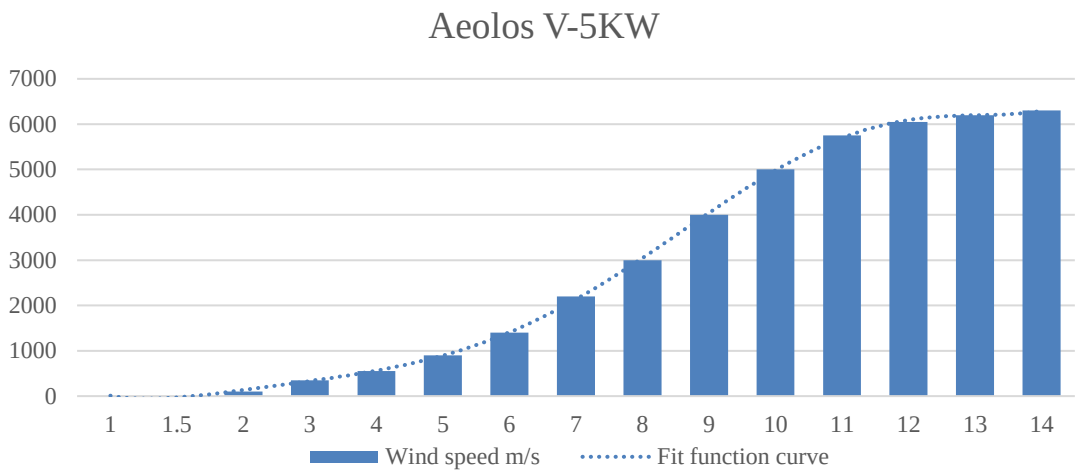

Figure 142: Aeolos V-5KW.

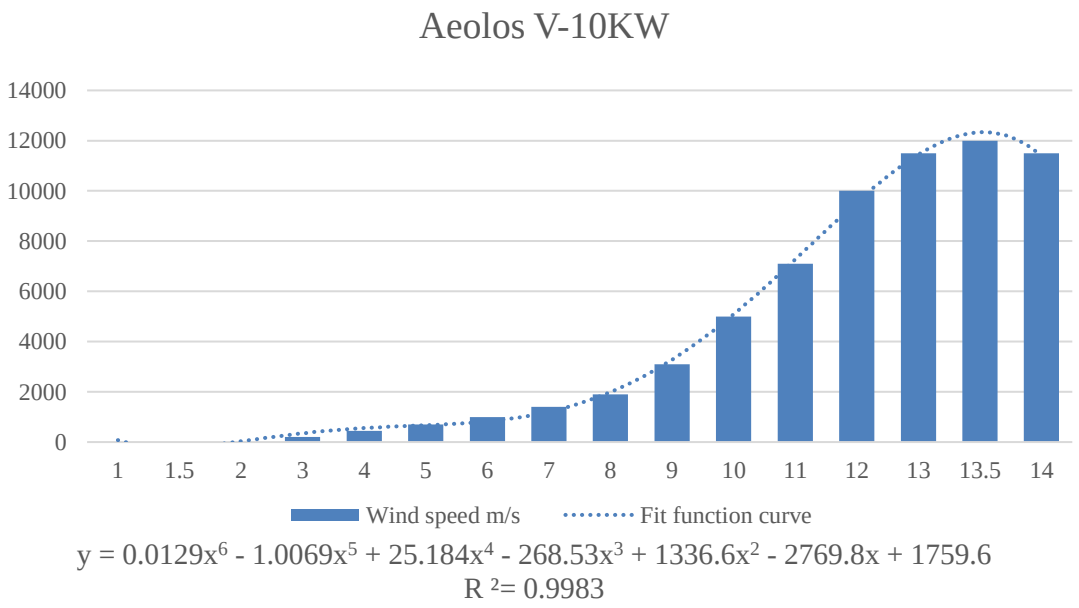

Figure 143: Aeolos V-10KW.

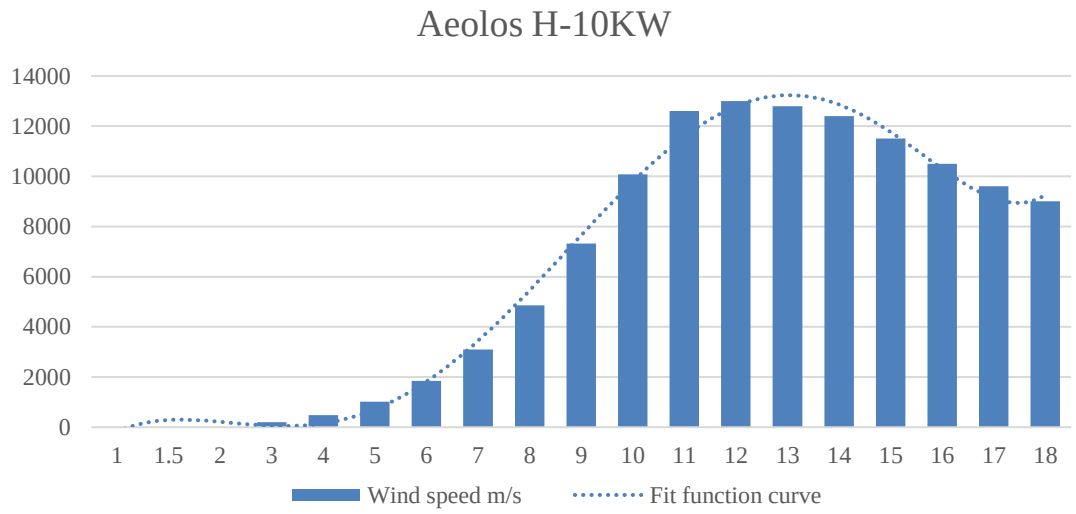

Figure 144: Aeolos H-10KW.

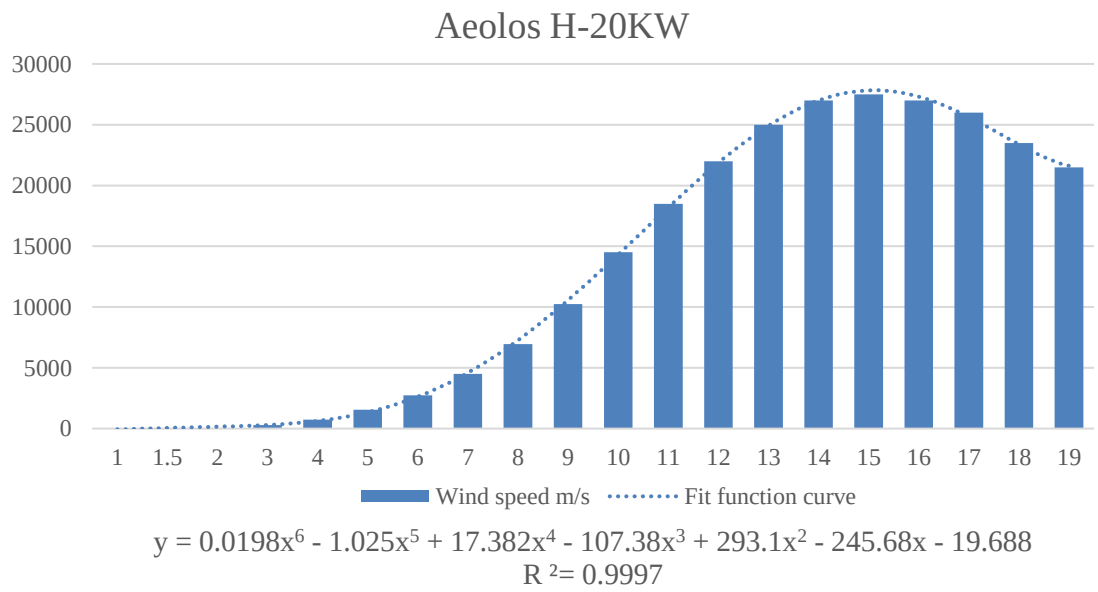

Figure 145: Aeolos H-20KW.

LUND UNIVERSITY

Dept of Architecture and Built Environment: Division of Energy and Building Design
Dept of Building and Environmental Technology: Divisions of Building Physics and Building Services